This is to certify that the
dissertation entitled

QUANTUM OPTICAL COMMUNICATIONS SYSTEM FOR
MICRO ROBOTS

presented by

JOHN DANIEL LEKKI

has been accepted towards fulfillment
of the requirements for the

Ph.D. degree in Electrical and Computer Engineering

Timothy Grotjohn
Major Professor's Signature

May 2, 2008
Date

QUANTUM OPTICAL COMMUNICATIONS SYSTEM FOR MICRO ROBOTS

By

John Daniel Lekki

A DISSERTATION

Submitted to
Michigan State University
in partial fulfillment of the requirements
for the degree of

DOCTOR OF PHILOSOPHY

Department of Electrical and Computer Engineering

2008

ABSTRACT

QUANTUM OPTICAL COMMUNICATIONS SYSTEM FOR MICRO ROBOTS

By

John Daniel Lekki

One way to improve the acquisition of planetary information from robotic landers is to use many smaller robotic explorers that can cover more ground than a single conventional rover. The development of such robots presents very significant technological challenges to enable essential functions, such as mobility and communication, given the small size and limited power generation capability. The research presented here has been focused on developing a communications system that has the potential for providing ultra-low power communications for robots such as these.

The communication system is a variant of photon-counting based communications. Instead of counting individual photons the system only counts the arrival of time coincident sets of photons that have distinct correlations. The utilization of sets of photons significantly decreases the bit error rate because they are highly identifiable in the presence of ambient light. The sets of photons can be generated in two ways. Quantum Entangled photons are one such set that can be generated through Spontaneous Parametric Down Conversion. This process is not energy efficient, but Quantum Entangled photons have an effective range that is hundreds of times greater than for photon sets that are not entangled. This is due to the highly correlated

momenta for entangled photons, which translates into positional correlation in the transmitted beam. A transmitter based on quantum entangled photons was built and tested. A one bit value was coded by sending photons of like polarization and a zero bit value was coded by sending photons with orthogonal polarizations. The system successfully transmitted data at a remarkably low power level, a received optical power of 1 Pico joule per bit, in the presence of significant background noise.

The second way to generate sets of photons is to utilize multiple sources that are pulsed simultaneously. This has the benefit of being much more energy efficient than a Quantum Entangled photon source. A transmitter utilizing this concept was built for evaluation. The components used in this system were chosen so that they could in the future be integrated into a cubic centimeter device. The experimental system was able to achieve a Bit Error Rate of 10^{-3} while transmitting data at a rate of 100 Kbits/ sec over a distance of 70 meters with a background level that was above the signal level (received Signal to Noise Ratio was -0.7 dB) using only 760 pW of transmitted power. Even with very low electrical to optical energy efficiency ~1%, an optimized optical system utilizing this technique would still use only 76 nw of electrical power. This is a power level that can be sustained by a power scavenging micro robot. The operating characteristics of this system have been modeled and used to extrapolate future performance improvements that can be achieved utilizing improved components that can be readily built.

To my wife Rebecca, my sons Ethan, Nathaniel and Caleb and also to my parents John and Helen. I so much appreciate the understanding and sacrifices that my wife and children have made while I completed this work. I also appreciate all the encouragement I got from my parents.

ACKNOWLEDGEMENTS

I would like to first acknowledge my advisor, Dr. Timothy Grotjohn, for his guidance and tutelage through this process. He not only helped me during the doctoral program but he also was my instructor for an independent study in optical systems during my undergraduate program. It was in this course that I realized how much I enjoyed this area of work and I have since followed a career path in this field. I am very grateful to him for his part in helping me to realize that I wanted to pursue a career in optical systems.

The work described here was part of a research project at the National Aeronautics and Space Administration Glenn Research Center. The experiments that were conducted as a part of this dissertation were accomplished with contributions from all of the members on that project team. I would like to recognize the talented team of researchers, engineers and technicians who have worked together on the Quantum Sensing and Communications project. This team includes Dr. Quang-Viet Nguyen, Mr. Binh Nguyen, Mr. Tom Bizon, Dr. Jun Kojima, Dr. Murad Hizlan, Mr. Quang Tran, Mr. James Williams, Mr. Ken Weiland and Mr. Bertram Floyd. Their friendship and collaboration made this one of the best experiences of my career.

TABLE OF CONTENTS

LIST OF TABLES

LIST OF FIGURES

NOMENCLATURE

$\langle N(1) \rangle$ = average number of photon coincidences for a '1' bit value

$\langle N(0) \rangle$ = average number of photon coincidences for a '0' bit value

CR = Contrast Ratio

$CR_{traditional}$ = Contrast Ratio for traditional photon counting communications

I = the entangled photon pair intensity generated from the transmitter (non dimensional counts / second)

i = is the background photon intensity captured by the receiver (non dimensional counts / second)

β = the fraction of transmitted photon pairs captured by the receiver

α = photon counter quantum efficiency

λ = wavelength (nm)

BER = Bit Error Rate (non dimensional bit errors / second)

SNR = Signal to Noise Ratio

f = frequency (Hz)

r_n = rate of ambient noise photons detected at photon counter n (non dimensional counts / second)

r_c = rate of photon coincidences due to ambient light (non dimensional counts / second)

δt = coincidence time window (in seconds)

T = bit period (in seconds)

CHAPTER 1

INTRODUCTION

The objective of this research is to develop a free space optical communication system that demonstrates the capability to transmit information over reasonable distances at very low radiated power levels. This work is in general inspired by the need to develop a communication capability that will be applicable for a planetary exploration concept that involves the mass spreading of very small robots, working in conjunction with small numbers of larger robots, on the surface of a planet. This method of exploration is meant to increase the information gathering capability of a mission while not increasing the mass that needs to be launched. In order for this to be possible it will be necessary to minimize the mass of these robots while retaining certain fundamental capabilities such as mobility, sensing and remote communications. The communication system developed and tested in this research has been designed with this usage as the primary motivator.

The communication system is optical because a small transmitter can confine an optical beam to a smaller divergence angle than is possible with radio frequency transmissions. Optical communication has the additional advantage that the receiver can have a very large gain when using photon counting detectors. These two reasons make optical communications a strong candidate for a small transmitter that must operate on very low power levels. Photon counting is very susceptible to ambient light conditions and it is for this reason that this research is focusing on a system that generates time coincident sets of photons that can be more easily recognized in sunlight. The research presented in this dissertation includes new work in two systems that both communicate using sets of photons but generate them in different manners. The first system generates a set of photons by creating quantum entangled photon pairs. The second system generates the set by pulsing pairs of diode lasers in coincidence. In this dissertation the underlying mathematics that describes these systems is presented as well as experimental tests that verify the operating characteristics of these systems.

1.1. Motivation

NASA's National Nanotechnology Initiative Grand Challenge

The proposed research path is motivated by the National Nanotechnology Initiative (NNI) Grand Challenge issued to the National Aeronautics and Space Administration (NASA) to develop Microcraft for Space Exploration and Industrialization. The vision for this Grand Challenge is summarized as: *"Continuous presence in space outside of the solar system with nanotechnology enabled low powered microspacecraft. Reduce the size and energy consumption ten fold."* [National Science and Technology Council 2000] This vision is further expanded upon as follows: *"Microspacecraft development is a key thrust for the exploration of space. Motivators for this demand include the high cost of launching into space, the desire to reach ever more remote and hostile environments in our solar system, and the unique capabilities of missions involving large numbers of cooperative spacecraft. To fulfill the promise that microspacecraft hold for exploring space, these spacecraft cannot be scaled down versions of larger spacecraft, limited in capability. This new breed of spacecraft must surpass the current state of technology in today's fleets of vehicles. Long duration missions (decades) to the outer reaches of the* *solar system; exploration into the interiors of planets, comets, and moons, searching for the subtle clues of the presence of life; fleets of telescopes, acting in concert, imaging Earthly planets around other stars; all these long range goals for space exploration in the 21st century will be enabled through the development of advanced nanoscale technology."* [National Science and Technology Council 2000] The strategy for implementing this vision states that there will be needs for research focused on nanostructured materials, nanoelectronics and biomimetic systems.

This research task will focus on the development of electronic and optical systems for the purpose of enabling microcraft communication as envisioned in the NNI. This research will focus on a communications system that is consistent with all the requirements that are unique for microspacecraft. These requirements are further described in the NNI: Initiative and Implementation plan as *"extreme demands on the electronics for ultra low power consumption, radiation tolerance, and safety."* These demands will require the *"development of transistors and other circuit elements utilizing single quantum excitations (electrons, Cooper pairs, photons) enable spacecraft to collect, process and then transmit information that will far surpass the capabilities of current missions."* [National Science and Technology Council 2000]

The requirements as described in the NNI are both challenging and vague. To further understand the requirements of a communications system for Microspacecraft some assumptions in regards to Microspacecraft (MSC) size and mission are needed. The first assumption is that due to the size of the MSC it is not possible for the MSC to send data directly to the Earth but instead will transmit information to a classically sized relay spacecraft. The size of the Microspacecraft should be driven by the requirements in the NNI which call for micro devices built from nano components. The micro devices are defined as devices on the dimensional scale from microns to centimeters that depend on the understanding and control of materials in the nanoscale. For this research effort the communications system will be assumed to be for a MSC with a length scale of 1 centimeter or less.

Power Requirements for Microspacecraft

The volume of the MSC will dictate the power requirements for the communications system. The power that can be generated by a MSC can be estimated from the volume, in the case of a battery type power supply, or from surface area in the case of photovoltaic power. In Figure 1.1 the power output estimate for a MSC with a high efficiency fuel cell is graphed in relation to the length scale. The assumptions used to create this graph are the following: the fuel tank takes up one half of the total volume of the MSC and the fuel is used for 24 hours of operation.

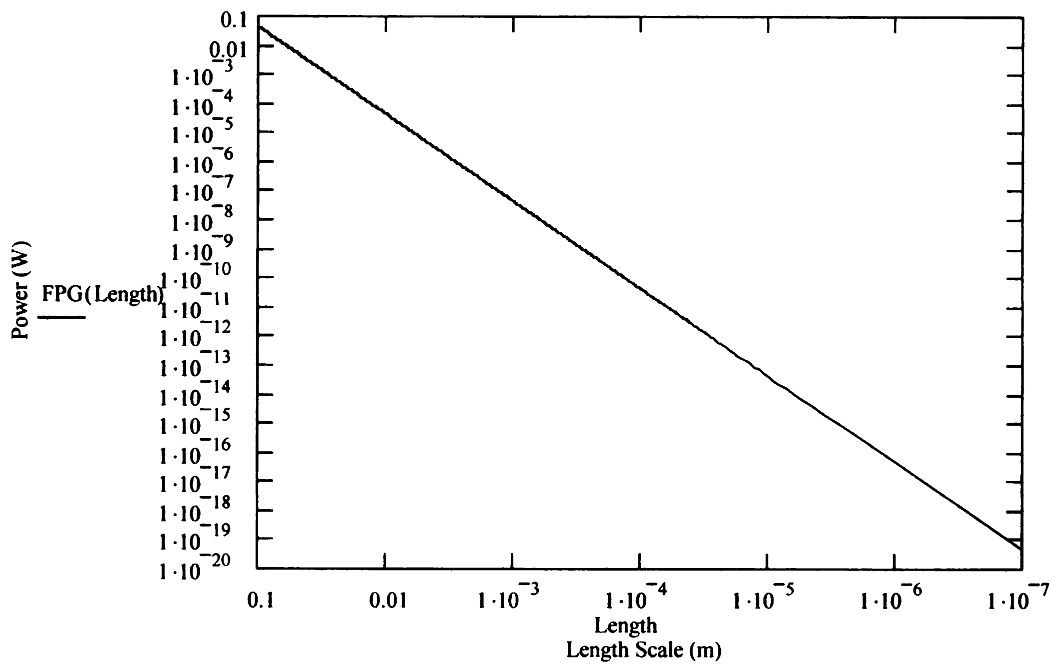

Figure 1.1: Graph of power output for a fuel cell that is assumed to linearly decrease as size decreases. Fuel cell Power Generation (FPG) is an estimate of the capability of future fuel cells.

For instance, for a MSC with 1 cubic centimeter of volume that is operating with a power supply that is an extremely efficient fuel cell, it is estimated that the power generation capability would be approximately 40 microwatts given a power generation capacity of 6.9 kW/L [Kimble 2004]. Given that only a fraction of the available power can be used for communications, the communication system must be designed to use only a quarter of that power, on the order of 10 microwatts of power. Since 1 centimeter is the length scale that is used as the maximum size for a MSC, 10 microwatts of communications power can be used as the maximum power usage for the MSC communication system.

Such a small amount of generated power implies that the device must be very efficient in signal transfer, or throughput, from transmitter to receiver. Throughput is defined as the ratio of signal energy received by the receiver divided by the energy sent from the transmitter. To achieve this level of throughput requires significant gain from beam forming, also described as a low level of beam divergence, or spreading, and a collector at the receiver the captures much of the transmitted beam. We will assume that the collector must be made of a reasonable size and so the parameter to optimize is the beam divergence.

The difficulty of building radio frequency antennas with significant gain given such very small dimensions is a second challenge that can further compound the power problem. The antenna gain is a function of both aperture size and signal frequency. Since the aperture is limited by the size of the transmitter the only parameter left to optimize is signal frequency. The relationship between beam divergence, θ_0, which is a measure of the beam forming gain, and frequency, υ, is

$$\theta_0 = \frac{c}{\pi W_0 \upsilon}, \qquad [1\text{-}1]$$

where W_0 is the beam waist radius and c is the speed of light [Saleh 1991]. Gain is inversely proportional to divergence, as a smaller divergence angle means greater long distance confinement of the beam and hence higher transmitter gain. So gain is therefore directly proportional to frequency. As gain is proportional to signal frequency, this suggests that the optimal frequency for remote communication, given robots of this scale, is in the highest frequency possible, which is in the optical region. Another benefit of optical frequencies is that it is possible to count photons at a receiver. This allows the receiver to be able to detect a signal that has very little energy, while at the same time providing a significant amount of intrinsic noise immunity from photons of energy below the band gap of the detector material. The advantages of beam forming and detectors capable of photon counting have made optical photons a very good candidate for communications for MSC devices. The research presented here is focused on a solution to the communication needs for MSC devices that is based on optical communication because of these reasons.

1.2. Objective

The overall goal for the National Aeronautics and Space Administration quantum optical communication research project is working toward energy-efficient, miniaturized, integrated (**photon source, modulator, receiver and antenna on a chip**) wireless technologies for robotic missions on planetary surfaces, on orbit and within space vehicles. The goal for this effort is to research a communication system, both transmitter and receiver, that is appropriate, in terms of power and capability to be fabricated in an extremely small package, for micro robotic communications. The manner in which this will be accomplished is in using an optical communication system that is based on quantum entangled, or highly correlated, photons.

Quantum Entangled (QE) photons are photons which are created by passing a pump beam through a nonlinear optical crystal. As the pump photons pass through the nonlinear crystal they sometimes spontaneously down convert into two photons whose individual energies add up to the pump photon energy. These two photons are created nearly simultaneously and because the two are created from one pump photon they are a part of a composite quantum state. An example of a 2 photon quantum state, $|\Psi\rangle_{12}$, that is composed of photons that are entangled in polarization, is

$$|\Psi\rangle_{12} = \frac{|H\rangle_1 |V\rangle_2 + |V\rangle_1 |H\rangle_2}{\sqrt{2}} \qquad [1\text{-}2]$$

where $|H\rangle$ indicates that a photon, 1 or 2, is horizontally polarized and $|V\rangle$ indicates that a photon is vertically polarized [Bouwmeester 2000]. The meaning of this quantum state is that either photon 1 is found horizontally polarized and photon 2 is found vertically polarized or photon 1 is vertically polarized and photon 2 is horizontally polarized. This quantum state is therefore a superposition of photon product states that cannot be factored. This means that it is impossible to describe the polarization state of one of the individual photons only in terms of itself. The photons therefore are highly correlated and this degree of correlation, along with the fact that they are produced simultaneously, makes them useful for low power communications in the presence of ambient noise.

The utility of QE photons for communication can be understood by considering the ambient photons detected by a receiver with two photon counters that detect specific wavelength and polarization photons. If a receiver has a narrow field of view and the ambient photons are sufficiently filtered by polarization and for narrow bands of wavelength, then even in the presence of sunlight the photon counts can be reduced to millions or even hundreds of thousands of counts per second. With photon counting detectors that can discriminate photon arrival times down to the nanosecond the detection of a photon can be considered a one nanosecond event. Even with a million of photons per second detected, the potential detector events are only one thousandth occupied. If only the times when both detectors detect photons within one nanosecond of one another are counted, then this significantly reduces the number of events from ambient photons. The number of coincident events in this scenario is only one thousand times per second. The mathematics supporting this will be further described in Chapter 3 but the important point is that the number of ambient noise events drops from one million per second to one thousand per second. The QE photons however pass through the optical and time coincidence filtering. They have highly correlated wavelengths and polarizations so the receiver filters can be matched to pass only photon pairs with these particular correlations. Also because the QE photons are generated at the same time they will arrive at the receiver at the same time and be time coincident. So while the receiver filters out a significant amount of the background noise, the QE signal is not attenuated and this makes the low power communication possible.

1.3 Planned Research Activities

There are three major activities planned for this research effort to develop low power communications for MSC. The first is to expand the development of communications systems based on QE photons. The second activity is to develop a system that emulates the QE communication system by coincidently pulsing individual sources. This system will hereafter be referred to as the Coincidently Pulsed Sources (CPS) system. Each of these systems has advantages and disadvantages that will be discussed later in this chapter. The last activity will be to develop the mathematical formulae that accurately predict the performance of both the expanded QE system and also the CPS system. Further details on these three efforts follow.

1.3.1 Modulated Quantum Entanglement State Communication Experiment

The idea of using photons that are quantum entangled for communication in very low signal-to-noise ratio (SNR) environments has been around for some time. Mandel [Mandel 1984] first proposed one such system in 1984 and a demonstration experiment was performed by Hong, et al., [Hong 1985] in 1985. In this experiment pairs of polarization entangled photons are generated and transmitted to the receiver over two beams of light that are on/off keyed with the data. In contrast to the system demonstrated by Hong et al. [Hong 1985], which encoded information through on/off keying, a system is presented here that instead encodes information with two symmetric entanglement states. This makes the receiver simpler to operationally implement than an on/off keyed system because the there is no threshold level, which is dependent upon ambient noise and hence influenced by the operational environment, to be concerned with. The QE system also has potentially greater range, as will be explained in Chapter 3, than the CPS system so further development of the QE system is appropriate as it may be the better choice for long distance low power communication.

This experiment also provided a good starting point because it is very similar to Hong's et al. [Hong 1985], and so this paper provided a good reference and provided a solid foundation to begin with. Also because the transmitter is an incremental improvement over the previous work, this experiment allowed many of the components for the CPS system, which is totally new, to be fully tested in a situation that has fewer unknowns. Upon completing this experiment critical experimental building blocks for the next stage, such as the photon counters and coincidence detection circuits, had been validated.

1.3.2 Monolithic Optical Transmitter Concept and Experiment

The general objective of the monolithic optical transmitter research activities was to develop a communication system based on time coincident photon pair communication that can be built into a miniaturized transmitter and is very efficient in terms of the amount of electrical power used to transmit a bit of information. The nonlinear generation of quantum entangled (QE) photons is extremely energy inefficient and is not feasible at present for usage in MSC devices. In order for this communication method to be used it is necessary to develop an energy efficient method for generating the signal photons. There is no known method for efficiently creating photon pairs that share a quantum state and are hence "quantum entangled". However, the QE communication method can be emulated. The communication method works because of the time coincident generation of photon pairs that have highly correlated wavelengths and polarizations. It is possible to build a transmitter that efficiently generates photons with these correlations. The subject of this research is a transmitter concept that will be able to generate correlated photon sets, which look like entangled photons to a receiver, in an energy efficient manner. This transmitter will be built from components that can eventually be incorporated into a very energy efficient monolithic device that is appropriate for a MSC.

As previously stated, the purpose of this work is to develop an optical transmitter that will meet the power and size requirements for a micro robotic device as was defined in the NNI. This means that the transmitter will have to have an overall diameter between 10 microns and 1 centimeter, and require less than 10 microwatts of power. It has been previously shown that quantum entangled photons are detectable even when swamped by background noise. The next step is to develop a monolithic source with driving electronics and optical sources integrated in a single solid state device with external beam forming optics. Since this source would require years of development, instead a prototypical transmitter that could in principle be built as a monolithic device was built and tested. The objective of the experiments performed with this system was to test the efficacy of both a transmitter that can generate the low power, highly detectable signal from commercial off the shelf components and a reciever to detect this particular signal. The commercial components for the transmitter were selected so that they can in the future be integrated into a low power monolithic device. This meant that a non linear crystal was not acceptable for this implementation. Instead solid state laser diodes and standard electronics were used to generate the detectable signal as they can be incorporated into a multi layer solid state device.

The block diagram for this transmitter concept is shown in Figure 1.2. The device works by modulating a signal from an oscillator or clock, for example at a 1 GHz rate. This modulated signal drives optical sources of different wavelengths. These sources (which may be LEDs, Laser Diodes, Quantum Wells or Quantum Dots) are driven with very small, and very fast pulses of electrical energy so that a burst of photons generally numbering less than one thousand per source, are generated. Since very small numbers of photons are required, the power can be significantly reduced from that of traditional On-Off Keyed optical transmitters, because very energy efficient optical sources can be used. The photons from all four optical emitters are sent coaxially along the same optical path to a receiver whereby they are decoded according to wavelength and polarization state. Various optical configurations can be used to spatially superimpose the signals from all emitters along a common optical path, inluding, but not limited to, dichroic beamsplitters and/or polarizing beam splitters, or a combination of a diffractive element such as a prism or grating and polarizers.

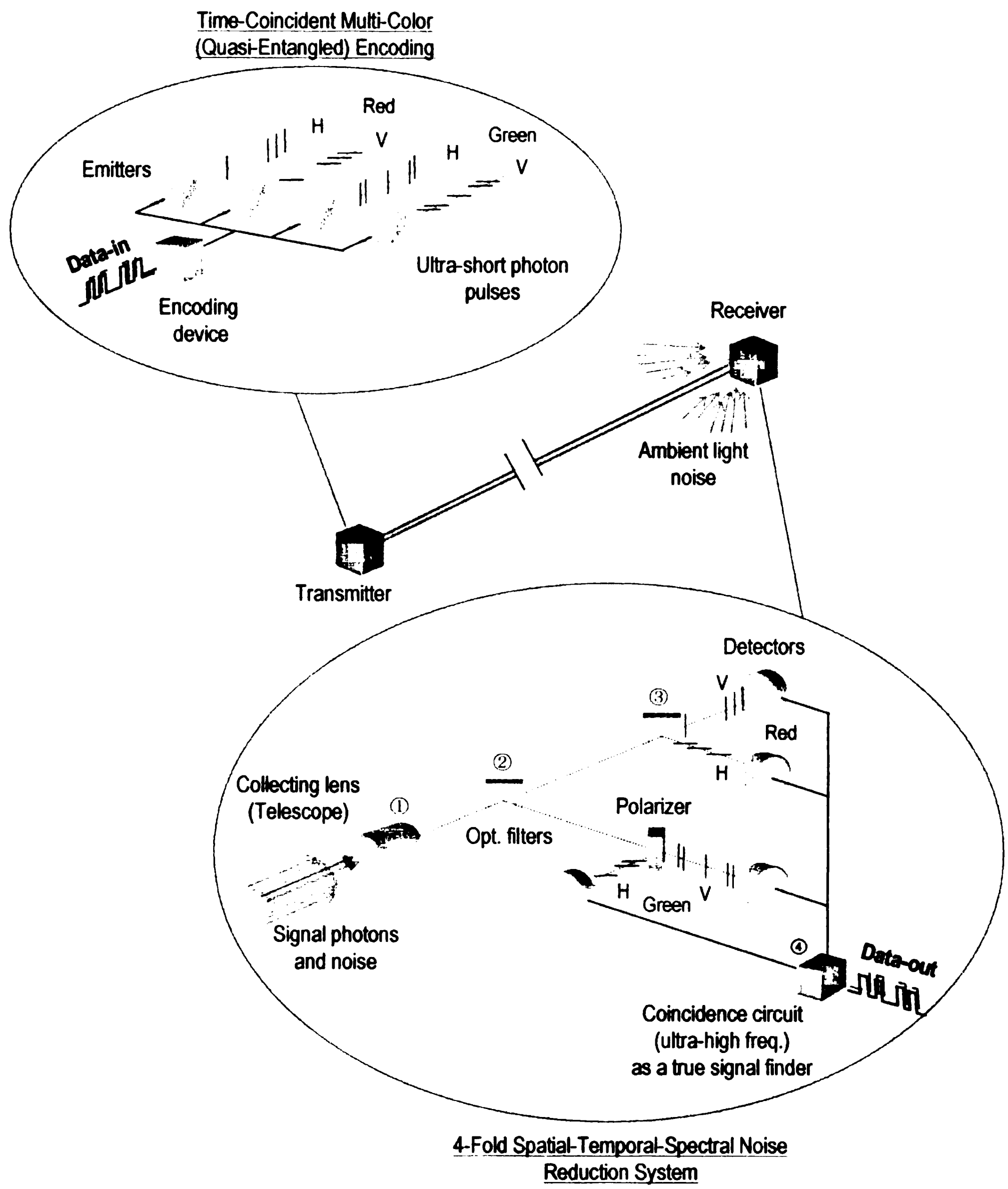

Figure 1.2: The conceptual system for generating highly correlated photon sets. Figure created by Dr. Jun Kojima of the Ohio Aerospace Institute.

In order to convey an idea of the power levels that are achievable, it is possible to estimate the power per bit of information transmitted for an integrated device that utilizes this signalling method. This calculation is best done by starting with the required signal at the receiver. It is known from the experiments performed up until now that the communication system has a reasonably low bit error rate if the number of coincidences registered by the receiver is greater than 10 per bit. Assuming a detector has a quantum efficiency of 70% means that the receiver must collect at least 14 photon pairs per bit to register 10 per bit. For the transmitter, it can be assumed that a very advanced nanolaser will have a 50% conversion efficiency of electrical to optical energy [Gourley 1998, Miyasawa 2005, Arakawa 2002, Mao 2004]. The transmission loss can be fixed as the range is bounded to the distance at which most of the transmitted photons are captured by the reciever [Jackson 2002]. This can be estimated as the distance where the transmitted beam falls off to 50% and so the transmission loss is set at 50%. From these assumptions it can be estimated that 56 photons / bit must be emitted from the transmitter to get 10 coincidences at the reciever. The electrical energy to generate these photons is equivelent to the energy of 112 photons per bit.

This is a simplified calculation and other factors, such as the inability to generate precise numbers of photons on demand and the fact that using two sources means there are two independent probabilities for generating a photon pair, capturing pairs and detecting pairs, will significantly increase the amount of electrical power required. If these additional considerations are roughly estimated to require an additional 400% of power then the energy the transmitter uses per bit would be around 500+ photons, which is about 150×10^{-18} joules. At 1 a Mbit/second data rate this works out to be a power of 140 picowatts, which is an extremely low power tranmitter. Again the fundamental goal of this dissertation is to take significant steps to demonstrate just such a transmitter as well as the requisite reciever.

1.3.3 Perform calculations to quantify the capabilities of this communication system

This communications system utilizes a simple technique for the production and transmission of time-correlated photon bursts over a multiplicity (minimum of two) of wavelengths or channels in a spectrum of wavelengths. Information is encoded by modulating the relative quantum state such as the polarization of the photons in each wavelength or spectral channel. The time-correlation of the photon bursts in addition to the modulation of the quantum states enable the detection of an ultra low-power signal that is comprised of at minimum, a single-photon from each spectral channel reaching a receiver. Thus, the transmitted signal comprised of multiple pairs of photons per bit is extremely low in radiated power (atto-Watts) making this technology useful for ultra low-power free-space optical communications applications. It should be noted that the time-correlation of photons at the separate spectral channels provides greater noise immunity than can be accomplished by increasing the radiated power from a single channel to a level equivalent to the combined power of the multiple channel transmission as described here. It is anticipated that the tranmitter described here will enable the development of ultra low-power free-space or fiber optic optical quantum systems using a simple and cost-effective electro-optics architecture.

1.4 Conclusion

In this chapter the motivation for developing a low power optical communication system for micro robots has been described. The research steps that have been taken, and are described in this work, have also been described. The planned accomplishments for this dissertation are to research, build and test, in a relevant environement, the efficacy of low radiated power communication system based on both quantum entangled sources and also coincidently pulsed sources. The new knowledge that has been generated from this effort include:

1. Quantified capabilities of both communication systems
2. Confirmation of the capabilities of a Quantum Entangled communication system with two-state coding through experiment
3. An original electronic photon pair communication system whose capabilities are confirmed through experiment.

The subsequent chapters support these three major efforts.

CHAPTER 2

BACKGROUND

In this chapter the key research in state of the art low power communications systems is discussed. First the previous work in utilizing quantum entangled photons for classical communications will be covered. From this previous research, particular equations that are important stepping stones for the research presented in this dissertation are discussed in detail, as well as known experimental demonstrations. Secondly, other state of the art low power communications systems, both RF and optical, will also be discussed in an effort to benchmark existing technology, so that the technological developments and results provided in later chapters can be evaluated.

2.1 Literature review of quantum entanglement for communication

State of the art optical systems include quantum communication systems which generate photons that share a quantum state, or in other words are entangled. It should be noted that in the literature quantum communications generally refers to the teleportation of a quantum state [Vilnrotter 2001, Lee 2000, Barnett 2001, Rarity 2003, Bouwmeester 2000, Nielsen 2000]. The other major area of quantum optical communication systems includes the used of single photons for both free-space and fiber optic Quantum Cryptographic Key communications. Single photons are used because it is possible to encode information in the quantum state of a photon in such a way that should an eavesdropper try to intercept the transmission they will not be able to reproduce the quantum state completely. If they cannot reproduce the state completely then the transmitter and receiver can detect that eavedropping is being attempted and will know not to use the transmitted key. This allows for the reliable communication of cryptographic keys. These systems have been demonstrated by, among others, Los Alamos National Laboratories. These systems typically utilize a bright, higher power, synchronization laser in conjunction with a low power photon source and so is not suitable for this low power micro robotic application [Nordholt 2002, Alde 2002].

The most important work in quantum communications that is applicable for low power optical communications has been work focused on utilizing quantum entangled photons to enhance the classical capacity of free space and fiber optic communications [Mandel 1984, Hong 1985, Jackson 2002, Banaszek 2004]. The systems that utilize entangled photon transmission are complicated large-scale systems requiring a ultraviolet (UV) pump laser to excite a non-linear crystal to produce time-coincident photons [Dmitriev 1999, Rarity 1990, Joobeur 1994, Kurtsiefer 2001, Kwiat 1995, Oberparleiter 2000, Takeuchi 2001, Eckardt 1990, Burnham 1970, Rarity 2003]. Because of the necessity of the pump laser and nonlinear photon pair creation the previous work by itself is not directly applicable to low power communication. However, the essentially important kernel from this work is the finding that enhanced signal recognition is achievable, even with a significantly higher level of background light, when utilizing entangled pairs of photons for classical communication. This kernel is the basis of the work contained herein and so the significant points of the prior research in this area will be discussed in detail to provide the basis for the research dedicated towards creating a system that generates these low power yet recognizable signals in an energy efficient manner.

Utilizing Quantum Entangled (QE) photons for communication was first proposed by Leonard Mandel. In 'Proposal for almost noise-free optical communication under conditions of high background' Mandel [1984] introduced this work. In this paper it was suggested that with quantum entangled photons "*it should be possible for weak signals that are greatly exceeded by background or noise to be used for communication, with relatively little loss of information*" [Mandel 1984]. Mandel's initial work has since been expanded upon by Hong et al. [1985] and Jackson [2002]. These analysis's support the assertion that optical communications utilizing pairs of photons that have an entangled quantum state have significant noise immunity benefits. They show that by only registering photons that are detected at the receiver in pairs, i.e. detected at the same time, a certain amount of noise immunity can be expected. This detection of photon coincidences can be thought of as an added level of temporal filtering to the system that further decreases noise effects.

Jackson's paper [2002] talked about particular communication instances such as when the sun was directly in line with the communication path. This paper concluded with two requirements: "(1) that an intrinsically two-photon detector be developed (this rejects noise without being saturated by it) and (2) that most of the transmitted photons be collected (which can be done in free space over distances up to about 1000 km)". The first conclusion is not completely applicable to the implementation for nanotechnology because detector saturation is dependent upon the environment where the MSC is used. This means the coincidence detector does not have to necessarily be an intrinsic two photon detector. The second conclusion however is critical for implementation of QE communication in MSCs because it will be a serious limiting factor for micro scale devices which will have significant beam divergence due to their small size.

Hong et al. [1985] not only expanded upon Mandel's [1984] analysis but also performed an experiment that demonstrated this noise immunity. In this experiment entangled photon pairs were generated by sending a 351 nm laser beam through a nonlinear crystal. The message was encoded using "on off" keying by turning the pump beam on and off. It was shown that a message that registered between 8 and 17 coincidences per bit was clearly distinguishable even when the individual photon counters detected an average of more than 2000 individual photons per bit.

From Mandel's and Hong et al. analysis, the total rate at which coincident photons are counted is a sum of the entangled photon pairs that are counted as well as the counted uncorrelated photons that accidentally overlap. The rate at which entangled photon pairs are counted, R_{CE}, is the product of the rate at which one of the conjugate photons is counted at one detector, $R_{1,2}$, and the probability that the second photon of the pair will be detected at the other detector, which is equal to the quantum efficiency of that detector $\alpha_{2,1}$. These rates are equivalent because the entangled photons are always produced in pairs

$$R_{CE} = R_1\, \alpha_2 = R_2\, \alpha_1\,. \qquad [2\text{-}1]$$

The accidental photon coincidence rate is the sum of the ambient noise photon rate for each detector, $r_{1,2}$, and also the rates, $R_1(1\text{-}\alpha_2)$ and $R_2(1\text{-}\alpha_1)$, which account for the case where one entangled photon of a pair is detected while the second one is not. From the accidental and conjugate photon coincident rates we have the following photon coincidence rate

$$R_c = [(1-\alpha_2) R_1 + r_1][(1-\alpha_1) R_2 + r_2]\delta t + R_1 \alpha_2, \qquad [2\text{-}2]$$

where δt is the time window in which the arrival of a photon at both detectors is registered as a coincidence.

When data is transmitted using on / off coding, the average number of coincidences registered when the pump laser is on, which represents a one data bit, is described by the equation

$$\langle N(1)\rangle = [(1-\alpha_2) R_1 + r_1][(1-\alpha_1) R_2 + r_2]\delta t T_s + R_1 \alpha_2 T_s, \qquad [2\text{-}3]$$

where T_s is the time period for each bit. When the laser is turned off, which represents a zero, the average number of photon coincidences detected is

$$\langle N(0)\rangle = r_1 r_2 \delta t T_s. \qquad [2\text{-}4]$$

The noise immunity of this system can be seen by looking at the effect of the coincidence time window. If the coincidence time window is very small, on the order of a nano second, then the average number of coincidences for a '1' bit value will largely be dependent upon the entangled photon rate until the background photon rates approach 10^9 photons per second. For a narrow region of the optical spectrum this is a fairly significant ambient optical power. As previously mentioned, this noise immunity of correlated pairs of photons forms the basis for the present research into low power optical communication.

2.2. State of the Art

To further understand how this research effort is beneficial an examination of the current State-of-the-art is necessary. The following sections covering Radio Frequency (RF) and optical communications are primarily focused on technological development rather than theoretical studies. The state of the art comparisons are therefore made to systems that have been, to some experimental level, built and tested.

2.2.1. Low power RF

State-of-the-art small-scale communications is presently achieved by very small RF transmitters. These transmitters have the benefit of omni directional communication but are limited in range. Currently, the development of the state-of-the-art miniature RF transmitters is being led by a group at U.C. Berkeley [Rabaey 2002]. The goal of the Berkeley group is to build RF transmitters so small and inexpensive that they will be ubiquitous in everyday uses and can be used as disposable embedded sensor/transmitters. The Berkeley group has demonstrated a micro-RF transmitter that is about 4 mm^2 in size, and requires less than 100 μW of power to operate at a frequency of 1.9 GHz. Perhaps one of the biggest challenges of their technology is the fact that they draw power (as much as 10 μW) even when they are not transmitting (standby mode). This type of drain alone can deplete the small energy reserves of micro-robotic exploration vehicles. Whereas optical communication technologies only require power when they are actually transmitting photons, thus they are more efficient in the long-run.

As advanced as this miniature RF technology is compared to existing RF technologies that use 10's of mW's, it still requires an external wire antenna that is of order cm's long in order to efficiently transmit its signal through space. It is the requirement of relatively large external antenna that poses a fundamental barrier to using RF technologies for micro- or nano-robotic exploration vehicles as the mass and size of the antenna alone may exceed that of the vehicle itself. It is in this area that by using free-space ultra-low power optical communications proves beneficial: the size of an optical antenna can be very small as the wavelength of light is much smaller. Thus, practical optical transmitters can be much smaller than 1 mm in size.

2.2.2. Low power optical

In general free space or wireless optical communications are primarily used for wireless network links for personnel computers or for high bandwidth trunk links between buildings [Heatley 1998]. State of the art optical systems also include classical optical communication systems based on lasers and single, as well as multiple, frequency transmissions [McEliece 1981, Atkin 1994, Polishuk 2003, Arnon 2003, Andrews 1998, Pierce 1978]. The classical multi-frequency free space systems utilize time coincident classical pulses on two or more wavelengths to overcome atmospheric scintillation [Kim 1997, Kim 1998, Strickland 1999, Grant 2005]. The wireless communication between buildings and for personnel computer networks are in general not as power limited as the research considered here and so they are not elaborated upon. Free space optical links are also considered for deep space communication [Wilson 2000, Pierce 1981], satellite links [Hemmati 2000] and also for communications for novel miniature sensors called by their designers "Smart Dust" [Warneke 2001, 2002]. Deep space networks are a somewhat similar problem because the signals are so very weak at their destination and so some description of this work will be made. The most similar state of the art work is in optical communications for integrated robots that are so small (~1cm) that they are called "Smart Dust". This work is considered the most relevant for comparison to the research described in this dissertation.

Optical communication for deep space networks has received more attention recently because of the increased bandwidths desired to support new technologies such as hyperspectral imaging and HDTV. A recent paper, summarizing efforts at the Jet Propulsion Laboratory, described a developmental laser communication system that is being used for various studies and demonstrations [Wilson 2000]. The transmitter utilizes a Q-switched Nd:YAG laser that encodes data using Pulse Position Modulation (PPM). The receiver is planned to be a 1 to 10 meter telescope with an avalanche photo diode as the detector [Ortiz 2000]. The deep space communication problem is a similar one to the micro robotic communication problem. The power levels of the transmitter are higher but the long distance and high background light make this a comparable case. By using PPM it is possible to achieve very low power communication. This is because PPM is a block encoding communication method where an entire block of data is sent by a single pulse. The data word sent is defined by the slot position of the transmitted pulse. The number of time slots, M, in a frame determines the number of bits that are transmitted with each pulse. So a system which has M = 256 will transmit 8 bits of information with each optical pulse, neglecting synchronization pulses. In comparison, the most common optical pulsed modulation system utilizes On Off Keying (OOK) with Manchester coding, and these systems require 1 laser pulse per bit. So PPM modulation in this case represents an average transmitted power reduction of a factor of 8.

In 2000, Gerardo Ortiz et al [Ortiz 2000] published a very good description of the design of a Mars to Earth optical communication link that included significant operational parameters such as data rates and background light. The Mars transmitter was specified as a one watt Q-switched Nd:YAG laser (wavelength 1064 nm), with a 10 cm aperture telescope that was PPM (M=256, pulse width = 25ns) modulated with Reed Solomon coding. The receiver included the following specifications: silicon APD detector, 10 meter diameter telescope aperture, an optical bandpass filter with a 0.2 nm bandwidth and a receiver sensitivity of 323 photons per pulse. The link distance is 300 million Km, the required bit error rate is 10^{-5}, and the number of nighttime background photons per pulse slot is in the range 156 photons per slot. The data rate obtainable with these parameters is 46 kbps and the received signal is 646 photons / pulse. The energy efficiency of this system is best examined from the required signal at the receiver. The received signal pulse of 646 photons is the amount of optical signal required to receive 8 bits of information, neglecting coding and synchronization. This works out to be one bit of information per 80 photons captured by the receiver. If the signaling method had been Manchester OOK then the required signal at the receiver would have been closer to the 646 photons per bit when the background is around 156 photons per pulse. In comparing the research in this text to this system, the comparison will be made in terms of the OOK parameters. The comparison will be to OOK because PPM is essentially a precoded version of OOK. That is an OOK system can be modulated as a PPM system. In referring to modulations such as PPM Hamkins wrote "All the other orthogonal modulations considered in this paper are constrained versions of OOK, in the sense that the other modulations can be viewed as a precoding operation followed by ordinary OOK." [Hamkins 2004]

The communication system considered for the Smart Dust project has a great deal of applicability as it is meant for essentially the same application and has size and power constraints very comparable to the goals of this research. The stated goal for Smart Dust is to develop a device, which is approximately a cubic millimeter in size, capable of sensing, computing and communicating that will work together with like devices to form a massive sensing array [Warneke 2001, 2002]. The device can be solar or battery powered. When solar powered the predicted power levels for a $1mm^2$ solar cell is 1 joule per day in sunlight and from 1 to 10 millijoules per day indoors [Warneke 2001]. In terms of watts this would be an average power of 11.5 microwatts outdoors and 11.5 to 115 nanowatts indoors. These are very similar to the estimate in Chapter 1, which was 10 microwatts, so the conclusions drawn from the Smart Dust research is very applicable.

The researchers in this program have pointed out several advantages of optical communication over RF communication for energy constrained devices such as these. They cite current RF transmitters requiring "minimum power levels in the multiple milliwatt range due to analog mixers, filters, and oscillators" [Warneke 2001]. They also address the need for an antenna of at least 1 cm as being a limiting factor in producing small RF transmitters that retain energy efficiency. Optical communication is in contrast described as "intrinsically small" while the "transmission and detection circuitry for on/off keyed optical communication is more amenable to low-power operation than most radio schema" and most importantly "optical power can be collimated in tight beams even from small apertures" [Warneke 2001]. These are essentially the same arguments that have been made in chapter one that motivates this optical communication research.

In the two papers cited [Warneke 2001, 2002], two different optical communication systems are described. The first is a passive optical transmitter built from a modulated Corner Cube Retroreflector (CCR) while the second is an active transmitter built from a laser diode with beam steering optics. The corner cube transmitter works by modulating the reftroreflection of an interrogation beam that originates from the device that is to be communicated with. The retroreflection is modulated by putting one of the mirrors that forms the corner cube on a swing arm that can be tilted. By tilting this mirror so that it is no longer orthogonal to the other two mirrors, the three mirrors will no longer work as a retroreflector and so the interrogation beam can thus be on/off modulated by tilting this mirror. This system has significant power advantage for a low power sensor node working with a higher power central node because the transmitter only uses the power required to move the mirror a slight angle, which for a micro mirror can be a very low power. The disadvantages are that devices that utilize a CCR will not be able to communicate with one another and the effective range is not easily extended beyond 1 km. For these reasons the researchers developing the Smart Dust devices state that the nodes "must be active and have their own onboard light source" [Warneke 2001].

The active system described in the Smart Dust project consists of a laser diode with a collimating lens followed by a steering mirror. In order to operate in outdoor ambient light the receiver has a narrow band filter and an imaging detector. The imaging detector further limits the ambient light because the individual cell in the detector array sees only a limited area of background light around the transmitter. The imaging detector also allows for multiple transmitters to be detected simultaneously. One issue with the imaging reciever is that the data rate is limited to video frame rates so an active research area for this project is to build an imaging array with an analog reciever associated with each pixel. Using this technique the Smart Dust project anticipates the need for a transmitte power of only 10 picojoules per bit for short ranged indoor communication. Since ambient outdoor light is about 1000 times greater than indoor light, the short range transmitted power estimate for outdoors communications is probably on the order of 10 nanojoules per bit. For 50 kbps transmission rate that would be a power of 500 μw outdoors and 500 pw indoors.

2.3. Summary

Previous work in utilizing quantum entangled photons for classical communication has been summarized. The optical systems that were used to generate entangled photons required large amounts of power and so they are not directly applicable to the present research. The signals however are foundational for the present work and so the summarized equations will be the basis in the next chapter to describe the low power quantum communication system.

State of the art short range RF devices are now at about 100 μw of power when transmitting and 10 μw in standby. They do not work efficiently when built so small that the antenna is less than one quarter wavelength in size. Pulsed optical communication systems have advantages in beam forming and in standby power usage. The required power level for these is dependent on ambient light conditions and is in the range of 500 pW to 500 μW. To build energy efficient classical optical transmitters, pulse position modulation is used to further reduce power. When comparing an OOK system to a PPM system, it is fair to compare the signal to noise ratio of the time slot containing the PPM signal pulse to the signal to noise ratio of an individual OOK pulse. This is because PPM is a precoded version of OOK and so an OOK system can always be made into a PPM system. The figure of merit in terms of required signal captured by the receiver, can thus be taken from the deep space optical communication research. That level is therefore 646 signal photons when the background is 156 photons. These parameters will be used for comparison in later chapters.

CHAPTER 3

COINCIDENT PHOTON COMMUNICATION THEORY

In this chapter the improvement in bit contrast ratio by utilizing quantum entangled photons for classical communication coded by on / off keying (OOK) is derived. An improved communication system utilizing quantum entangled photons for symmetrically coded communications is introduced and the Bit Error Rate (BER) for this system is derived. The BER for a system that electronically generates photon pairs is also derived. Finally this chapter includes a section where the ranges of the two different communication systems are examined.

3.1 General theory for On / Off keyed Quantum Entangled Photon Communication – improvement in bit contrast ratio

A comparison of the bit contrast ratios for the technique based on utilizing Quantum Entangled (QE) photons and traditional single source photon counting communications shows the utility of utilizing QE photons for low signal power situations. From Shannon information theory it is known that the larger the noise, or background, in a discrete channel, the lower the rate at which information can be transmitted [Shannon 1948]. If the noise level were to exceed the signal then the information becomes useless. The obvious way to overcome the noise for successful communication is to increase the signal strength. However with a fixed signal strength, which is below the ambient noise, the proposed optical system using quantum entangled photos for communication becomes necessary. The QE system can perform favorable even when the signal strength is as low as a few photons and noise level is extremely high. By further analyzing the equations derived by Mandel it is possible to derive a comparison of QE photonic communication system versus a traditional single source photon counting communication system [Mandel 1984]. Hereafter the typical single source and single detector photon counting system will be referred to as the traditional photon counting system.

The effectiveness of this signaling technique can be realized by looking at the contrast ratio for the '1' and '0' bit value. The contrast ratio in the case of registering single photons or QE photon coincidences is defined as the following ratio:

$$CR = \frac{\langle N(1) \rangle}{\langle N(0) \rangle}, \qquad [3\text{-}1]$$

and is described as the ratio for the average number of single photons or coincident photons for the one bit level, $\langle N(1) \rangle$, to the average number of single photons or coincident photons for a zero bit level, $\langle N(0) \rangle$. For traditional photon counting these values are

$$\langle N(1) \rangle = \alpha\, i + \alpha\, \beta\, I \qquad [3\text{-}2]$$

$$\langle N(0) \rangle = \alpha\, i \qquad [3\text{-}3]$$

where I is the signal photon intensity, i is the noise intensity, α is the quantum efficiency of the detector and β is the fraction of transmitted photons that are captured at the receiver. From Equations [3-1,2,3] the contrast ratio for traditional photon counting optical communication ($CR_{traditional}$) is

$$CR_{tradional} = 1 + \beta \cdot \frac{I}{i}, \qquad [3\text{-}4].$$

The contrast ratio for the QE based photon counting communication can be derived using Equations [2-3], [2-4] and [3-1]. It can be presented in a clearer manner by assuming the rates of the photons going to the two detectors is equal for both the entangled photons (R_n) and the ambient noise photons (r_n) and representing these parameters as R and r respectively.

$$CR_{QE} = \frac{R\alpha + \left[(1-\alpha)R + r\right]^2 \delta t}{r^2 \delta t} \qquad [3\text{-}5]$$

The equation can be further simplified by expanding the R and r photon rates to account for beam divergence and quantum efficiency of the detectors through the following relationships:

$$R = \alpha \beta I_{QE} \quad and \quad r = \alpha i, \qquad [3\text{-}6]$$

where I_{QE} is the entangled photon intensity generated from the transmitter. This substitution produces a Contrast Ratio for the entangled photon communication that is

$$CR_{QE} = \frac{\alpha^2\,\beta\,I_{QE} + \left[(1-\alpha)\alpha\,\beta\,I_{QE} + \alpha\,i\right]^2 \delta t}{\alpha^2\,i^2\,\delta t}. \qquad [3\text{-}7]$$

By looking at the case where the quantum efficiency is assumed to be equal to 1 it is easier to compare the QE contrast ratio to the contrast ratio for traditional photon counting communication. Setting α to one further simplifies the QE Contrast Ratio to:

$$CR_{QE} = 1 + \frac{\beta\,I_{QE}}{i^2\,\delta t}. \qquad [3\text{-}8]$$

From this equation and the traditional photon counting contrast ratio equation, the Contrast Gain (*CG*) can be expressed, in terms of decibels, by:

$$CG = 10\left[\log\left(\frac{1+\dfrac{\beta\,I_{QE}}{i\,\{i\,\delta t\}}}{1+\dfrac{\beta I}{i}}\right)\right] = 10\left[\log\left(\frac{i^2\,\delta t + \beta\,I_{QE}}{i^2\delta t + i\delta t\beta I}\right)\right]. \qquad [3\text{-}9]$$

If the intensity of QE photons is equal to the intensity of traditional source then from this equation it is apparent that the entangled photon communication method can produce significant gain as long as the i and δt product is smaller than one. This bounding equation provides a means to calculate the maximum background intensity where this technique will prove useful. Assuming that the minimum coincidence window that is possible to obtain with existing electronics is approximately 100 pico seconds, this makes the maximum background photon rate at the detector to be approximately 10^{10} photons / second for this method to prove useful. If the QE intensity is less than the intensity for traditional photon counting, then this difference directly reduces the maximum background photon rate where the system has merit. The need for high efficiency QE sources is apparent from this relationship.

A plot that compares the bit contrast ratio of classical on-off keying optical communication with this non classical technique is shown in Figure 1. For this plot the following parameters were used: fraction of captured photons $\beta = .3$, coincidence resolving time $\delta t = 1$ ns, detector quantum efficiencies $\alpha = 1$ and a fixed signal rate I of 10^4 photons/s. The amount of noise was varied to generate different levels of Signal to Noise Ratio (SNR).

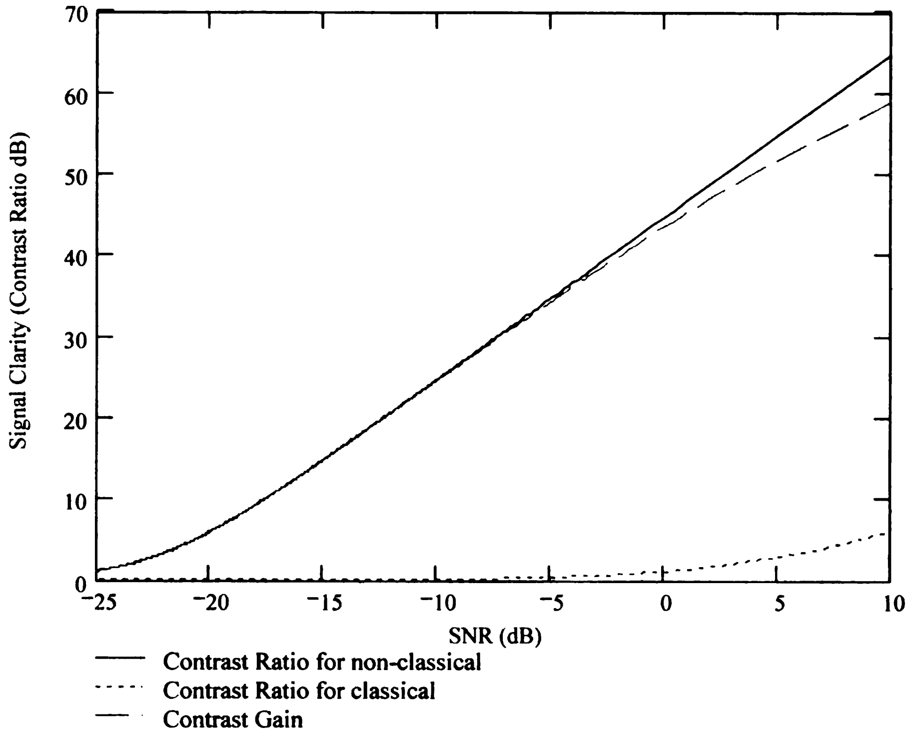

Figure 3.1: This figure gives a plot of the increased contrast ratio that is possible when utilizing quantum entangled photons (non-classical) for communication at low SNR when compared to classical optical communications.

At less than -25 dB, the noise and background dominate and the QE signal photons are largely lost in the noise. Below this SNR communication would be impractical because the contrast ratio of the quantum entangled optical system is similar to the traditional photon counting system and there are no contrast gains. However at slightly higher signal-to-noise ratios (greater than -22 dB) the contrast ratio of QE system improves significantly in comparison to the traditional photon counting system and the contrast gain is greater than 3 dB at SNR of -20 dB. This region between -20 dB and 10 dB is where communication with entangled photons is useful. Beyond SNR of 10 dB it is unnecessary to utilize the QE photon based technique and the contrast gain begins to drop significantly. The use of entangled photons together with photon coincidence detection permits good discrimination against background noise at the SNRs that an ultra-low power MSC can be anticipated to operate at.

3.2 Bit error rate for communication utilizing quantum entangled photons with on off keying for bit coding

The experiment performed by Hong, *et. al.,* in 1985 is illustrated in Figure 3.2 [Hong 1985]. The pairs of polarization entangled photons are generated and transmitted to the receiver over two beams of light that are on-off keyed with the data. The receiver detectors can detect individual photon arrivals. The coincidence detector circuit produces a pulse when a pair of photons triggers detectors 1 and 2 in temporal coincidence. If there is no signal present, ambient light incident on the detectors will produce what are called *accidental coincidences* at a rate $r_a = r_1 r_2 \delta t\, T_s$, where r_1 and r_2 are the detector 1 and detector 2 count rates due to ambient light, in photons/s, and δt is the two-sided coincidence window size in seconds and T_s is the bit period. By making the coincidence window time smaller, the rate of accidental coincidences from ambient light can be made to be much smaller than the rate of coincidences due to the arrival of entangled photon pairs, which are inherently time coincident. In general, more than one set of entangled photons will be transmitted during a bit period. Bit value decisions can be made by comparing the number of coincidences per data bit duration to a threshold value. This process results in a relatively high detector output SNR from a very small detector input

SNR, making reliable communications possible where classical detectors would be swamped by the presence of ambient light.

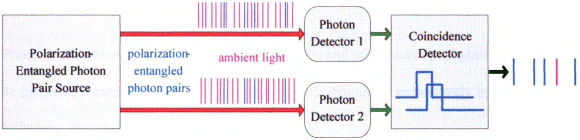

Figure 3.2: Concept for on/off keying quantum entangled communication

The experiment performed by Hong et al, was for quantum entangled photons used in an on/off keying mode. In this case, bit values are determined by comparing the number of photon pairs received to a threshold value, *k*. If the number of photons pairs received is larger than *k* then it is a '1' bit value and if less coincidence photons are received than the threshold it is a '0' bit value. The error rate for this coding scheme is tied to the average number of transmitted correlated photon pairs that are received (m), the average number of noise pairs received during a '0' bit (m_0), the average number of noise pairs received during a '1' bit (m_1) and the threshold value. These averages are defined [Hong 1985] by

$$\begin{aligned} m &= \alpha_1 R_2 T_s = \alpha_2 R_1 T_s \\ m_1 &= \left[(1-\alpha_2)R_1 + r_1\right]\left[(1-\alpha_1)R_2 + r_2\right]\delta t\, T_s\,, \\ m_0 &= (R_1 + r_1)(R_2 + r_2)\delta t\, T_s \end{aligned} \qquad [3\text{-}10]$$

where $R_{1,2}$ are the rates of conjugate signal photons detected by detectors 1 and 2 except for the m_0 equation where they are the rates of photons from a compensation light that was turned on when the laser was off, and $\alpha_{1,2}$ is the quantum efficiency of the two detectors.

Photon coincidence counts obey Poisson statistics and so the error probability of a '1' to be incorrectly interpreted as a '0' and vice versa is described respectively by the following probabilities [Hong 1985]

$$P(0\,|\,1) = e^{-(m+m_1)} \sum_{r=0}^{k-1} \frac{(m+m_1)^r}{r!} \qquad [3\text{-}11]$$

$$P(1\,|\,0) = 1 - e^{-m_0} \sum_{r=0}^{k-1} \frac{m_0^r}{k!} \qquad [3\text{-}12]$$

where r is the summation variable. These error probabilities are asymmetric because an increase in noise increases the probability for a '0' to be mistaken as a '1' bit value, by increasing m_0, and decreases the probability for a '1' to be mistaken as a '0' bit value, because m_1 is increased. This will force the selection of a threshold that needs to be biased toward the '1' bit value depending upon the amount of noise.

The Bit Error Rate comes directly from these error probabilities and is equal to the average of the error probabilities [Saleh 1991]

$$BER = \frac{P(1|0)+P(0|1)}{2}. \qquad [3\text{-}13]$$

The BER calculation produces some remarkable results given these sample conditions: 10 QE photon pairs detected per bit, over 6000 noise photons per bit, and a coincidence time of 1 ns produces a minimum BER of 1.5×10^{-3} with a k of 3.

3.3. Bit error rate for communication using quantum entangled photons with two state coding

The necessity of setting a threshold value for an OOK system that is asymmetrically affected by noise is not optimal. To resolve this problem, a two state coding scheme has been developed. What is meant by the two state coding scheme is that a '0' bit is represented by a zero state rather than simply by off or lack of a signal. The '0' bit in a two state coding is represented by a particular set of photon states and a '1' bit is represented by another orthogonal set of photon states.

In contrast to the system demonstrated by Hong, which encoded information through on/off keying, this system encodes information with two symmetric entanglement states and will therefore have nominally symmetric affects from noise. Figure 3.3 shows the block diagram of the architecture for the two-state implementation. The optical source consists of a UV laser-pumped spontaneous parametric down conversion (SPDC) entangled photon source which generates two beams of light with identical, but random polarizations, similar to the source described by Kwiat et al. [Kwiat 1995]. For the receiver, photon detectors 1 and 2 are set to detect only H photons whereas detector 3 is set to detect only V photons through the use of a polarizing filter and polarizing beam splitter. Binary data modulates a variable phase retarder, keeping H and V photons intact under state "1," and changing H photons into V, and V photons into H under state "0." As a result, photon detectors 1 and 2 trigger H photon coincidences in coincidence detector 1 when state "1" is transmitted, and detectors 1 and 3 trigger V photon coincidences in coincidence detector 2 when state "0" is transmitted. Decisions are made by comparing the number of coincidences per data bit from the two coincidence detectors. If coincidence detector 1 count is greater than coincidence detector 2 count then the receiver records a "1;" if not the receiver records a "0". As in the conceptual system, accidental coincidences due to ambient light and un-entangled photons from the laser source are expected to be much smaller than signal coincidences, affording reliable communications under very low SNR.

In comparing Figure 2 and Figure 3 it can be seen that the essential differences from the on/off keying experiment conducted by Hong are that a polarization rotator is added to the transmitter and a third detector is added to the receiver. When the polarization rotator is off the quantum entangled photon pairs are only detected by detectors 1 and 2. This is nominally the same as having the laser on with OOK and so the average number of coincidences detected by coincidence detector 1 are the likewise the same. The bit value can be defined as a one with the polarization rotator off and so the average number of coincidences for a one value is

$$\langle N(1)\rangle = [(1-\alpha_2)R_1 + r_1][(1-\alpha_1)R_2 + r_2]\delta t\, T_s + R_1\,\alpha_2\, T_s. \qquad [3\text{-}14]$$

When the polarization rotator is 'on' the coincidences are then detected with detector 1 and 3 and this is defined as the zero value for a bit. The average number of coincidences when a zero is being transmitted is simply determined by replacing the detector 2 parameters with detector 3

$$\langle N(0)\rangle = [(1-\alpha_3)R_1 + r_1][(1-\alpha_1)R_3 + r_3]\delta t\, T_s + R_1\,\alpha_3\, T_s. \qquad [3\text{-}15]$$

The value of a bit is determined at the receiver by comparing the number of coincidences registered for a 1 to those registered for a 0 during a given bit period. Since a comparison is being made between coincidence detector 1 and 2 to determine a received bit value, the coincidences registered by coincidence detector 2 represent noise when a one is being transmitted and likewise the coincidences registered by coincidence detector 1 are noise for a zero. The average number of these noise coincidences [$\langle N(1|0)\rangle$, $\langle N(0|1)\rangle$] is derived from the expressions for $\langle N(0)\rangle$ and $\langle N(1)\rangle$ by accounting for the lack of entangled photons registered at detector 3 when a one is transmitted and also lack of entangled photons registered at detector 2 when a zero is transmitted. The expressions for these noise coincidences when a zero is transmitted is therefore

$$\langle N(1\,|\,0)\rangle = [(1-\alpha_2)R_1 + r_1][r_2]\delta t\, T_s \qquad [3\text{-}16]$$

and the noise coincidences when a one is transmitted is likewise

$$\langle N(0 \mid 1) \rangle = [(1-\alpha_3) R_1 + r_1][r_3]\delta t \, T_s . \qquad [3\text{-}17]$$

The probability for an error when a 1 is transmitted is

$$P(0 \mid 1) = P[N(1) < N(0 \mid 1)] \qquad [3\text{-}18]$$

and likewise the probability for an error with a zero is

$$P(1 \mid 0) = P[N(0) < N(1 \mid 0)]. \qquad [3\text{-}19]$$

The probability of error therefore is the probability that a random value from the noise probability distribution will be equal or larger than a random value from the signal probability distribution. This probability that a random number from one distribution function is larger, by a value z, than a random number from another distribution function can be found by summing all of the probabilities for positive values in the difference between the two functions. This is expressed for the case of a '0' bit error by

$$P\big[N(1 \mid 0) > N(0)\big] = \sum_{z>0} P\big[N(1 \mid 0) - N(0) = z\big]. \qquad [3\text{-}20]$$

The difference between Poisson variables has been shown [Haight 1967]

$$P\left[N(1\,|\,0)-N(0)=z\right]=e^{-\left(\langle N(1|0)\rangle+\langle N(0)\rangle\right)}\left(\frac{\langle N(1\,|\,0)\rangle}{\langle N(0)\rangle}\right)^{\frac{z}{2}} I_z\left(2\sqrt{\langle N(1\,|\,0)\rangle\langle N(0)\rangle}\right),$$

[3-21]

where $I_z()$ is a modified Bessel function of the first kind. The probability of error for a '0' bit is therefore

$$P(1\,|\,0)=\sum_{z=1}^{\infty} e^{-\left(\langle N(1|0)\rangle+\langle N(0)\rangle\right)}\left(\frac{\langle N(1\,|\,0)\rangle}{\langle N(0)\rangle}\right)^{\frac{z}{2}} I_z\left(2\sqrt{\langle N(1\,|\,0)\rangle\langle N(0)\rangle}\right). \quad [3\text{-}22]$$

In the same manner the probability of error for the '1' bit is found to be

$$P(0\,|\,1)=\sum_{z=0}^{\infty} e^{-\left(\langle N(0|1)\rangle+\langle N(1)\rangle\right)}\left(\frac{\langle N(0\,|\,1)\rangle}{\langle N(1)\rangle}\right)^{\frac{z}{2}} I_z\left(2\sqrt{\langle N(0\,|\,1)\rangle\langle N(1)\rangle}\right). \quad [3\text{-}23]$$

The difference between the summation for the '1' bit error starting at $z=0$ and the '0' bit error starting at $z=1$ comes from an arbitrary decision to assign a tie in coincident counts as a '0' bit. The BER is again the average of these two error probabilities

$$BER=\frac{P(1\,|\,0)+P(0\,|\,1)}{2}.$$

[3-24]

The BER for a symmetric system with 10 signal pairs per bit, 6000 noise single photon counts per bit and a coincidence time of 1 ns, is $5.4\text{x}10^{-5}$. While the BER is significantly lower than the BER OOK system, the signal for this system is 3 dB higher than for the OOK system. If the signal levels are equal then the performance for the two systems is very similar. With the two-state system however, there is the added improvement of consistently optimal operation no matter what the noise level is. In contrast, with an OOK system the threshold level has to be dynamically set in order to achieve the optimal BER because of variations in ambient noise.

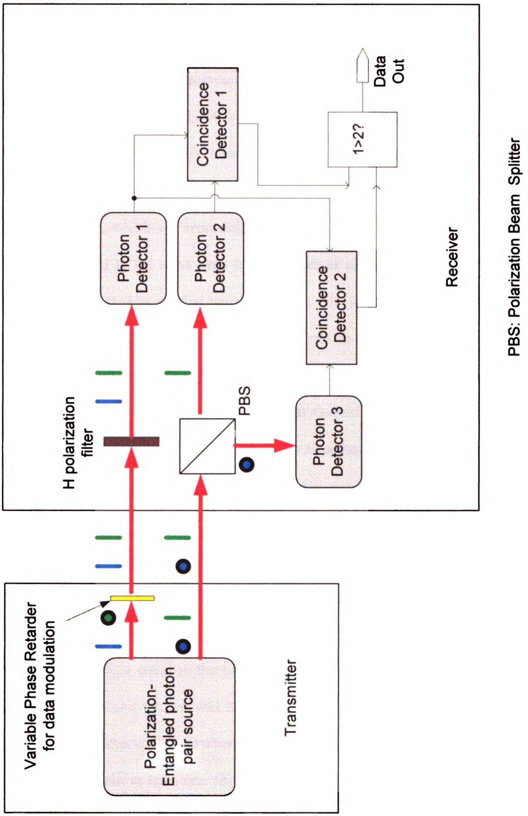

Figure 3.3: Block diagram of the two state system utilizing photons with an entangled state.

3.4 Bit Error Rate for time coincident communications

A time coincident photon communication system is shown as a block diagram in Figure 3.4. In this figure the details of how the beams are put together at the transmitter and likewise separated at the receiver are left out, to be included in later chapters of course, so that the basics of the signaling method can be understood. To transmit a one, photon source 1 and 2, which are separately identifiable by either wavelength, polarization or both, are pulsed at the same time to send pairs of photons to the receiver. A zero is likewise transmitted by pulsing sources 3 and 4. The sources will be pulsed several times during the bit period so that a significant count can be recorded at the receiver. The pairs are detected by photon detectors 1 and 2 for a 'one' and 3 and 4 for a 'zero' and, assuming they arrive at the same time, result in a coincidence detected by the coincidence detectors. The receiver compares the number of coincidences from coincidence detector 1 to coincidence detector 0 to determine the value of the bit.

The photons from pulsed photon sources are not definitely produced in pairs as they are with a QE source. They instead can be designed so that both sources produce an average of one or more photons per pulse. The probability of a pair being detected during a pulse time T_p is therefore equal to the product of the average counts at detector one and the probability a second photon will be counted by detector 2. The probability a second photon will be detected is a function of the quantum efficiency for detector 2, the ratio of pulses that contain at least one photon captured by detector 2 and also the ratio of the coincidence time to the pulse width. When a one is transmitted the average coincidences at the receiver due to photons from the sources one and two will therefore be

$$R_1 \frac{\alpha_2 R_2}{R_p} \frac{\delta t}{T_p}, \qquad [3\text{-}25]$$

where R_p is the pulse rate and T_p is the pulse width. This equation is valid for $T_p \geq \delta t$, otherwise $\delta t \ / \ T_p = 1$. When a second photon of a pulsed pair is missed another contributor to coincidences are due to a photon from one of the transmitters being detected in coincidence with a noise photon expressed by

$$\left[(1-\alpha_2) R_1 r_2 + (1-\alpha_1) R_2 r_1\right] \delta t \, T_s . \qquad [3\text{-}26]$$

The last contributor to coincidences is due to accidental coincidences from ambient photons expressed by $r_1 r_2 \delta t \, T_s$. Adding all these contributions gives the average number of coincidences detected by detectors 1 and 2 when a '1' is transmitted

$$\langle N(1) \rangle = R_1 \alpha_2 \frac{R_2}{R_p} \frac{\delta t}{T_p} T_s + \left[(1-\alpha_2) R_1 r_2 + (1-\alpha_1) R_2 r_1 + r_1 r_2\right] \delta t \, T_s . \qquad [3\text{-}27]$$

The noise that can contribute to a '1' being misinterpreted as a zero is only due to ambient photons being detected by detectors 3 and 4 and is

$$\langle N(0|1)\rangle = r_3\, r_4\, \delta t\, T_s . \qquad [3\text{-}28]$$

Because the data is coded in a symmetric fashion the equation for the average numbers of coincidence when a '0' is transmitted is the same as for a '1' only with photon counter 3 and 4 replacing the 1 and 2 subscripts

$$\langle N(0)\rangle = R_3\,\alpha_4 \frac{R_4}{R_p}\frac{\delta t}{T_p} T_s + \left[(1-\alpha_4)\,R_3\, r_4 + (1-\alpha_3)\,R_4 r_3 + r_3 r_4\right]\delta t\, T_s \qquad [3\text{-}29]$$

and likewise the equation for noise when a '0' is transmitted is

$$\langle N(1|0)\rangle = r_1\, r_2\, \delta t\, T_s . \qquad [3\text{-}30]$$

The probability for an error when a 1 is transmitted is, as with the symmetric QE two state coding,

$$P(0\,|\,1) = P\,[N(1) > N(0\,|\,1)] \qquad [3\text{-}31]$$

and likewise the probability for an error with a zero is

$$P(1\,|\,0) = P\,[N(0) < N(1\,|\,0)] . \qquad [3\text{-}32]$$

These error probabilities have the same solution as the previous section with only the average values for the number of coincidences being different. This leads to a BER which is an average of these two error probabilities.

It should be noted that the performance of the two coincident channel system with data encoded by on-off keying can be predicted using several of the previous equations. In the two channel case $<N_1>$ is still calculated using Equation [3-27] and $<N_0>$ is calculated by equation [3-30] with $<N_0>$ replacing the $<N(1|0)>$.. The error probability equations for this system are the same as they are for the QE based system so Equations [3-11] and [3-12] are used to calculate the probability of error. The BER is again the average of these two error probabilities.

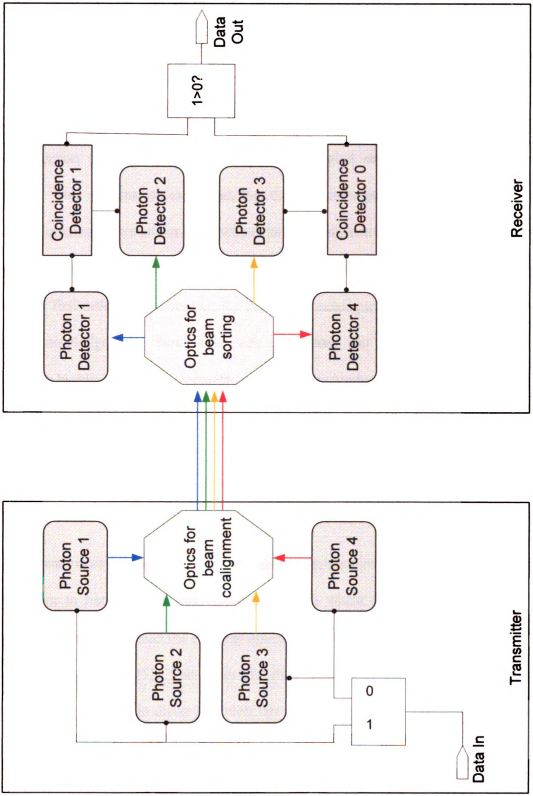

Figure 3.4: A time coincident photon communication system made from classical sources.

3.5. Theory for time coincident photon communication range

In this section the signal intensity as a function of range is considered for optical communication systems that utilize quantum entangled sets photons for information encoding. Two systems are examined, one that generates pairs of photons that have an entangled quantum state and another where the pairs of photons are generated from a pair of pulsed photon sources. The signal intensity as a function of range is analyzed as a qualitative first order approximation for these two techniques. For the first time, to this author's knowledge, it is shown that pairs of photons that share a quantum state, and hence have highly correlated momenta, can produce communication systems that have a high degree of noise immunity and are viable for ranges significantly beyond the collimated range of the transmitter, which up until now is considered the maximum range.

Optical communications systems utilizing time coincident pairs, or sets, of photons have been shown to have great utility in circumstances where the transmitted signal is of significantly less power than the ambient optical environment [Mandel 1984, Hong 1985, Jackson 2002, Lekki 2005]. Two cases that illustrate this are for optical communication where the transmitter is in direct line with the sun and also for a very low power optical transmitter operating in sunlight.

3.5.1 Communication Range for Quantum Entangled source system

Time coincident photon signals can be generated through Spontaneous Parametric Down Conversion (SPDC) or by simply pulsing two photon sources at the same time [Kwiat 1995, Takeuchi 2001]. In the case of SPDC a photon from a pump beam passing through an appropriate nonlinear crystal can down convert into two photons that meet the conservation of energy and momentum criteria

$$\omega_p = \omega_s + \omega_i, \qquad [3\text{-}33]$$

$$\boldsymbol{k}_p = \boldsymbol{k}_s + \boldsymbol{k}_i, \qquad [3\text{-}34]$$

where $\omega_{p,s,i}$ the frequency and $\boldsymbol{k}_{p,s,i}$ is the wave-vector for the pump, signal and idler photons. It should be noted that the pump, signal and idler photons have a bandwidth so that equation 1 can be expressed

$$\left(\omega_{p0} \pm \Delta\omega_p\right) = \left(\omega_{s0} \pm \Delta\omega_s\right) + \left(\omega_{i0} \pm \Delta\omega_i\right), \qquad [3\text{-}35]$$

where $\omega_{p0,s0,i0}$ are the average frequencies and $\Delta\omega_{p,s,i}$ are the bandwidths for the pump, signal and idler beams. For the purposes of communication, the crystal and pump beam can be selected so that the down converted photons are collinear or the down converted beams can be combined using a geometrically symmetric optical system.

The second way to generate the set of photons is to pulse a pair of single photon sources at the same time and use a geometrically symmetric optical system to combine the two beams into one. Both of these techniques will generate a signal that will be recognizable at signal power levels significantly below the ambient noise and, at short ranges, have nearly identical signal to noise ratios. In this second case, the photon pair signal can be generated using significantly less power than in the first case, because pulsing two micro sized photon sources is very energy efficient whereas generating SPDC photon pairs is a very power inefficient non linear process.

At the distance where the signal beam diameter starts to spread to be larger than the receiver aperture, R_s, however these two communication techniques are not equivalent. In the first case the entangled photons are highly correlated by momentum, and therefore the probability that a photon pair will be detected is a conditional probability relationship between each of the probabilities the receiver will capture each individual photon (P_n) of the pair

$$P_C = P_1 \cap P_2 = (P_1 \mid P_2)(P_2). \qquad [3\text{-}36]$$

The relationship between the two momentum entangled position probabilities is shown in Figure 3.5. In this figure an example is illustrated where a pump beam with a Gaussian intensity distribution generates two down converted quantum entangled beams that also have Gaussian distributions which represent the photon positional probability distributions. The down conversion depicted here is for a nonlinear crystal that has good phase matching, which produces nearly degenerate signal and idler beams with momentum vectors that have opposite components of equal magnitude that are perpendicular to the pump beam momentum vector. For clarity of the diagram the nonlinear crystal that is in the **x** plane is not shown. A single line is shown in the pump intensity distribution to denote an arbitrary point in **x** where a pump photon down converts into a signal – idler photon pair. In these conditions, this pair of photons will have highly correlated angles relative to the momentum of the pump photon they were created from [Abouraddy 2001, Friberg 1985, Pittman 1995]. The momentum uncertainty of the pump photon will translate into an uncertainty of the nominal center of the signal and idler pair, but does not affect the relative momentums of the signal and idler to each other.

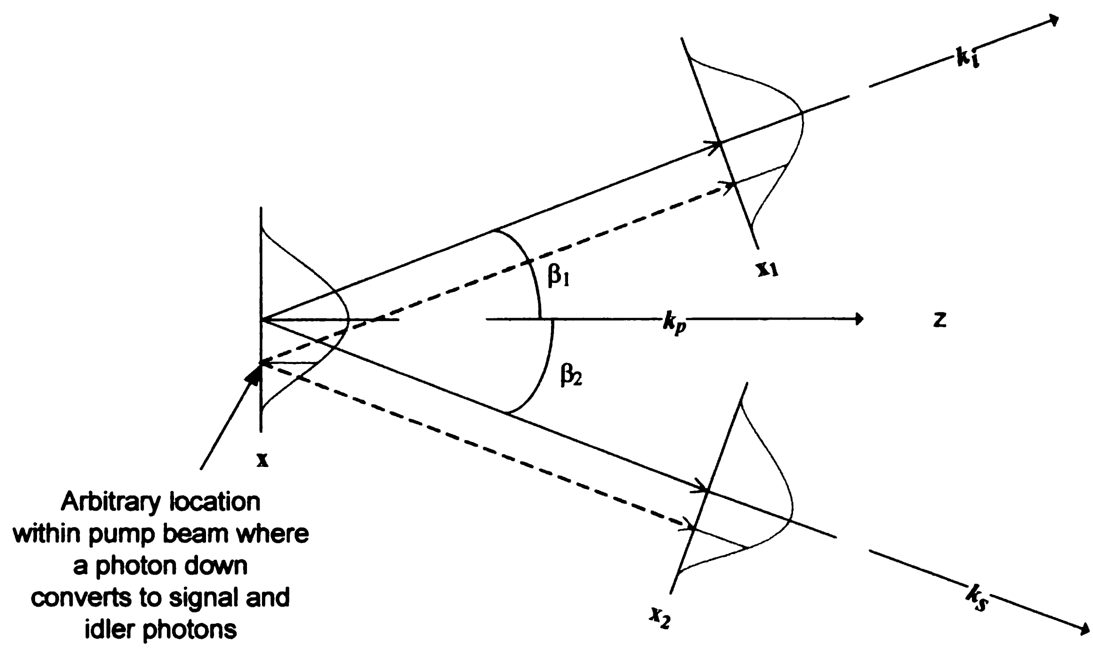

Figure 3.5: Drawing of Spontaneous Parametric Down Conversion of a pump beam (Plane X) with a Gaussian intensity distribution and wave-vector k_p into signal and

idler beams (Planes X_1, X_2) with Gaussian photon positional probability distributions and wave-vectors k_s and k_i.

The relative momentum of the photon pair dictates the conditional probability of capture by a receiver and is derived here. The difference in relative momentum between the two down converted photons is derived from bandwidth of the photons. In degenerate down conversion the signal and idler beams are the same center frequency, denoted by ω_0. If the down converted photons are filtered at the output by a narrow bandpass filter they will have the same bandwidth as the filter denoted $\Delta\omega_{bp}$, which represents the Full Width Half Maximum (FWHM) bandwidth of the filter. In the following calculations the derivation of the range at which the combined degenerate signal and idler photons remain close spatially is developed. In order to develop a bounding equation, two new frequencies will be introduced, ω_1 and ω_2, that represent the lower and upper bounds of the signal and idler frequencies so that

$$\omega_1 = \omega_0 - \Delta\omega_{bp} \quad and \quad \omega_2 = \omega_0 + \Delta\omega_{bp}. \qquad [3\text{-}37]$$

This bandwidth definition for ω_1 and ω_2 is used so that a large percentage of the transmitted photons have frequency differences smaller than the ω_1 and ω_2 difference. If the filter is approximated as Gaussian then the difference of 2 times the FWHM between ω_1 and ω_2 translates to a bounding of well over 90% of the photons. The angles of the signal and idler photons $\beta_{1,2}$ will vary slightly depending upon the range of photon frequencies, ω, and is determined by the following relationship

$$\omega_1 \sin \beta_1 = \omega_2 \sin \beta_2 . \qquad [3\text{-}38]$$

By using the bounding frequencies the largest angles, and hence the greatest spatial separation, will be identified. From this relationship, and the illustration of the recombination of the signal and idler beams shown in Figure 3.6, it is apparent that the maximum transverse distance d_r between the two photons as a function of the propagation distance, R, is

$$d_r = (\sin \beta_1 - \sin \beta_2)\, R . \qquad [3\text{-}39]$$

The situation of most interest is to determine the range at which the detection of a second photon given the detection of one photon is nearly unity. This range, R_u, derived from Equations [3-38] and [3-39] is approximately the range in which the pair of photons are separated by less than half the receiver aperture diameter A_r.

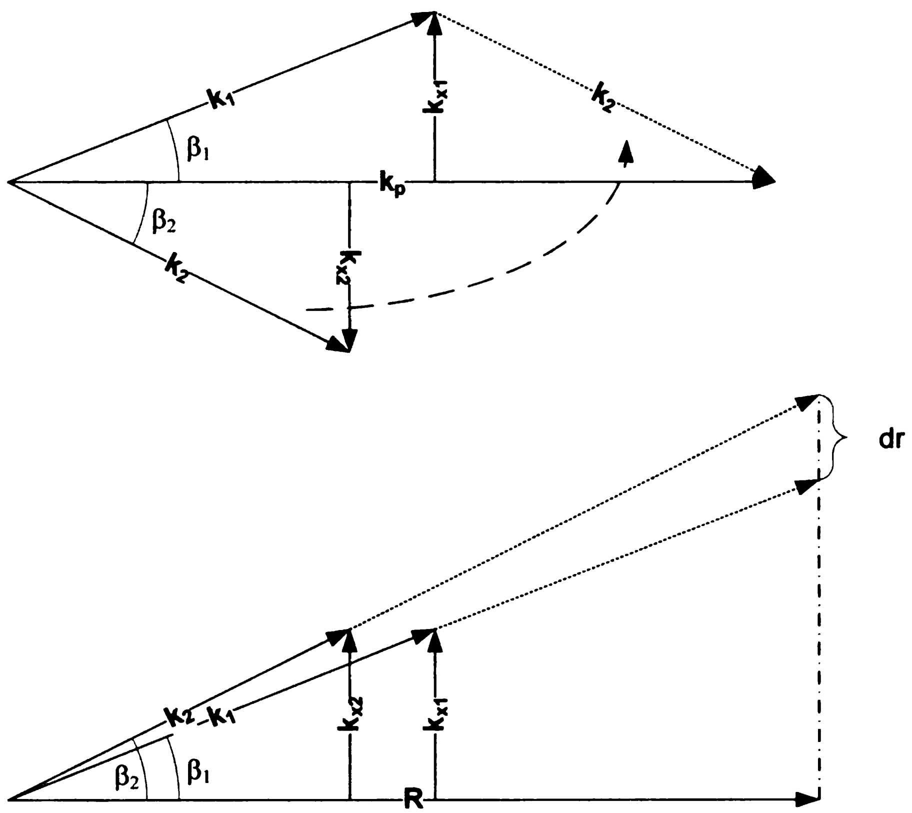

Figure 3.6: The top portion of this figure shows how the down converted photon vectors are linked so that momentum is conserved in down conversion. The bottom portion illustrates how the geometrically recombined beams will have differing angles when the magnitude of momentum is not equivalent between the two photons.

The derivation of R_u begins with a substituting for *sin* β_1 from Equation [3-38] into Equation [3-39] and also replacing the photon separation distance d_r with the aperture diameter A_r to obtain

$$A_r = (\frac{\omega_2}{\omega_1} \sin \beta_2 - \sin \beta_2)\, R_u. \qquad [3\text{-}40]$$

By solving for R_u the equation becomes

$$R_u = \frac{A_r\, \omega_1}{(\omega_2 - \omega_1)\sin\beta_2}, \qquad [3\text{-}41]$$

and recognizing that ω_1 subtracted from ω_2 is equal to $2\Delta\omega_{bp}$ simplifies the equation to

$$R_u = \frac{A_r\, \omega_1}{2\Delta\omega_{bp}\sin\beta_2}. \qquad [3\text{-}42]$$

This can also be expressed in terms of wavelength

$$R_u = \frac{A_r\, \lambda_1}{2\,\Delta\lambda_{bp}\sin\beta_1}. \qquad [3\text{-}43]$$

Note that the different beta subscripts in these two equations come from the inverse relationship of wavelength and frequency and also the ratio of photon frequencies and angles in Equation [3-38].

The probability P_n of a transmitted photon being captured by the receiver in an ideal case, where there are no losses due to scattering etc. and the quantum efficiency of the detector is unity, is only a function of beam spreading given a fixed receiver aperture. At a range where the transmitted beam expands to a diameter larger than the receiver aperture the photon capture probabilities for each beam, $P_{1,2}$, are proportional to $1/R^2$ [Siegman 1986].

If the beams have been symmetrically co-aligned and the distance between the transmitter and receiver is less than R_u then the conditional probability for a photon pair being detected is unity (or more exactly greater than 90%), because of the momentum correlation [Friberg 1985]. This reduces the coincidence probability to $P_c = P_2$. Thus the coincidence probability of quantum entangled, momentum correlated photons is simply reduced to the probability of a limited aperture capturing a photon in an angularly diverging spherical wave, which is a probability proportional to $1/R^2$ for $R < R_u$. This result, incidentally, is the same proportion for signal intensity as a function of range for classical optical communication.

3.5.2 Range of time coincident photon communication

The effective range for the second case, where two separate sources are used to generate the time coincident photons, is much more limited. For two separate photons, with Gaussian positional probability distributions that have been collinearly combined, there is no position correlation between one photon generated in one beam and the second photon of the pair generated in the second beam. Therefore the probability of capturing a photon pair in the aperture of the receiver is a function of two independent probabilities, one corresponding to each source. The probability of the individual photons being captured by the receiver again is proportional to $1/R^2$ when the photon probability distribution is larger than the receiver aperture. The probability of coincident photon capture at large distances is

$$P_c = P_1 P_2 \approx \frac{1}{R^4} \qquad [3\text{-}44]$$

which significantly limits the range of this type of transmitter. In Figure 3.7 the manner in which the quantum entangled source and the two independent sources fall off as a function of range is summarized.

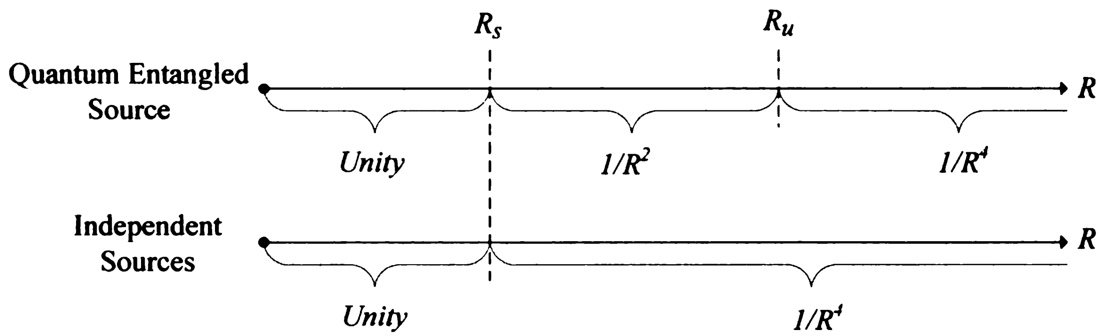

Figure 3.7: In this figure the fall off of the two different signaling sources are compared as a function of range *R*. Both sources have near unity while the beams are collimated. After the range at which the beams begin to spread, R_s, the two independent sources fall off at $1/R^4$ while the entangled photon source falls off at $1/R^2$ until the photon pairs begin to separate significantly at the range R_u.

3.6 Range Comparison

To further illustrate the difference between these two techniques these ranges can be calculated for a case where a transmitter and receiver both have 1 meter optical apertures and are utilizing a wavelength of 1500nm. In this case the range at which the receiver captures nearly 100 percent, R_S, of the transmitted photons can be approximated as the collimated range $[A_r^2/(\pi\lambda)]$ [Siegman 1986]. This range, where there is essentially no signal loss, is therefore about 212 km. In the case of two independent sources the signal falls off at $1/R^4$ beyond this range and therefore this represents a nominal effective range for this technique.

In the case of the quantum entangled photons β_l must be calculated to determine the range, R_u, at which the probability of photon pair capture will fall off in proportion to $1/R^2$. This angle is determined by the type of nonlinear crystal used, the cut angle of the crystal and the tuning angle of the pump beam relative to the input face of the nonlinear crystal. This calculation is well covered in the literature so it is not included here [Dmitriev 1999].

The effect of the collimating transmitting optics, illustrated in Figure 3.8, must also be accounted for. The angle β_n is reduced because of the beam diameter magnification. Also, because the photons separate in the distance between where they are created and where they enter the collimating optics another parameter is included, represented by d_0, that accounts the initial lateral separation of the photon pair. This separation is increased by the subsequent magnification of the beam diameter by the collimating optics and so this magnification of d_0 must be included in the calculation.

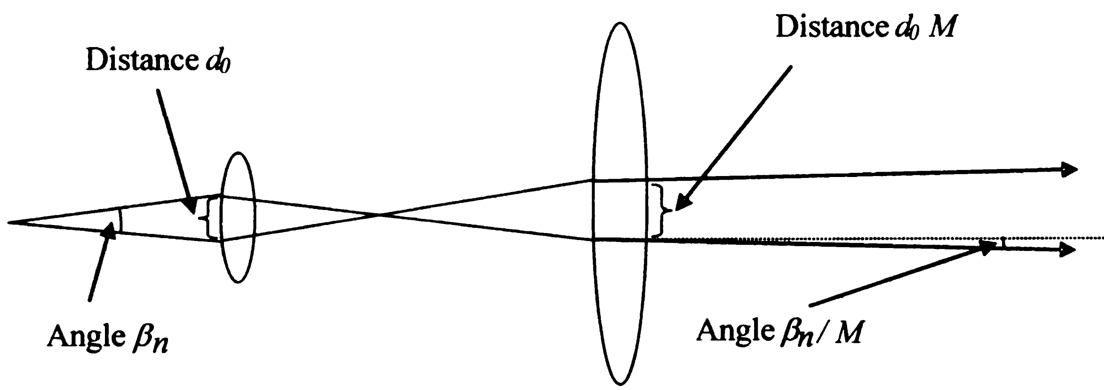

Figure 3.8: An illustration of the affect that collimating optics has on the photon pair system. The angles and lateral distances are exaggerated for illustrative purposes.

These parameters associated with the collimating optics will modify Equation [3-43] in the following manner

$$R_u = \frac{(\frac{A_r}{2} - d_0 M)\lambda_1}{\Delta\lambda_{bp} \sin\frac{\beta_1}{M}}, \qquad [3\text{-}45]$$

where M is the magnification of the beam diameter. To perform this calculation the following parameters are assumed: λ_p is 1500 nm, $\Delta\lambda$ is 1 nm, β_n is 2 mrad, and M is 200. It should be noted that the wavelength bandwidth is a very significant parameter. If the bandwidth were smaller the range would be increased but the number of photons generated would likewise decrease and it should be noted that the system still has a $1/R^2$ loss to overcome between $R_s < R < R_u$. The selection of 1 nm is a reasonable trade off between the loss of transmitted photons from making the bandwidth smaller and the probability that a photon counting receiver will be saturated by making the bandwidth larger. If the nonlinear crystal is fairly close to the beam expansion optics, ~10 cm, then the maximum separation of the entangled photons d_0 is 0.2 mm. With these parameters R_u is 69,000 km which gives the momentum correlated photons an effective range that is 325 times that of the photon pair that does not have a momentum correlation.

In summary, the two sources of correlated photons have been discussed. The first source, generating momentum correlated pairs of photons, has application at significantly greater ranges than the second source, which consists of two independently pulsed photon sources. The momentum correlated source is very energy inefficient and so it should only be considered for longer ranges. It should be noted that the energy efficiency of these sources has improved significantly in the last 15 years but more improvement is necessary for a source to be used in this application. The second source can be made to be energy efficient but has a range effectively limited to the distance where the transmitted beams diverge to become larger than the receiver's aperture. The first source has a range that makes it usable for intra orbit or ground to orbit communications. The second source should be considered only for ranges of less than 200 to 1000 km, depending on wavelength.

3.7 **Summary**

In this chapter the supporting mathematics for the contrast gain and the BER has been developed for the multiple configurations of time coincident photon communications. The different configurations addressed included a summary of the on/off communications system developed by Hong and the two state QE photon communications developed as a part of this dissertation to improve signal to noise ratio. The BER for the electronic photon pair system has also been described. This system is included because it has very good potential for very power efficient communication. Also the range for QE photon source and electronic photon pair source has been developed. Here it has been found that the effective range of the QE based system can be significantly greater than the electronic pair system. This is because the momentum correlation of the QE photons can be used to generate a positional correlation that increases the range at which photon pairs fall off a rate equivalent to classical optical communications.

CHAPTER 4

EXPERIMENTAL SETUP FOR QUANTUM ENTANGLED PHOTON COMMUNICATION

4.1 Introduction

In this chapter experimental setup for a two-state communications system based on Quantum Entangled (QE) photons is presented. This system exploits the temporal coincidence property of quantum-entangled photons to communicate at power levels several orders of magnitude less than what is currently achievable through classical means. Quantum entangled photons are studied here because there are multiple benefits, such as the photons are always generated at very close to the same time, within picoseconds, and also there are advantages to utilizing entangled photons at longer ranges. As shown in Chapter 3, a system based on QE photons can have a effective range that is hundreds of times greater than a system based on coincidentally pulsed sources. The main disadvantage to utilizing quantum entangled photons is that there is no known way to generate the photon pairs efficiently. The low efficiency to generate the signal is a significant drawback but the other advantages coupled with the potential that the efficiency may be increased, makes this a technique that deserves continued attention.

4.2 Concept

In this experiment pairs of polarization entangled photons are generated and transmitted to the receiver over two beams of light that are on-off keyed with the data. The receiver detectors can detect individual photon arrivals. The coincidence detector circuit produces a pulse when a pair of photons triggers detectors 1 and 2 in temporal coincidence. If there is no signal present, ambient light incident on the detectors will produce what are called *accidental coincidences* at a rate

$$R_a = R_1 R_2 \tau \qquad [4\text{-}1]$$

where R_1 and R_2 are the detector 1 and detector 2 count rates, in photons/s, and τ is the two-sided coincidence window size in seconds. By making the coincidence window time smaller, the rate of accidental coincidences from ambient light can be made to be much smaller than the rate of coincidences due to the arrival of entangled photon pairs, which are inherently coincident. In general, more than one set of entangled photons will be transmitted during a bit period. Bit value decisions can be made by comparing the number of coincidences per data bit duration to a threshold value. This process results in a relatively high detector output SNR from a very small detector input SNR, making reliable communications possible where classical detectors would be swamped by the presence of ambient light.

4.3 Experimental Setup

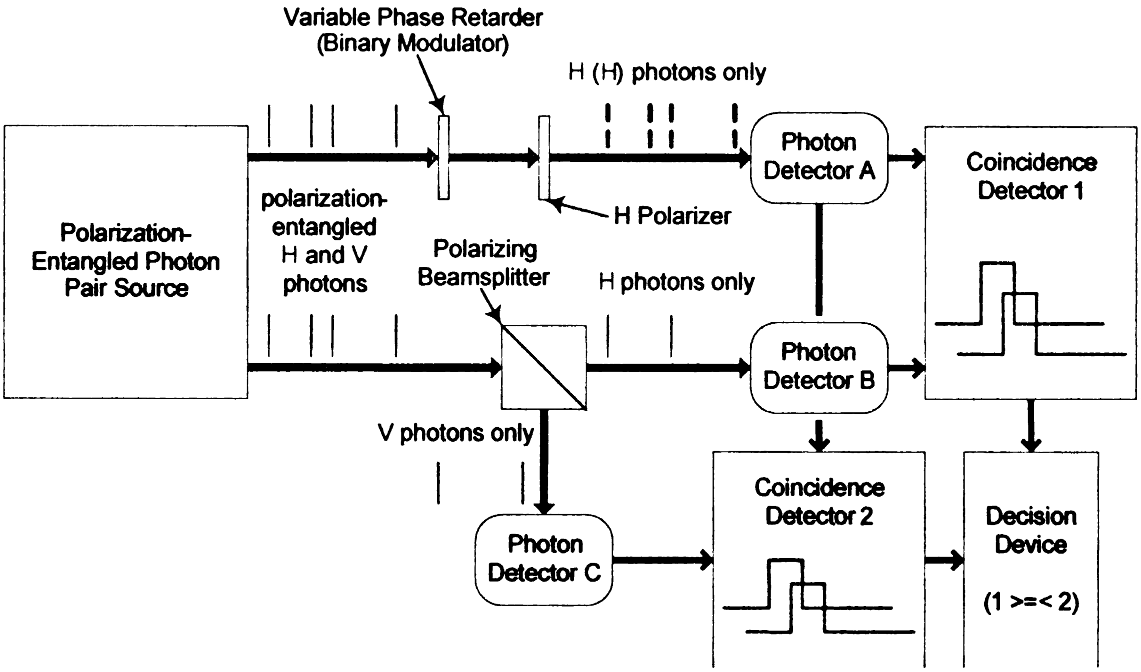

Figure 4.1: Quantum Entangled Photon Communicator Block Diagram

The block diagram for the advanced version of the quantum communicator is shown in Figure 4.1. In contrast to the system demonstrated by Hong et al. [Hong 1985], which encoded information through on/off keying, this system encodes information with two symmetric entanglement states. Figure 4.1 shows the block diagram of the architecture of the two-state implementation. The optical source consists of a UV laser-pumped spontaneous parametric down conversion (SPDC) entangled photon source which generates two beams of light with identical, but random polarizations. For the receiver, photon detectors A and B are set to detect only H photons whereas detector C is set to detect only V photons through the use of a polarizing filter and polarizing beam splitter, as shown in Figure 4.1. Binary data modulates a variable phase retarder, keeping H and V photons intact under state "1," and changing H photons into V, and V photons into H under state "0." As a result, photon detectors A and B trigger H photon coincidences in coincidence detector 1 when state "1" is transmitted, and detectors A and C trigger V photon coincidences in coincidence detector 2 when state "0" is transmitted. Decisions are made by comparing the number of coincidences per data bit from the two coincidence detectors. If coincidence detector 1 count is greater than coincidence detector 2 count then the receiver records a "1;" if not the receiver records a "0". As in the conceptual system, accidental coincidences due to ambient light and un-entangled photons from the laser source are expected to be much smaller than signal coincidences, affording reliable communications under very low SNR.

The experimental implementation of the above architecture is schematically shown in Figure 4.2. Here, the beam from a 351 nm (< 150 mW) single-frequency argon-ion laser is first spectrally filtered using a UV dispersing prism (not shown), and then passes through a UV dielectric polarizing beam-splitter cube to produce a pump beam with better than 1000:1 polarization purity. A zero-order quartz half-wave plate sets the polarization state of the beam to 45 degrees prior to passing through two thin (0.69 mm), optically contacted, orthogonally-aligned, Type-I beta Barium Borate (BBO) crystals to generate the SPDC light. Due to the 45 degree orientation of the polarization state of the pump beam, it then has an equal probability of producing either a HH or VV SPDC photon pair from either crystal. Thus, the photon pairs emitted from this source have identical but random (in time) polarizations, constituting an efficient hyper-entangled photon source as first described by Kwiat et al. [Kwiat 1999]. Similar setups have also been previously described to use blue diode pumped twin BBO crystals with good success [Dehlinger 2002]. The SPDC photons are emitted in a cone, with entangled photons arranged diametrically along the cone. By selecting a fraction of the cone emission using apertures, two beams of hyper-entangled photons are created. Although the photons are hyper-entangled, only utilize the polarization properties of the photons in this report. One of the beams then passes through a digital logic controllable liquid crystal phase modulator set to act as a bi-state half-wave plate (0 or $\lambda/2$) which encodes information onto the beam via polarization rotation (either H or V). The beam then passes through a polarizing beam splitter analyzer, and is filtered using a bandpass filter centered at 702 nm (2 nm FWHM) before being focused with a 75 mm focal length lens onto the active area of a single-photon counting module (SPCM) consisting of a thermo-electrically-cooled (TEC), actively quenched, avalanche photodiode (APD) operated in a Geiger mode (Perkin Elmer SPCM-AQR-13). These detectors have an approximate 60% quantum efficiency at 700 nm and a 50 ns dead-time between pulses, with < 250 dark counts/s. In the Detector B & C beam path, similar optical components are used with the exception of the polarizing beam-splitter analyzer which acts as polarization state sorter. Detectors B & C use band pass filters centered at 702 nm but with a 5 nm FWHM.

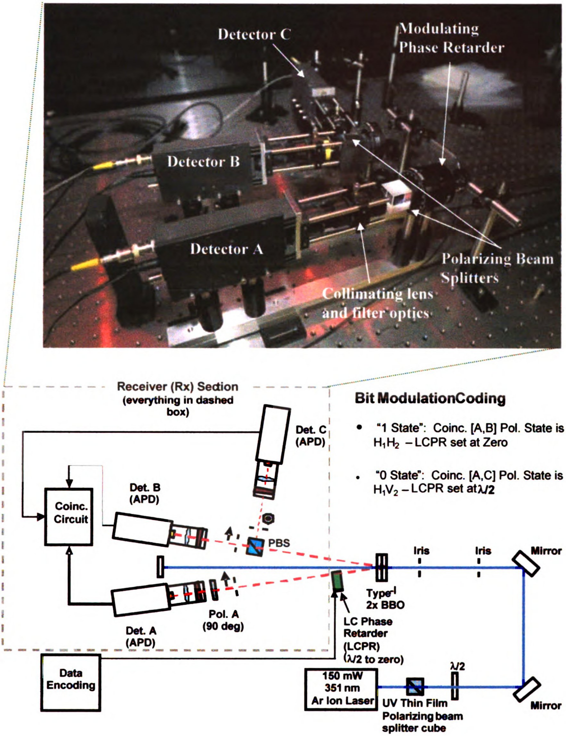

Figure 4.2: Schematic of Quantum Communication System with a picture of the experimental setup

The photon arrivals at the detectors produce TTL logic signals that are resolved to within 350 ps and are coincidence-gated using discrete CAMAC logic modules to produce a 6.5 ns coincidence window. The coincidence pulses are then counted using two photon counters controlled by a PC running a custom developed LabView software interface. The whole apparatus is contained within a light-tight enclosure with black walls. In order to simulate an ambient light source, an array of individually selectable incandescent light bulbs (typical 60 W, 120 VAC) was placed above the system *inside* the enclosure. The amount of background light is controlled by turning on various combinations of three red and one white light bulbs, and a variable intensity fiber optic light source aimed at a white cardboard diffuser placed around the BBO crystal housing. After careful alignment of the optical system, typical single photon rates from the BBO crystal were in the 250,000 counts/sec range for 60 mW of laser pump power.

In order to determine the bit-error rate (BER) performance of the GRC Quantum Communicator, custom software on National Instruments LabView 7.0 platform was developed for generating, transmitting and receiving pseudorandom data sequences (Figure 4.3). The software interfaces with two Dual Channel Gated Photon Counters connected to coincidence detectors and photon detectors, controls the variable phase retarder (modulator) and also therefore handles the synchronization of data transmission and reception. With this set-up, the BER for any data rate with varying laser power and background light intensity is determined. The software collects statistics and full histogram data from individual photon detectors and coincidence counters, and determines BER within any desired confidence level and interval.

The data transmission is real-time and the data rate is determined as the reciprocal of the counting time allocated for each data bit. This is due to the 5 to 20-ms switching time required by the liquid crystal variable phase retarder used for modulation. In fact, the major contributor to the detection error in the laboratory setup is this particular modulator, as will be discussed in the experimental analysis in Chapter 5.

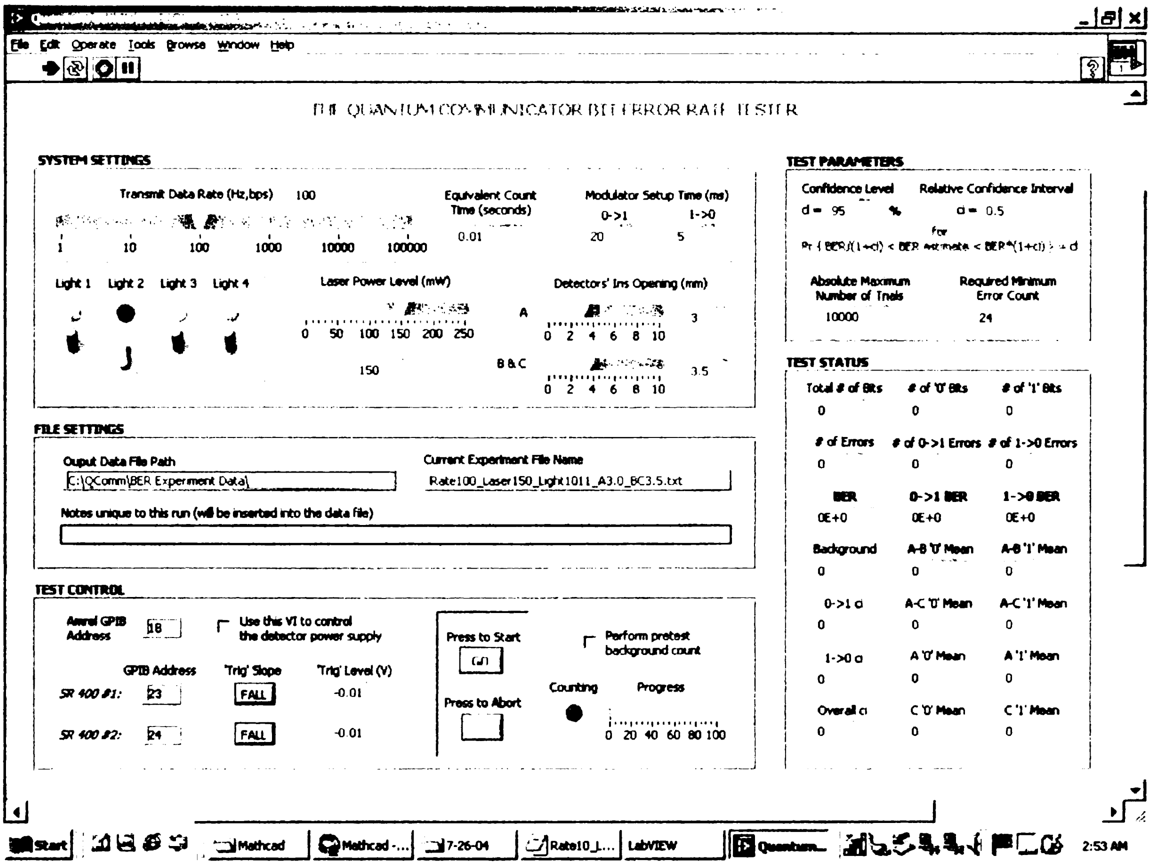

Figure 4.3: GRC Quantum Communicator BER Tester interface.

4.4 Summary

In this chapter the system concept for a two-state communication system based on quantum entangled photons is presented. This system utilizes a pump laser with a nonlinear crystal that generates quantum entangled photons through spontaneous parametric down conversion. Information is encoded by rotating the polarization of one of the entangled photons so that the entangled photons are either both horizontally polarized for a '1' bit or one is horizontally and the other vertically polarized for a '0' bit. The receiver consists of three detectors, which are photon counting avalanche photodiodes, as well as a coincidence circuit to determine when photons are detected within the coincidence time. The advantage of this system is that it always operates at an optimal bit error rate for given ambient light conditions. This is because in contrast to OOK, the two-state method does not require a threshold level to determine bit values. With OOK systems the threshold level has to be dynamically set, based on ambient light conditions, in order to minimize the bit error rate. A two-state system always operates at the optimal bit error rate for a given set of conditions because the bit value is determined by comparing the coincidence counts of one state to the other and assigning a bit value to whichever state is higher for that bit. This simplifies the receiver operation in an environment which has dynamic ambient light levels, which includes just about all natural environments.

CHAPTER 5

EXPERIMENTAL RESULTS AND DISCUSSION FOR QUANTUM ENTANGLED PHOTON COMMUNICATION

5.1 Introduction

The two-state communication system based on Quantum Entangled (QE) photons was described in Chapter 4. The tests that were conducted on this system and experimental results are discussed in this chapter. Several tests were conducted and the experimental data is compared to values that were calculated from the mathematical formulae for this system in Chapter 3. There were some limitations to the modulator used in this system as has been described in Chapter 4. These limitations are examined more closely in this chapter and so some predictions of how the system would perform with an improved modulator are presented at the end of this chapter.

5.2 Experimental Results

Numerous tests have been conducted with varying data rates, laser intensities, background light levels, coincidence window sizes, modulator setup times, optical aperture settings and various other parameters. In Figures 5.1 and 5.2, representative BER results are plotted for data rates of 10, 30, 100, 300 and 1000 bps at laser source power levels of 3, 5, 10, 30, 50 and 100 mW and two-sided coincidence window size of 3.5 ns in the presence of two extreme background light intensities. Figure 5.1 shows the

BER plots in the presence of minimal background light, corresponding to approximately 900 photons/s total detected on the three photon detectors, whereas Figure 5.2 shows the same plots in the presence of maximum background light, corresponding to approximately 250,000 photons/s total.

It can be immediately observed from Figures 5.1 and 5.2 that there is very little difference in BER performance, especially for higher data rates, between the case with minimal background light intensity and that with maximum background light intensity. This is due to the relatively small size of the coincidence window that results in approximately 20 accidental coincidences per second under maximum light and almost none under minimal light. If the per-bit coincidences are considered, the comparative detrimental effect of the two different background light intensities becomes relatively insignificant, especially at higher data rates. The effect of background light can be diminished even further by the use of smaller coincidence window sizes.

Another interesting observation is the relatively poor performance of the system at higher data rates. Worse performance at higher data rates is expected since, for any given laser power level, average coincidences per second will stay fixed but average coincidences per data bit will decrease with increasing data rate. This closes the gap between the '1' state and the '0' state in terms of the Poisson mean coincidence rate per bit, resulting in higher error probabilities. However, the degradation in BER performance was found to be much worse than what the theory predicted. This can be attributed to the less-than-perfect modulator that was used in the laboratory setup and this will be further discussed later in this chapter.

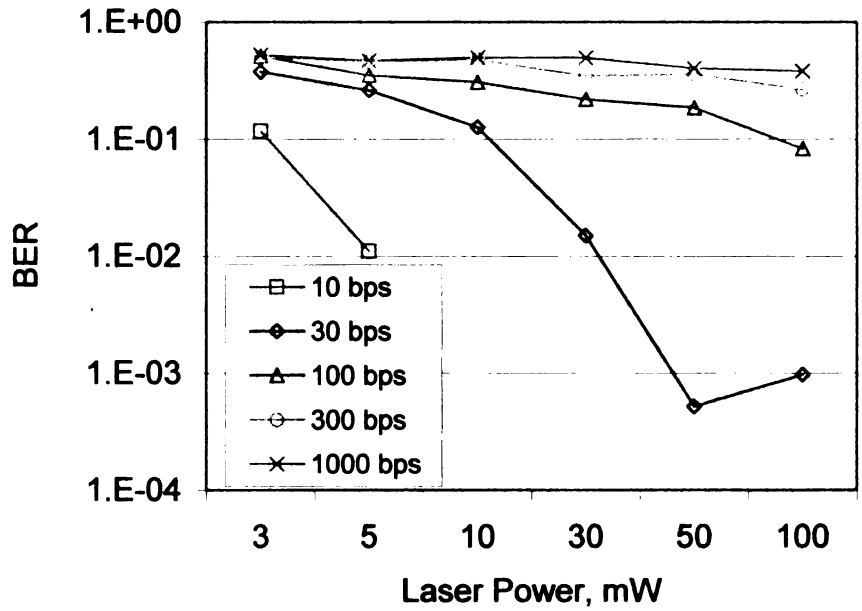

Figure 5.1: BER with minimal background light

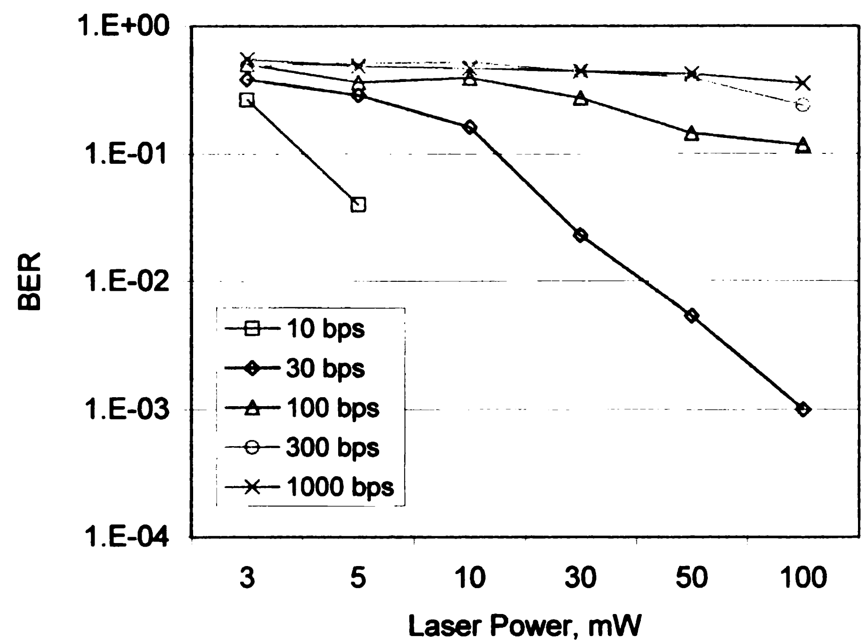

Figure 5.2: BER with maximum background light

The liquid crystal variable phase retarder used for the modulator requires a finite setup time, on the order of 5 to 20 ms, in order to completely switch states. As explained earlier, this was accounted for in the BER test procedure. However, even after significantly increasing the setup time, it was found that the phase retarder frequently failed to completely switch states; more so at higher data rates. Table 5.1 displays the average coincidence detector counts per second accumulated during the BER tests for various data rates at a 30-mW laser source power in the presence of minimal background light. It can be observed from this table that the ratio of transmitted state to opposite state (contrast ratio) coincidence counts drops from about six at 10 bps to about one or two at 1000 bps, while the total counts stay reasonably fixed for each detector. These ratios would stay virtually fixed for a perfect modulator. Obviously, the dropping ratios significantly affect the BER performance by severely degrading the separation between the two states. It is also observed from Table 1 that at higher data rates, the modulator somewhat prefers the "0" state, as evidenced by the slight increase in ratio for the AC coincidence detector counts at 300 bps to 1000 bps. Table 5.2 displays the detector counts per second under steady state for various laser power levels in the presence of minimal background light. This data shows that in the steady state condition, the contrast ratios (AC:AB for the '0' state and AB:AC for the '1' state), are very good, generally ranging from 24 to 68. This demonstrates that by using an improved polarization modulator, a significantly improved BER performance would be expected.

Table 5.1: Test average coincidence detector counts per second at 30 mW laser power in the presence of minimal background light

Data Rate, bps	AB counts per second				AC counts per second			
	AB | "0"	AB | "1"	AB Total	1:0 Contrast Ratio	AC | "0"	AC | "1"	AC Total	0:1 Contrast Ratio
10	99	612	711	6.2	607	113	720	5.4
30	180	464	624	2.6	464	188	652	2.5
100	257	456	712	1.8	433	268	701	1.6
300	282	423	705	1.5	372	234	606	1.6
1000	350	390	740	1.1	500	270	770	1.9

Another source of inefficiency in the laboratory setup is the generation of coincident photons through the use of parametric down conversion. Because of this inherent disadvantage, a relatively large laser source power was used in order to obtain a very small number of coincident photons per second. The actual received energy may be calculated by using the formula

$$E_r = \frac{h \cdot c}{\lambda} N \qquad [5\text{-}1]$$

where h is Planck's constant, c is the speed of light, λ is the wavelength of the light source (7.02×10^{-11} m), and N is the photon count. In order to gain a better understanding of the actual energy levels involved, the plots in Figure 5.1 were recalculated as a function of *received energy per bit* using the data from Table 5.2, where the received energy per bit is determined by the average total number of photons received per bit on detectors A, B and C. Figure 5.3 shows the BER plots as a function of received energy (Joules) per bit in the presence of minimal background light. It is observed from Figure 5.3 that reliable communication is possible, with the addition of error correction coding when necessary, at remarkably low received energy levels on the order of a picoJoule per bit. It can also be seen from this figure that, when normalized with respect to received energy per bit, performance differences among different data rates become insignificant, especially considering the possible use of an improved phase modulator.

Table 5.2: Steady-state detector counts per second in the presence of minimal background light

Laser Power (mW)	State "0" counts per second					State "1" counts per second				
	A	B	C	AB	AC	A	B	C	AB	AC
3	1530	880	1230	1	24	2140	910	2150	24	0
5	4300	2620	2950	2	100	5250	2530	3000	110	1
10	9500	6000	6200	5	220	11000	5900	6200	260	1
30	31000	18100	15000	23	740	32500	17900	17200	760	9
50	44000	28000	24400	40	1250	40000	28000	27800	1375	20
100	94000	57200	55100	85	2540	97400	56000	59500	2750	46

In order to visualize the effect of background light, the plot in Figure 5.2 is recalculated as a function of *optical signal-to-noise ratio* (SNR), where the data from Table 5.2 is used for the average total number of photons received per second on detectors A, B and C, and a background average total count of 250,000 photons/s, corresponding to the maximum light setting, is used. The sum of the singles from Table 5.2 is proportional to the signal power and the background average total count is proportional to the noise power. Figure 5.4(A) shows the BER plots as a function of this SNR in the presence of maximum background light. It can be observed from Figure 5.4(A) that reliable communication is possible at very low optical signal-to-noise ratio levels.

The singles in Table 5.2 are in effect mostly noise. In the calculation for Figure 5.4(A) all of the singles registered from Table 5.2 have been counted as signal because they are generated by the signaling device. However, most of these single photons are not detected in pairs, and therefore appear as noise to the receiver, even though they are generated by the signaling device. These photons are not detected in pairs because, due to slight misalignment, the three detectors are seeing slightly different spatial portions of the quantum entangled light. To illustrate how low the signal level is, the ratio of coincident photons to single photons have been calculated, where the single photons are those that are from both the background light and the uncorrelated singles from the quantum entangled light. In the instance where the pump laser is at 30 mW this correlates to an SNR of -5.8 dB in Figure 5.4(A). The coincident photon count to single photon count ratio for this same instance is -26.6 dB. If the system were designed so that photon pairs generated by the transmitter were reliably detected by the receiver then the SNR for Figure 5.4(A) would be shifted lower by 20.8 dB. Figure 5.4(B) shows the BER for the system with maximum background light with the SNR calculated from the coincident photon count to single photon count ratio. It is believed that this type of reliable transmission is possible, and so this result dramatically illustrates that reliable communication is possible even when the transmitted signal power is significantly less than the noise power.

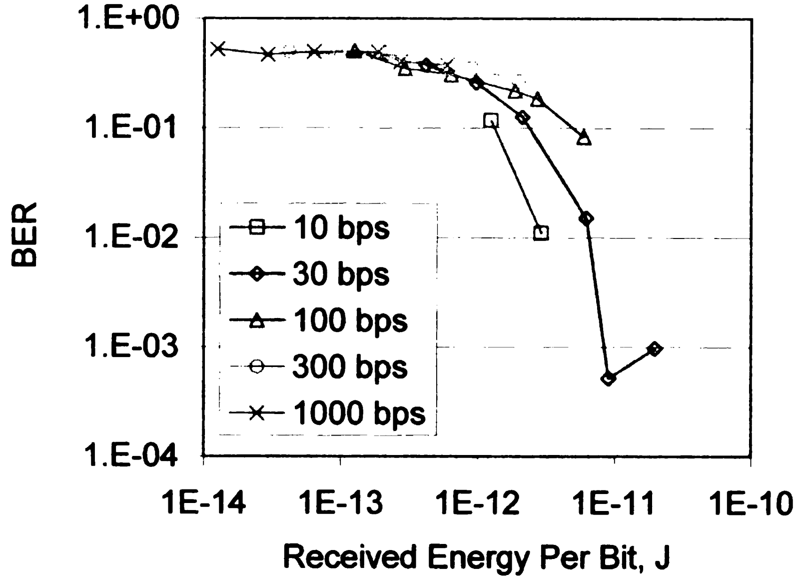

Figure 5.3: BER with minimal background light

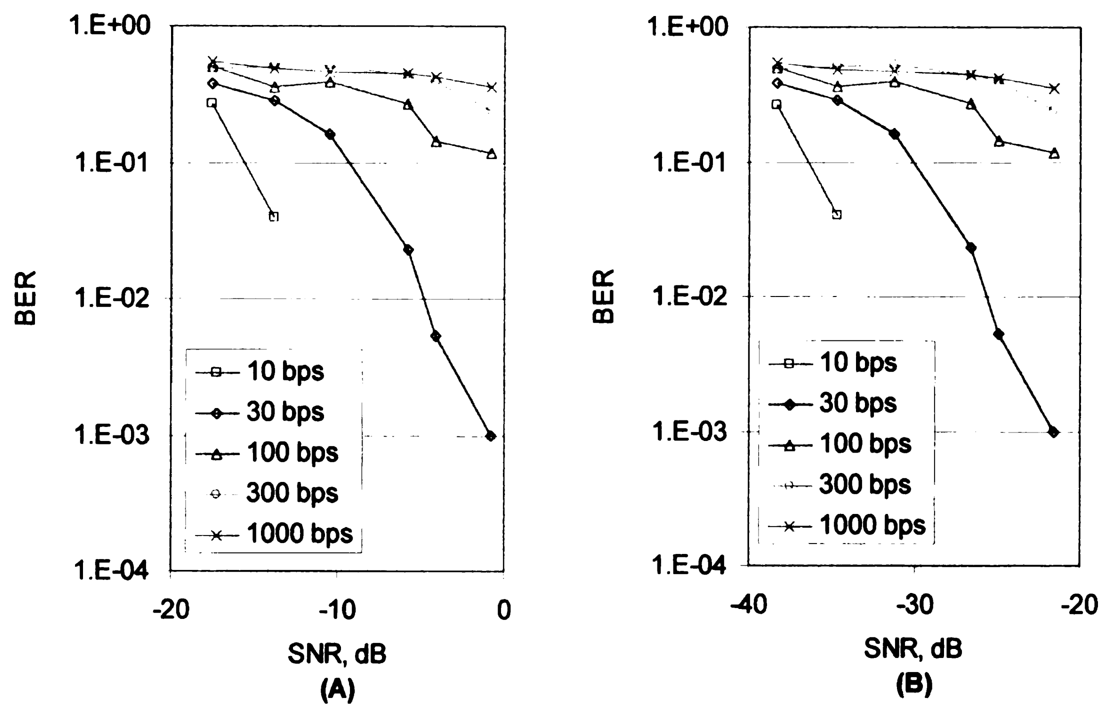

Figure 5.4: (A) BER with maximum background light. (B) BER with maximum background light and SNR calculated as ratio of coincidences to single photons.

5.3 Discussion

The limitations in switching of the liquid crystal phase retarder have made the data obtained from this experiment disappointing in the higher bit rates. It can however be used to compare the predicted results from the two state bit error rate equations derived in Chapter 3. The equations derived in Chapter 3 [3-14, 15, 16, 17, 22, 23, and 24] are repeated here in the same order:

$$\langle N(1)\rangle = [(1-\alpha_2)R_1 + r_1][(1-\alpha_1)R_2 + r_2]\delta t\, T_s + R_1\,\alpha_2\, T_s \qquad [5\text{-}2]$$

$$\langle N(0)\rangle = [(1-\alpha_3)R_1 + r_1][(1-\alpha_1)R_3 + r_3]\delta t\, T_s + R_1\,\alpha_3\, T_s \qquad [5\text{-}3]$$

$$\langle N(1\,|\,0)\rangle = [(1-\alpha_2)R_1 + r_1][r_2]\delta t\, T_s \qquad [5\text{-}4]$$

$$\langle N(0\,|\,1)\rangle = [(1-\alpha_3)R_1 + r_1][r_3]\delta t\, T_s \qquad [5\text{-}5]$$

$$P(1\,|\,0) = \sum_{z=1}^{\infty} e^{-(\langle N(1|0)\rangle + \langle N(0)\rangle)} \left(\frac{\langle N(1\,|\,0)\rangle}{\langle N(0)\rangle}\right)^{\frac{z}{2}} I_z\left(2\sqrt{\langle N(1\,|\,0)\rangle\langle N(0)\rangle}\right) \qquad [5\text{-}6]$$

$$P(0\,|\,1)=\sum_{z=0}^{\infty}e^{-\left(\langle N(0|1)\rangle+\langle N(1)\rangle\right)}\left(\frac{\langle N(0\,|\,1)\rangle}{\langle N(1)\rangle}\right)^{\frac{z}{2}}I_z\left(2\sqrt{\langle N(0\,|\,1)\rangle\langle N(1)\rangle}\right) \qquad [5\text{-}7]$$

$$BER=\frac{P(1\,|\,0)+P(0\,|\,1)}{2} \qquad [5\text{-}8]$$

Equations [5-2, 3, 4, 5] give the coincidence rates registered by the receiver as a function of bit period, transmitted entangled photons (signal), noise photons and detector coincidence window. It would have been ideal to calculate the BER as a function of these parameters but it was not possible to measure both the coincident photons and the individual channels concurrently because the equipment to record five channels (2 for coincidence counting and 3 for the photon counting detectors) of photon counting signals was not possessed at the time. Equations [5-2] to [5-5] have been verified by Hong et al. [Hong 1985] so it is primarily necessary to verify the Equations [5-6] and [5-7] in order to have confidence that Bit Error Rate is correctly calculated.

To verify these two equations the BER was calculated using these equations from the coincidence counts measured in this experiment. The 30 bps data rate was used to do this calculation because, as can be seen in Figure 5.4, this data rate does capture a good range of bit error rates for very low signal to noise ratios. At low SNR the BER is very high and at about -5 dB SNR the BER drops to a reasonable level for data transfer. The data used for calculating this BER is shown in Table 5.3. Mathcad software was used to make these calculations and the worksheet is shown in Appendix A.

Table 5.3: Average Coincidence counts per bit in the presence of maximum background light at a data rate of 30 bps

SNR (dB)	State "0" counts per second		State "1" counts per second	
	AB or $\langle N(1\mid 0)\rangle$	AC or $\langle N(0)\rangle$	AB or $\langle N(1)\rangle$	AC or $\langle N(0\mid 1)\rangle$
-17.1	0.8	1.2	1.1	1.0
-12.7	1.5	3.1	2.5	1.4
-9.7	2.6	5.6	5.5	2.8
-4.8	7.0	16.3	16.3	7.2
-2.7	11.9	27.8	28.3	12.0
0.5	23.3	54.0	55.7	23.7

In Figure 5.5 the calculated BER is obtained by using Equations [5-6, 7, 8] and the measured coincidence numbers in Table 5.3. It has been compared to the directly measured BER and the agreement is excellent. The single point in positive SNR do not appear to be close but in this case there was one measured error is 1002 bits collected so the variance is larger than the difference between the two values. Based on the precision of the measurement the overall agreement is excellent.

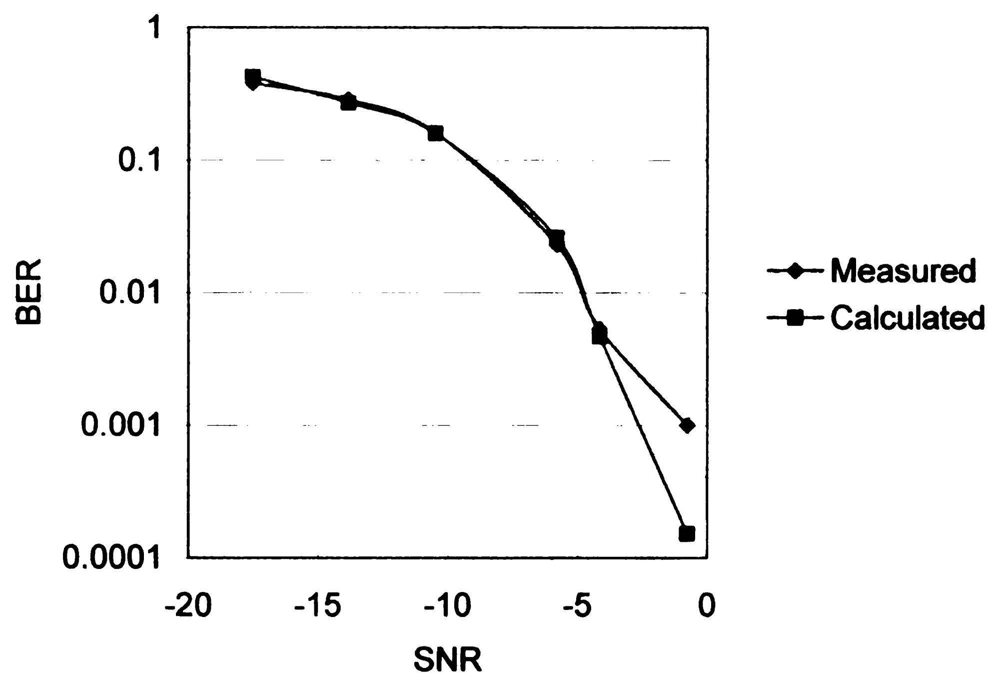

Figure 5.5: The calculated BER in this figure is obtained by using equations measured coincidence numbers is compared here to the directly measured BER as a function of SNR for 30 bps data rate.

5.4 Discussion of potential given high contrast modulator

The previous discussion and analysis confirm that he BER can be reliably calculated from by knowing the number of coincidences detected for the '0' and '1' coincidence detector. Though this system did not achieve the contrast ratio necessary to confirm that a low BER can be maintained even when SNR is negative, in terms of decibels, it did confirm the equations that predict BER and so some estimate can be made of potential system performance given a higher contrast system.

The performance of the system given a higher contrast modulator can be estimated by using the data Table 5.3 and adjusting the error coincidences to approximate a modulator that has a contrast ratio as good as the steady state contrast ratio that was achieved with the modulator used in the experiment. So the error coincidences in Table 5.3 were adjusted according to the following formulae

$$\langle N(1|0)\rangle = \frac{\langle N(0)\rangle}{CR_{ss}(0)} + \langle Noise\rangle \qquad [5\text{-}9]$$

$$\langle N(0|1)\rangle = \frac{\langle N(1)\rangle}{CR_{ss}(1)} + \langle Noise\rangle \qquad [5\text{-}10]$$

where the $<N(0)>$, $<N(1)>$ and $<Noise>$ values are all what was measured in the experiment and $CR_{ss}(0)$, $CR_{ss}(1)$ are the lowest steady state contrast ratios measured for the '0' and '1' states obtained from Table 2. These calculated values are summarized in Table 5.4.

The values in Table 5.4 and Equations [5-6, 7, 8] have been used to calculate the potential BER if the modulator maintained a high contrast ratio when switched. These bit error rates are plotted in Figure 5.6 as a function of signal to noise ratio. The measured BER is also plotted in this Figure. From this plot it can be seen that the BER could have been low (less than 10^{-2}) even when the SNR is as low as -7 dB. The calculated BER values are not much different for SNR less the -9 dB because the signal is low enough that the lack of signal is starting to drive the error rate. Even without noise there is a significant chance to receive no coincidences (signal) for a bit when the average number of coincidences is less than 5.6 per bit.

Table 5.4: Average Coincidence counts per bit in the presence of maximum background light, with a data rate of 30 bps and modified error coincidence rates to represent the operation of a better modulator

SNR (dB)	State "0" counts per second		State "1" counts per second	
	AB or $<N(1\vert 0)>$	AC or $<N(0)>$	AB or $<N(1)>$	AC or $<N(0\vert 1)>$
-17.1	0.62	1.2	1.1	0.8
-12.7	0.67	3.1	2.5	0.52
-9.7	0.9	5.6	5.5	0.91
-4.8	1.52	16.3	16.3	1.21
-2.7	2.53	27.8	28.3	1.94
0.5	4.66	54.0	55.7	3.33

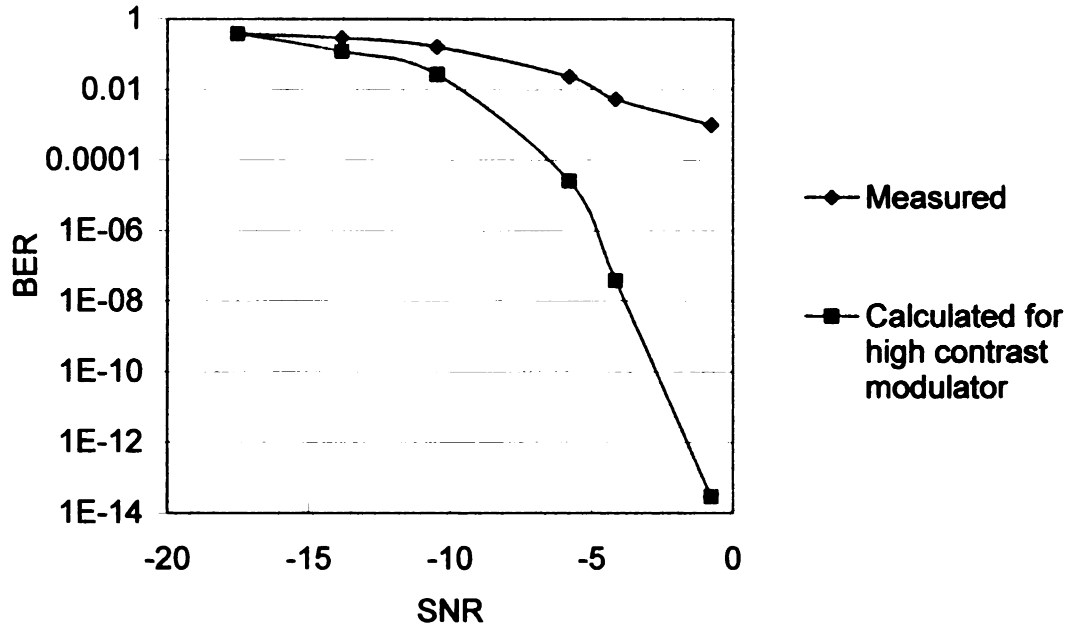

Figure 5.6: This graph illustrates the potential of the communication system if the modulator had higher contrast. The calculated series is generated by modifying the off state data by reducing it to a contrast level equal to the steady state contrast.

5.5 Conclusion

Through the use of quantum-entangled photons, it has been shown that reliable communication is possible at remarkably low received energy levels on the order of one picoJoule per bit in the presence of an overwhelming background light equal to over 100 times the signal, resulting in exceptionally low optical signal-to-noise ratios. While the experimental setup suffers from the inherent inefficiency of current quantum-entangled photon generation processes, and the use of an imperfect liquid crystal phase retarder as the modulator, it successfully demonstrates the feasibility of the concept.

The equations developed in Chapter 3 to describe the bit error rate of the two state communication system have been checked against the data gathered in this experiment. It was shown that the BER as predicted by those equations agrees very well with the BER measured in this experiment. A further calculation to illustrate the potential of the system developed here with a more capable polarization modulator has shown that the system could have sustained low BER communication to a SNR of up to -7dB.

The demonstration of the feasibility of the two state quantum entangled photon communication system and the confirmation of the two-state BER equations are the important steps that have been taken in this chapter. The two-state system makes synchronization between the transmitter and receiver much easier, as it allows bipolar forms of encoding such as Differential Manchester signaling. The confirmation of the BER equations is important because it is a significant building block for the further developments in the time coincident system. It is a step beyond the formalism developed for on / off keying by Hong, Friberg and Mandel [Hong 1985] and it is a step in the direction of the time coincident system which is described in the next two chapters.

CHAPTER 6

EXPERIMENTAL SETUP FOR COINCIDENT COMMUNICATIONS EXPERIMENT

6.1 Introduction

In this chapter the concept and the experimental design of the time coincident photon communication system, which is based on pulsing sets of sources simultaneously, is described along with a series of experiments that have been conducted to examine the efficacy of the system. The primary experiment to confirm the predicted functionality of the communications system was conducted over a significant range with ambient light levels that are in the range of a typical scene on a moderately sunny day. Ideally it would have been very interesting to fabricate a source that would have nearly ideal characteristics utilizing a quantum well source but this was impractical given the time and resources allotted. The experimental system was instead built using mainly components that are off the shelf. The off the shelf components were chosen so that they in theory could be incorporated into a monolithic micro transmitter. This means the control / driving electronics, optical sources and beam forming lens all can be incorporated into a device the fits the NNI grand challenge, which is to have an overall dimensional scale from microns to centimeters while incorporating nanometer scale components. The receiver is made from macro components and is not necessarily adaptable to fit the NNI scheme. Since the concept system is for micro robots working in cooperation with macro scale robots there is not a need for the receiver components to be potentially "shrinkable".

In the first part of this chapter the concept and experimental design for the transmitter made from time coincident pulsed sources is introduced. The photon counting reciever is subsequently covered. The chapter is concluded with a description of the experimental plan as well as the overall setup of the experiments. This leads into Chapter 7 which will cover the results and a discussion of these experiments.

6.2 Transmitter

6.2.1 Optical Transmitter Concept

The goal of the communication system described in this chapter is to emulate the communication system based on quantum entangled photons with a much more energy efficient transmitter. The system concept is based on multiple energy efficient sources that are fired simultaneously. Like quantum entangled photons, these sources have the same wavelength and polarization correlations essential for communication in the presence of significant background light. The sources either have different wavelengths, or sources of the same wavelength have orthogonal polarizations, and the sources emit bursts of photons with these wavelength and polarization correlations simultaneously. It should be noted that the photon pairs from the multiple sources do not have entangled quantum states. They only have the same correlations that make the photon pairs readily identifiable to a reciever that detects pairs of quantum entangled photons in the presence of ambient noise, such as the reciever that was described in Chapter 4.

This transmitter is unique in that it is the only known transmitter utilizing the time coincident photon information coding scheme in conjunction with traditional optical sources, such as LEDs and Laser Diodes. This system has the unique advantage of not requiring the use of a non-linear crystal and high power laser source for the generation of single-photon pairs for the purposes of time-coincident communications.

The advantage of this system is that it will enable the transmission of information at very low power levels and with a very small device. The scheme fits very nicely with very small, low threshold sources that are very energy efficient but also limite in total power. The calculated power levels are lower than any known transmitter. Another advantage of this system is that everything can be fabricated on a single chip using conventional microchip fabrication technologies with the only exception being the beam forming optics. This would make the system very compact and also potentially low-cost if manufactured in mass quantities.

The pulsed optical sources that would produce pairs or sets of photons at nearly the same time have stringent but readily obtainable requirements. The optical sources should have a narrow spectral linewidth, with a Full Width Half Maximum (FWHM) in terms of wavelength less than 2nm, and also have an optical lifetime for the radiative state that is less than 1 ns. The narrow linewidth is a requirement so that the receiver spectral filter can be narrow enough so that the photon counting detector is not saturated. A shorter radiative lifetime will lead to shorter coincidence time at the receiver and therefore improved noise immunity. The coincidence time would also nominally dictate the maximum data transmission rate if there were no dead-time between received pulses of the single-photon detectors. However current detectors made from high quantum efficiency Avalanche Photodiodes are actively quenched, which means they have a dead-time of 40 ns which limits the maximum data rate to 25 MHz.

A block diagram of the driver for the four channel system is shown in Figure 6.1. In this diagram the manner in which the logic signals are converted to an electrical pulse for exciting the diode laser such that it emits energy efficient photon bursts is presented. In the experimental implementation the driver electronics will transmit data bits at a frequency of 100 kHz, except where the frequency has been purposely varied. There will be 10 pulses per bit emitted (to get 10 photon pairs per bit) that will have between 10-20 ns pulse duration. This pulse duration is the lower limit of the available laser diodes.

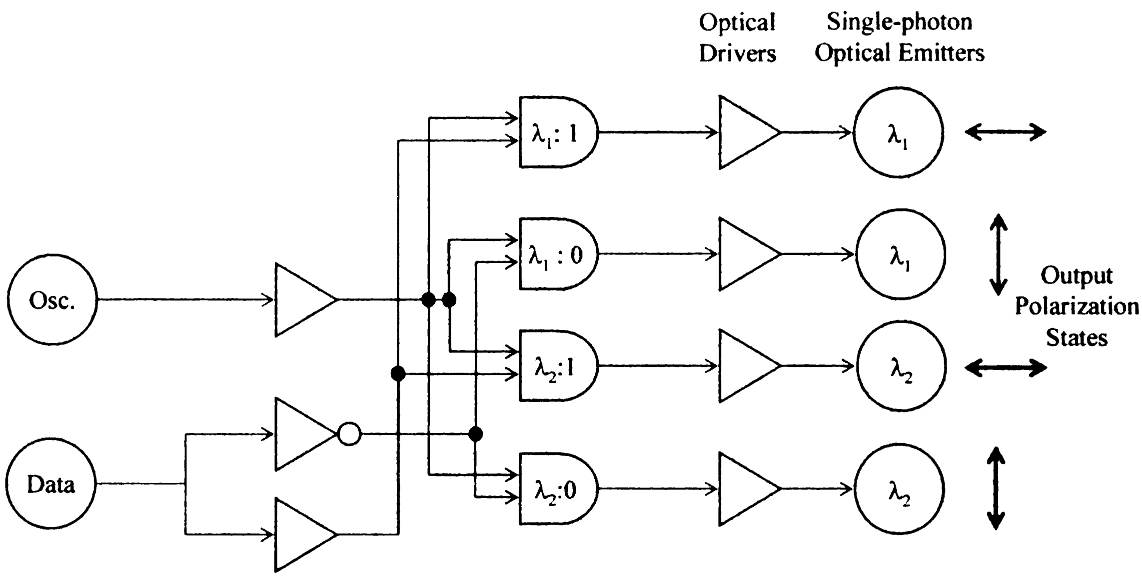

Figure 6.1: Schematic of the logic diagram for the multi-wavelength time-coincident optical transmitter. The oscillator provides a steady stream of alternating low (0) and high (1) digital clock pulses at say, 1 GHz. The data stream is sent to the appropriate AND gate which then determines which optical emitter to fire. The AND gate allows the clock signal to control the pulse width of each source. The clock period is much smaller than the data bit period so that multiple pulses are sent during one data bit. The logic states are shown in the truth table in Table 1. The optical emitters can be, but are not limited to light emitting diodes (LED) or diode lasers, quantum-dots, etc. Depending on the emitter that is fired, each has a certain wavelength or spectral channel and a polarization associated with it. In this way, both wavelength and polarization states are used to effectively increase the SNR for single-photon data transmissions.

Oscillator (Clock)	Data Input	Optical Output (λ, polarization)
0	any	0
1	0	λ_1 Vertical, λ_2 Vertical
1	1	λ_1 Horizontal, λ_2 Horizontal

Table 6.1: Truth table or logic chart for schematic shown in Fig. 6.1. Light emitters fire in pairs with complementary wavelengths and identical polarizations.

The modulated signal drives optical sources of different wavelengths or polarizations. These sources (which may be LEDs, Laser Diodes, Quantum Wells or Quantum Dots) can be driven with low amplitude and very short pulses of electrical energy so that a pulse of photons is generated. The photons from all four optical emitters are sent coaxially along the same optical path to a receiver whereby they are decoded according to wavelength and polarization state. Various optical configurations can be used to spatially superimpose the signals from all emitters along a common optical path, including dichroic beam splitters, polarizing beam splitters, or a combination of a diffractive element such as a prism or grating and polarizers.

This method of communicating using correlated photons provides many possibilities for the assignment of physical parameters to bit values. In Table 6.1 a truth table defining the way in which the information bits are encoded. According to Table 6.1, when the receiver counts photons from wavelengths λ_1 and λ_2 in temporal coincidence that have identical and vertical polarizations then information bit is a "0"; when the receiver counts photons that are in horizontal polarization states, then the information bit is a "1". Of course, other polarization coding schemes can be employed to achieve the same effect, such as orthogonal polarizations for a "0" and identical polarizations for a "1" and vice versa.

Note that by use of additional logic gates, a system can be devised to send up to 2 bits (2^2) of data to yield a possible of 4 combinations versus the 2 possible combinations. The truth table for this bit coding is shown in Table 6.2. For the communication schemes shown Table 6.1 and Table 6.2, only two photons per pulse, one at each wavelength, have to be captured by the reciever. Since only two photons have to make it to the reciever, this implies that very few photons must be transmitted from the transmitter. The actual number of photons transmitted depends on the reciever size and quantum efficiency, the distance of the transmission and the directional capability of the transmitter.

Oscillator (Clock)	Data Input	Optical Output (λ, polarization)
0	any	0
1	0, 0	λ_1 Vertical, λ_2 Horizontal
1	1, 0	λ_1 Horizontal, λ_2 Vertical
1	0, 1	λ_1 Vertical, λ_2 Vertical
1	1, 1	λ_1 Horizontal, λ_2 Horizontal

Table 6.2: Truth table or logic chart for an alternate embodiment (not shown) but based on Figure 6.1 where up to 2-bits (4 states) of information can be sent at a time through the use of perpendicular polarization states of λ_1 and λ_2.

Alternate configurations are shown in Figures 6.2 and 6.3. Figure 6.2 shows the schematic of a transmitter that utilizes three optical channels with the data being encoded on one wavelength while a timing pulse is sent on another spectral channel. The logic chart or truth table for Figure 6.2 is shown in Table 6.3.

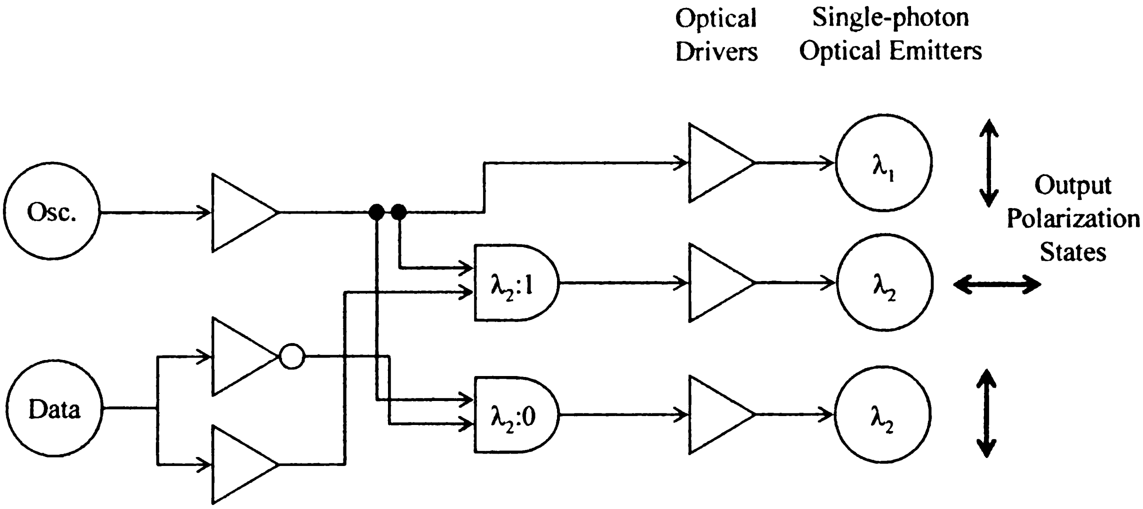

Figure 6.2: This is a schematic of the three channel configuration. Here, the emitter that is of wavelength 1 provides synchronization and a reference polarization. This emitter has a fixed wavelength and polarization. The second set of emitters is of a different wavelength than the sync emitter. The data is encoded by the relative polarization of the emitter that is fired from the second wavelength when compared to the reference emitter polarization. When the emitter of wavelength 2 that is fired is the same polarization as the wavelength 1 emitter then this encodes a zero bit. When the emitter of wavelength 2 that is fired has a different polarization than the wavelength 1 emitter then this encodes a one bit.

Oscillator (Clock)	Data Input	Optical Output (λ, polarization)
0	any	0
1	0	λ_1 Vertical, λ_2 Vertical
1	1	λ_1 Vertical, λ_2 Horizontal

Table 6.3: Truth table or logic chart for schematic shown in Figure 6.2. Light emitters fire in pairs with complementary wavelengths and polarizations.

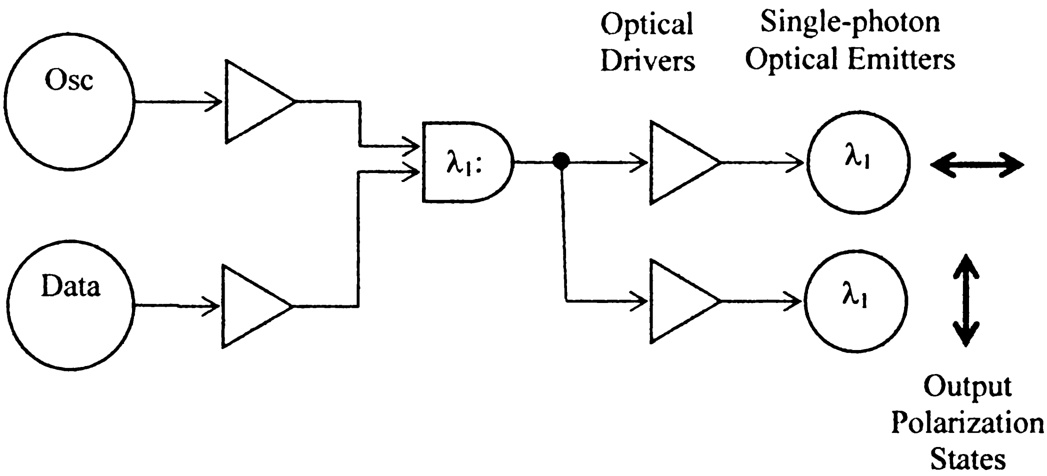

Figure 6.3: Schematic of the two channel configuration. In this case the data is encoded using on / off keying. A '1' is communicated by transmitting the complimentary photons of the same wavelength and orthogonal polarizations. A '0' is communicated by the lack of signal. This scheme requires the receiver to compare the number of photon pairs received to a threshold to determine the bit value.

6.2.2. Experimental Transmitter

The experimental version of the transmitter was built using commercial off the shelf components. The components used were chosen with an emphasis on their potential to eventually be incorporated into a very energy efficient monolithic device that is appropriate for a miniature robot. For example laser diodes have been used along with collimating optics limited to an aperture diameter of 1 cm. The lasers and optical components of the transmitter are shown in Figure 6.4. There were 2 laser diode sources at 669 nm and 2 at 673 nm. They were arranged so that one laser of each wavelength was polarized vertically and the other was polarized horizontally. The lasers were pulsed 10 times per bit and the pulse duration of the laser pulses was approximately 10 to 20ns. This pulse duration is the lower limit of the commercially available diodes and was slightly different for each individual laser.

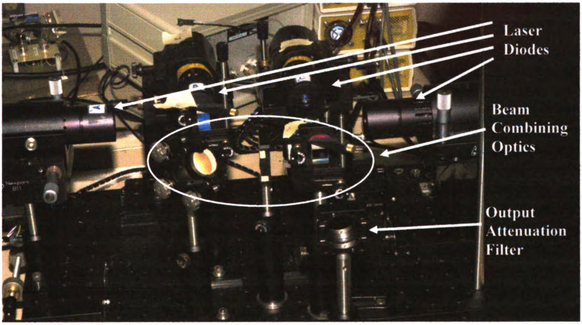

Figure 6.4: Front view of the experimental transmitter. The four laser diodes are utilized in the multiple configurations described previously. The output attenuation filter is set so that an average of one photon per pulse is detected at the receiver.

The electronic components of the transmitter are shown in Figure 6.5. The data source is custom built specifically for these experiments. It has the option of using an internal or external clock. The data bit period is programmable with dip switches and can be varied from 1 to 256 microseconds. The data can either be alternating ones and zeros or can be a preprogrammed text message. The output of the data source gates a Berkeley Nucleonics BNC 555 pulse generator. This pulse generator has four outputs that can produce pulses of varying amplitude, duration and period. The outputs from the BNC 555 are used to trigger the laser diodes.

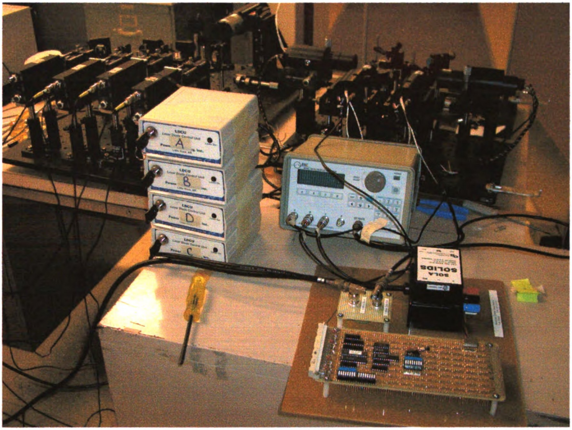

Figure 6.5: The electronic components of the transmitter consist of a custom built data source (lower right) and a Berkeley Nucleonics BNC 555 pulse generator.

6.3 Receiver

A complimentary receiver for the transmitter described previously has been developed. The receiver recognizes when photons are received within the coincidence window and depending upon the wavelength and polarization of the coincident photons, the receiver turns these coincident photon events into bit values. The optical components of the receiver are functionally diagramed in Figure 6.6 and the receiver built for the experiments is shown in Figure 6.7. The receiver has a 50.8 mm diameter telescope to collect the photons and also collimate the received beam for the rest of the optical system. Immediately after the collection optics is a bandpass optical filter, denoted λ_1, that passes a 2 nm bandwidth centered at 669 nm. The filter reflects the 673 nm photons which are guided to another 2 nm bandpass filter, denoted λ_2, centered at 673 nm. With this set of filters the photons of wavelength 1 go to one set of photon counting detectors and the photons of wavelength 2 to a separate set of photon detectors. The photon counting detectors are Perkin Elmer Single Photon Counting Modules that have about 70% quantum efficiency for 670 nm photons. These detectors are actively quenched Geiger mode Avalanche Photodiodes which have built in cooling and signal conditioning. After the filter, the photons of wavelength 1 are separated by a Polarization Beam Splitter (PBS) into horizontal and vertical polarizations and then detected by photon counters. The photons of wavelength 2 are likewise separated by polarization and detected.

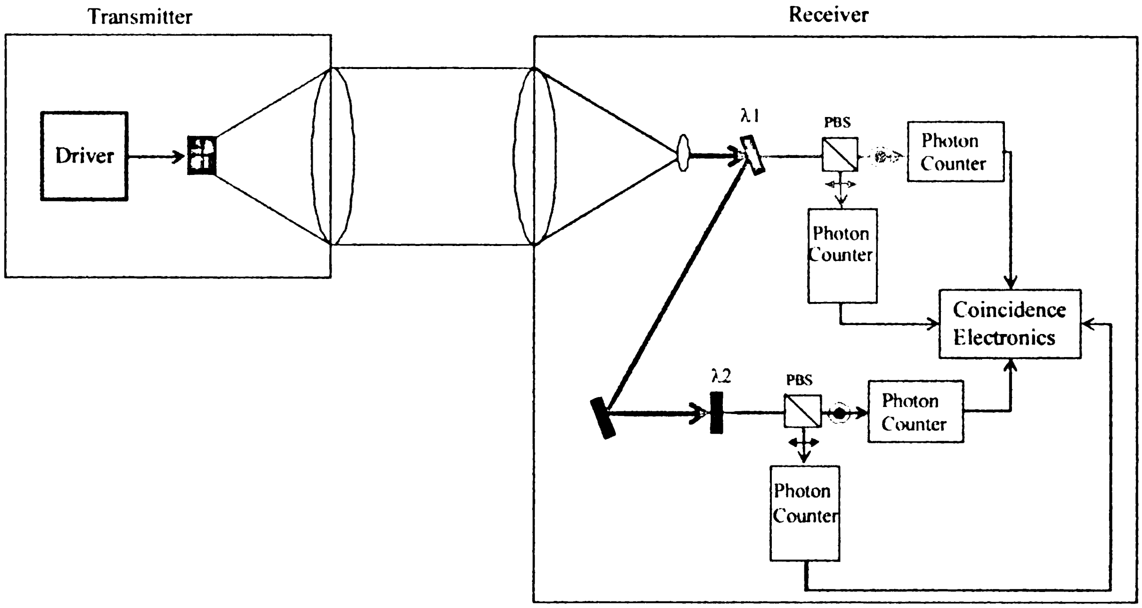

Figure 6.6: In this schematic the transmitter is shown working in conjunction with a receiver. The internal optics of the receiver that sorts the received photons starts with a telescopic front optic that collects and collimates the received photons. After this there are two filters, one that passes photons in band 1 while reflecting all other wavelength photons and a second that passes photons in band 2. Behind the two filters are Polarization Beam Splitters (PBS) that have extinction ratios of 1000:1 which they sort horizontally polarized photons from vertically polarized photons. The front end optics therefore sorts the beams so that the photon counters only see photons of a particular wavelength and polarization.

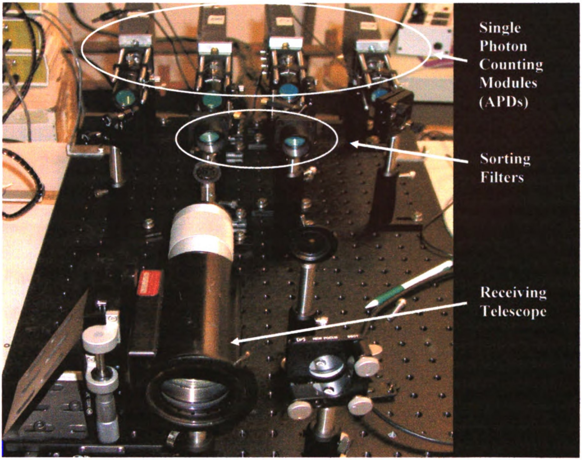

Figure 6.7: Picture of the optical components of the receiver that is diagrammed in Figure 6.6.

The coincidence electronics, pictured in Figure 6.8, determine which photon counters fire at the same time and thereby decode the data in bits of ones and zeros. The coincidence electronics have been built using a Field Programmable Gate Array operating at 400 MHz and the coincidence time window is programmable between 3 ns and 11.75 ns. When this circuit detects a coincidence a pulse is output to a logic analyzer which logs the time the pulse occurred.

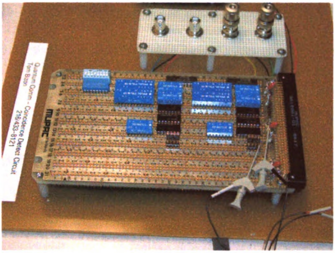

Figure 6.8: Custom built coincidence detector takes pulse outputs from two pairs of photon counting detectors and determines if a pair of detectors fire within the programmable coincidence time window. When a coincidence is detected the circuit outputs a pulse to a logic analyzer which logs the time the pulse occurred.

The selection of the coincidence time window is influenced by the laser pulse duration. It cannot be too small compared to the pulse duration or a photon from one source early in the pulse will not be time coincident with another photon from its paired source late in the pulse. The number of coincidences, r_c, due to noise photons is directly proportional to the coincidence time window, δt, and is approximately equal to [Mandel 1965]

$$r_c \approx \prod_n r_n \, \delta t^{n-1} \, T \qquad [6\text{-}1]$$

where n is the number of channels used for coincidences, r_n is the photon count for channel n, and T is the bit period. The nominal coincidence window for the experiments was 11.75 ns. Additional noise reduction would have been possible if a coincidence time of 1 ns were used but this would have resulted in significant signal loss because the laser pulses were of 10-20 ns duration.

6.4 Experimental Plan

As previously mentioned the experimental tests of the system were conducted in both the laboratory and also in a hallway where longer ranged communication could be tested. For each experiment run the quality of the transmitted information was determined by measuring the Bit Error Rate for a transmitted message. The system parameters that were varied during the experiment were the receiver aperture diameter, transmitter optical pulse power, ambient light conditions, data rate and coincidence time window. By varying the receiver aperture it is possible to simulate both how the system will perform for different sized transmitter apertures or different ranges with a fixed aperture. Varying the optical pulse power and ambient light are straightforward measurements of the signal quality as a function of signal power and noise. The experiment varying the coincidence time window will effect both the signal and noise coincidences. The signal coincidences are reduced as the coincidence time gets smaller than the pulse duration of the sources. Likewise the coincidences due to noise are proportional to the coindidence time. Signal synchronization could be accomplished with a number of different preamble signals, such as a clock, sync word or a unique signal such as firing all sources at the same time but for these experiments a simple data pattern of alternating '1's and '0's was used to make the synchronization straightforward during the data analysis.

Summary of Performed tests

1. Identify how the system works with 1, 2, 3 and 4 channels with varying SNRs. The signal level was fixed and the noise level was varied. This tests the affect of the noise level on system performance. This experiment was conducted in the hallway.
2. The signal intensity was varied with 1, 2, 3 and 4 channels while leaving the noise level fixed. This tested how signal intensity affects system performance. This experiment was conducted in the hallway.
3. The coincidence time window was varied to 3 different settings with 2, 3, and 4 channels with a fixed signal level, noise level. This experiment tested the affect of coincidence time on system performance. This experiment was conducted in the hallway.
4. The bit rate was varied between 50 kHz and 1 kHz while keeping average signal power per bit constant. This experiment examined what affect the bit period has on system performance. This experiment was conducted in the laboratory.
5. Vary the aperture of the receiver while keeping the signal, noise and coincidence window constant. This experiment emulates the transmission over multiple distances. This experiment was conducted in the hallway.

6.5 Experimental Setup and Experiment Operation

The experimental setup diagram is shown in Figure 6.9. The test was conducted in a hallway, shown in Figure 6.10, with the transmitter and receiver located next to one another, shown in Figure 6.11. This allowed for the longest transmission distance and also made aligning the two easier. A white paper screen, with a small hole in it to allow for the transmitted beam to pass through, was placed in front of the transmitter. This screen provided a uniform reflector so that the background light seen by the receiver could be controlled by illuminating it with different brightness lights. In order to achieve the highest ambient light levels a fiber optic light source was located next to the beam path and directed towards the receiver. The screen and light sources are shown in Figure 6.12.

The highest background light levels were similar to outdoors on a sunny day while the lowest were similar to outdoors with heavy clouds. In this experiment the signal power for all configurations was attenuated by neutral density filters so that for each channel approximately 1 photon per pulse was detected at the receiver. When one system parameter was varied all others were kept constant.

Multiple experiment configurations were tested. The baseline configuration was just a single channel (no coincidence) that was used for traditional on/off keyed photon counting communication. In the second configuration photons were transmitted in time coincidence over 2 channels. A clock signal was transmitted and the bit values were encoded by on/off keying. The third configuration used 3 channels and fourth used 4 channels. In this configuration the data was keyed as shown in Table 6.3 and 6.1 respectively. In general the transmitted power in the hallway experiments for the single channel case was 180 pW, the 2 channel case was 360 pW, the three channel case 580 pW, and for the 4 channel case 760 pW.

The conditions of this hallway were not ideal. There was a very significant temperature change between the room where the transmitter and receiver were located and the hallway the mirror was in. There was also significant turbulence in the hallway from the heating and cooling system. This caused a significant amount of beam wander, on the order of 1.5 to 2 cm linear displacement, which was probably very similar to what would be encountered outdoors. It was observed that the multiple beams did appear to stay together as they moved which was expected since the beams were at nearly the same wavelength. There were no active measures taken in the transmitter or receiver to counteract this beam wander so it should be noted that this was a significant contributor to the Bit Error Rate (BER).

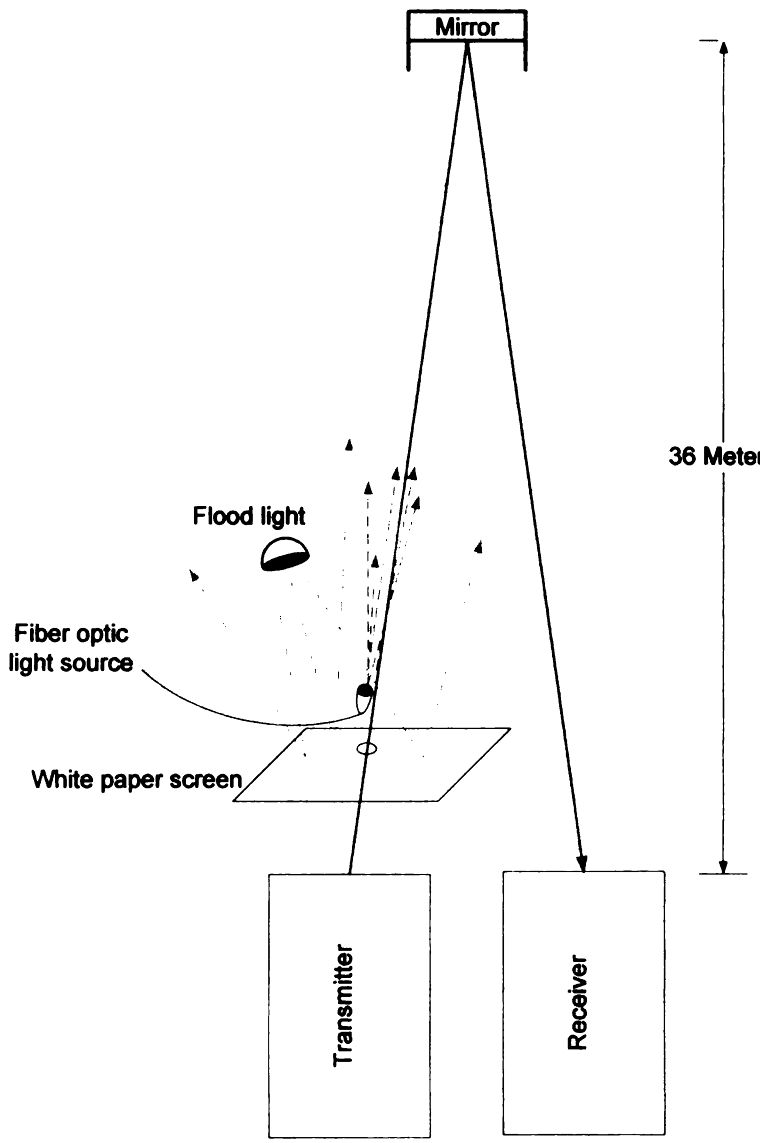

Figure 6.9: This figure shows the configuration of the ranged experiment. The experiment was performed in a hallway that allowed for a total of 72 meters of distance between the transmitter and receiver.

Figure 6.10: This picture shows the hallway where the long range experiments were conducted. The picture is taken from the location where the transmitter and receiver is located and the mirror that reflects the beam back to the receiver can be seen at the end of the hallway.

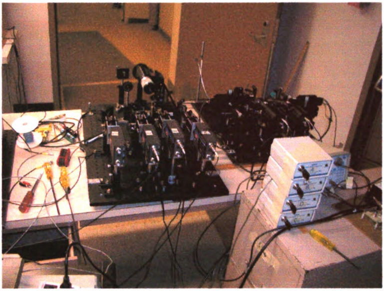

Figure 6.11: For ease of alignment the transmitter and receiver were located next to one another. Both are pointed down the hallway at the top of the picture.

Figure 6.12: Front view of the transmitter and receiver with the white cardboard to reflect the light sources located in front. The receiver was covered in black cloth so that very little of the noise photons go directly to the photon counters but instead reflect from the screen to the mirror and back to the receiver.

6.6 Summary

In this chapter the concept for the transmitter utilizing pairs of pulsed sources to generate time coincidence photons has been presented along with the transmitter and receiver that were built to test this concept. The experiments that were conducted were likewise described along with the experimental setup and conditions. The results of these experiments and a comparison of the predicted performance with measured performance are the subjects of the following chapter.

CHAPTER 7

EXPERIMENTAL RESULTS AND DISCUSSION FOR COINCIDENT PHOTON COMMUNICATIONS EXPERIMENT

7.1 Introduction

In this chapter the results from the experimental tests to determine the efficacy of the time coincident photon communication system, as described in the previous chapter, will be presented and discussed. The experimental results will also be compared to the predicted results, which are calculated from the mathematical formulation described in Chapter 3, to test how well the mathematical representation predicts the system performance. The data processing and analysis of the time coincident photon communication will be discussed first and then the results of the five different experiments will be presented and discussed. After the discussion of the individual experiments a general discussion of the overall experiment, covering the common results and some general observations on this system will conclude this chapter.

7.2 Experimental Measurement and Data Analysis

The data acquired at the receiver for all of these experiments is a series of single photon and coincident photon detection times. In the base line cases, where a single transmitting channel was used, the photon arrival times of that channel were recorded. In the other cases where time coincident photon communications were utilized the coincidence times for either one or two coincidence channels were recorded. This data record was then transferred to a computer for post processing and analysis.

The processing of the data was accomplished using Mathcad programs which have been provided in Appendices B and C. One of the programs processes on/off keyed data (Appendix B) for the one and two channel data and a second program (Appendix C) processes two state data for the three and four channel cases.

There were several sources of experimental error. A systematic error was caused by the lasers not completely shutting off between pulses. The photons generated by the partially on laser add a bias (non-zero off state) to the measured signal level. This bias level was measured to be 24% of the overall signal level and is treated as a background noise signal. Another source of error was caused by conditions in the experimental environment (lab hallway) not being ideal. There was a very significant temperature change between the room where the transmitter and receiver were located and the hallway that the mirror was in. There was also considerable turbulence in the hallway from the heating and cooling system. This caused a significant amount of beam wander, on the order of 1.5 to 2 cm linear displacement, which is probably very similar to what would be encountered outdoors. It was observed that the multiple beams did appear to stay together as they moved which was expected since the beams were at nearly the same wavelength. There were no active measures taken in the transmitter or receiver to counteract this beam wander so it should be noted that this was a significant contributor to the Bit Error Rate (BER).

7.3 Experiment 1: Effect of varying background noise

The data taken in these experiments has been tabulated and graphed in Figure 1 to show the BER as a function of SNR. Three data sets consisting of approximately 10 Kbits of data were transmitted through the system and the BER was measured for each data set. In Figure 7.1, each data point is the average of the three BER measurements that were taken for each condition point and the error bars show the maximum and minimum values. SNR was measured by independently counting the number of noise photons received by the individual detectors while the background lights were on and the transmitter was off and also by counting the number of signal and noise photons received when the transmitter and background lights were both on. The noise measurement was subtracted from the signal with noise to give the signal photon count. Then the SNR was determined from the ratio of the signal photon counts divided by the noise photon counts. The background light was varied to 4 different levels that were approximately equal for each configuration. The reason that the data points do not have the same SNR for each configuration is because the laser power levels could not be exactly matched and also by adding channels the amount of noise is increased linearly with the number of channels. A significant reduction of the BER is shown for the 2 channel coincidence compared to the single channel baseline. The 4 channel configuration also shows a significant reduction in BER from the baseline but the improvement from the 2 channel case was not as significant.

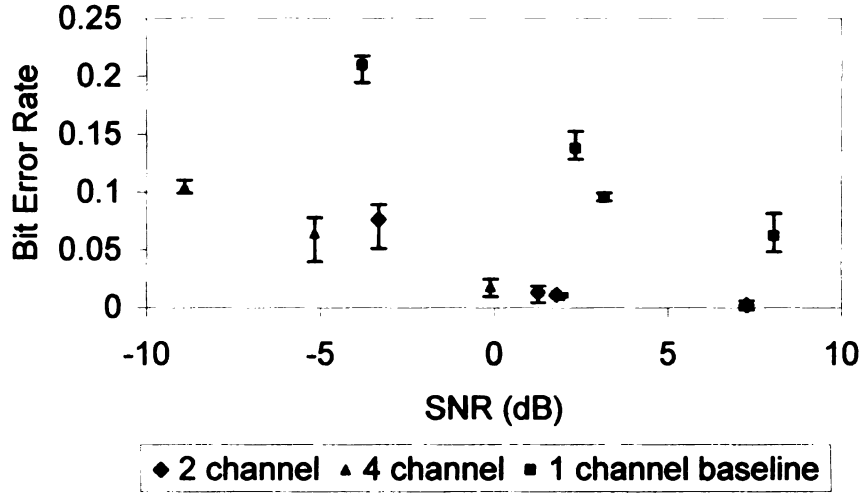

Figure 7.1: In this figure a comparison of single channel photon counting communication to time coincident photon counting communication for different noise levels can be made. This graph directly compares the measured SNR to BER. The variation in the magnitude between the maximum and minimum for the different data points was caused by varying amounts of beam wander. The beam wander would change because there was a large temperature difference along the hallway where the experiment was conducted that was made worse by the building heating system turning on periodically during the experiment.

In Figure 7.2 a sample of the raw data from the single channel (top) and two channel (bottom) configurations is shown. The single channel data plots photon detections as function of time. The two channel data plots photon coincidence detections over time. The data rate was 100 Kbit/sec so there were 10 microseconds of 'on'/ '1' bit with photon pulses and 10 microseconds 'off' / '0' bit without pulses. In the single channel case it can be seen that there are 10 microsecond time periods with more photon counts and periods in between with less but the contrast between these is not very strong. In the

2 channel case the 10 microseconds of coincidence counts are readily apparent as there is almost no noise between them. The data clearly shows the noise immunity obtained by using coincident photon communication. The data however also shows some periods where the 2 channel coincidence counts are low. For example, in the 2 channel data the period between 30 and 40 microseconds there are only 4 coincidence counts. With some low counts such as these it is apparent that signal loss due to beam wander was probably one of the most significant sources of error.

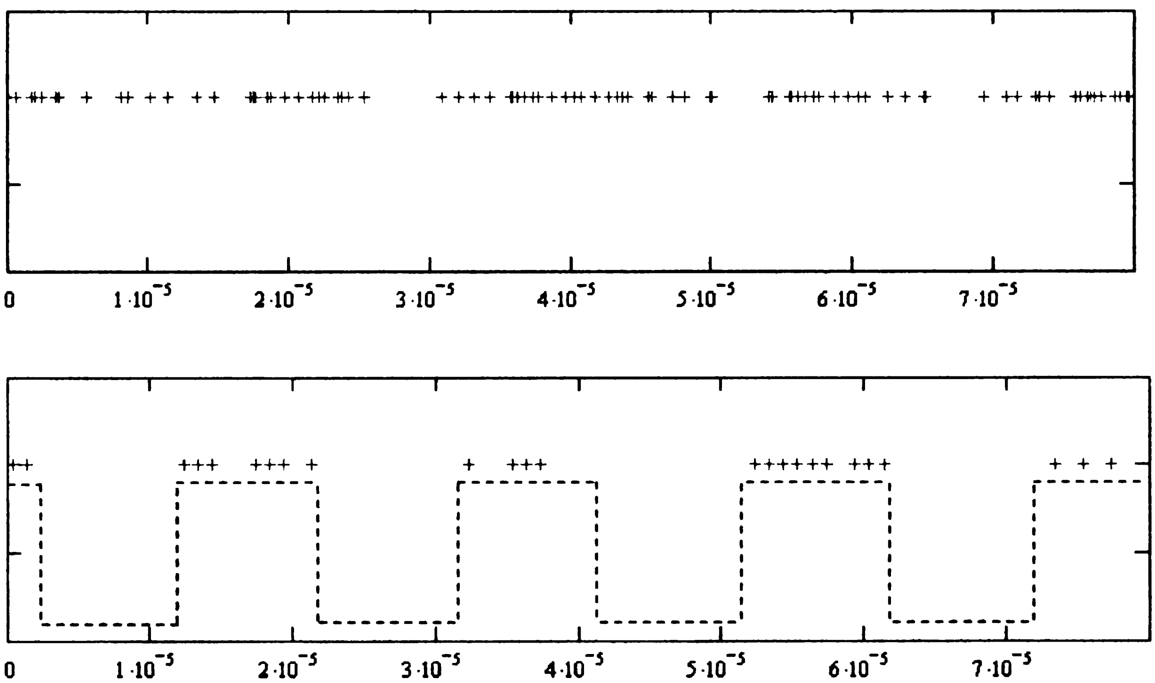

Figure 7.2: Top: A graph of photon detections as a function of time for the single channel baseline. Bottom: A graph of photon coincidence detections as a function of time for the 2 channel configuration. The bottom axis for both of these graphs is in units of seconds. The dashed line shows the transmitted waveform for reference.

In order to more fairly evaluate the data shown in Figure 7.1, a second graph has been generated in Figure 7.3 where the SNR is calculated in a way that compensates for the deflated SNR that results from inflated noise levels caused by additional channels. Here the signal is still the sum of the signal photons from each channel. The noise however is now calculated as the single channel average number of noise photons, rather than the sum of the noise photons from all channels. In Figure 7.3 it can be seen that again a significant improvement comes from using the 2 channel photon coincidence as opposed to a single channel photon counting system. A 5 to 7 db improvement has been measured in these tests. The data however does not show an improvement of the 4 channel system over the 2 channel system. In this case the 4 channel system would probably have to be coded with multiple bits, as in Table 6.2, for a given bit period to see an improvement.

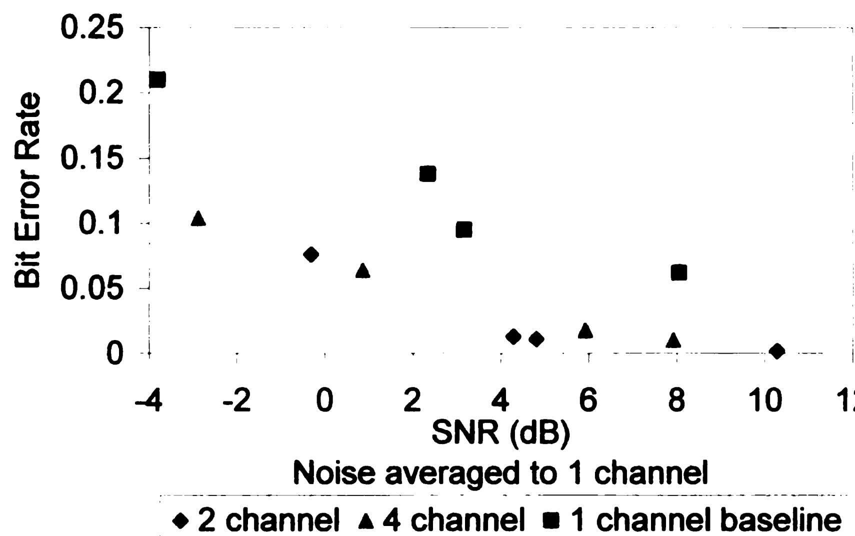

Figure 7.3: In this graph the signal-to-noise ratio has been calculated with the signal summed for all of the channels used in a particular configuration. The noise however was calculated as an average for a single channel.

In order to test how well the equations derived in Chapter 3 [3-22, 23, 24, 27, 28, 29, and 30] predict the system behavior, a comparison of the expected BER calculated from those equations and the measured BER is shown in Figure 7.4. In this comparison it should be noted that the bias caused by the laser not completely turning off has been compensated by counting the laser photon counts outside of the pulses in the noise for that detector. These compensated signal and noise photon counts for each individual detector were then used, along with the BER equations, to obtain the calculated BER for each condition. In this figure it can be seen that there is fairly good agreement between the calculated BER and the measured BER. The two potential sources of the discrepancies between the measured BER and the calculated BER are the beam wander that dynamically changes the signal strength and also the fact that the photon counts were measured independently from the data transmission. This independent measurement, which was not taken from the data transmission record, took place a couple of minutes before or after the data transmission. This, along with the dynamics added from beam wander, probably caused the majority of the discrepancies.

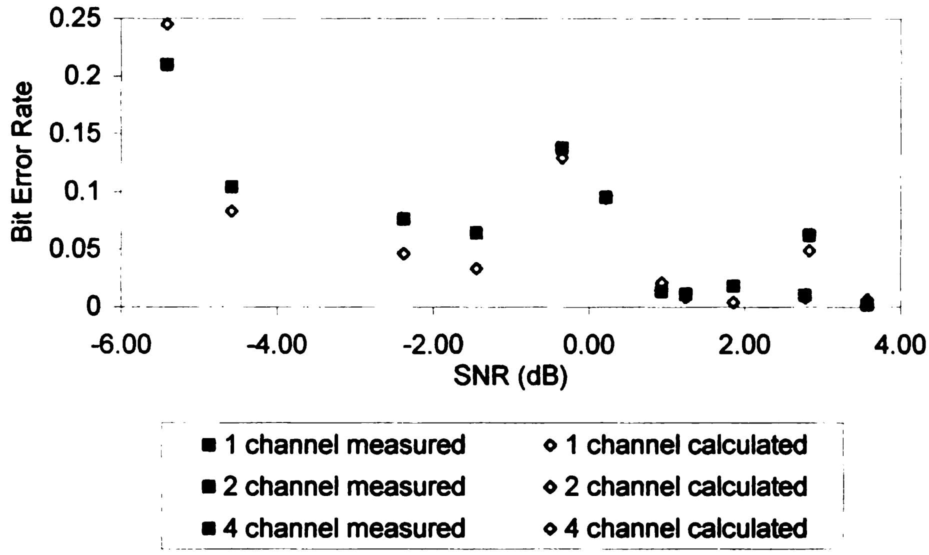

Figure 7.4: In this graph a comparison of the expected BER calculated from the BER equations and the measured BER is shown. In this case the bias caused by the laser not completely turning off has been compensated by counting the laser photon counts outside of the pulses in with the noise for that detector.

Since the equations from Chapter 3 effectively predict the measured BER, they can be used to further compare and contrast the difference between the one channel traditional photon counting communication and two channel coincident photon communication. Using these equations, and parameters that are close to those measured in the experiment, the Bit Error Rate for the one and two channel systems for varying background photon count per channel is calculated and shown in Figure 7.5. Here the signal level for the one channel system has been doubled so the total signal photons are the same as the two channel system and the threshold was kept at a constant level. In the experiment the threshold level was optimized for each individual measurement to produce the lowest BER. In this case that would have produced a curve that would have had steps in it and so the threshold was held constant for better comparison.

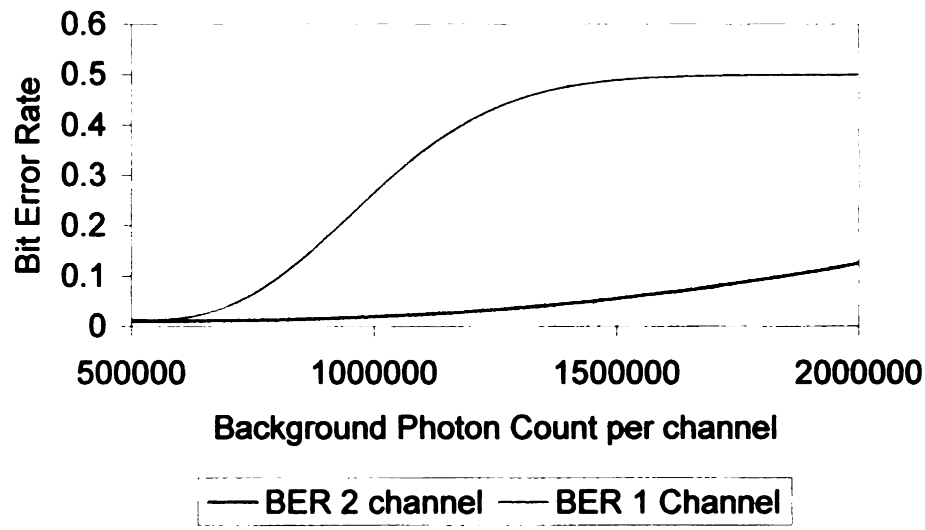

Figure 7.5: In this figure the BER of the two channel system and one channel system are directly compared for the following conditions. The signal is held constant at one million photon counts per second for both cases. The one channel system has a signal level equal to 1 million photons per second in the single channel the two channel system has 500000 photons per second in each channel. The threshold level for determining the bit value was held constant.

This graph produced from the simulated data shows that the single channel system degrades much more quickly from noise than the two channel system does. This further supports the conclusion that the coincident photon technique appreciably suppresses noise and enables photon counting communications in the presence of significant background noise.

7.4 Experiment 2: Effect of varying signal levels

In this experiment the affect of varying signal level on the coincident communication system is studied. The signal level was varied by placing various neutral density filters at the output of the transmitter. The noise was kept constant so that only the changing of the signal level changed the SNR. In this experiment a single channel (traditional photon counting) OOK baseline was obtained as well as data from 3 channel and 4 channel coincident photon counting with two state coding. A graph of the experimental results is shown in Figure 7.6. In this graph several of the modifications mentioned in the previous experiment have been used. Here the laser noise has been counted in with the noise figure to obtain the calculated values. Also in this figure the calculated BER from an independent measurement of the signal and background photon counts is shown. The noise level in this experiment was 4 times higher per channel than the maximum signal level per channel.

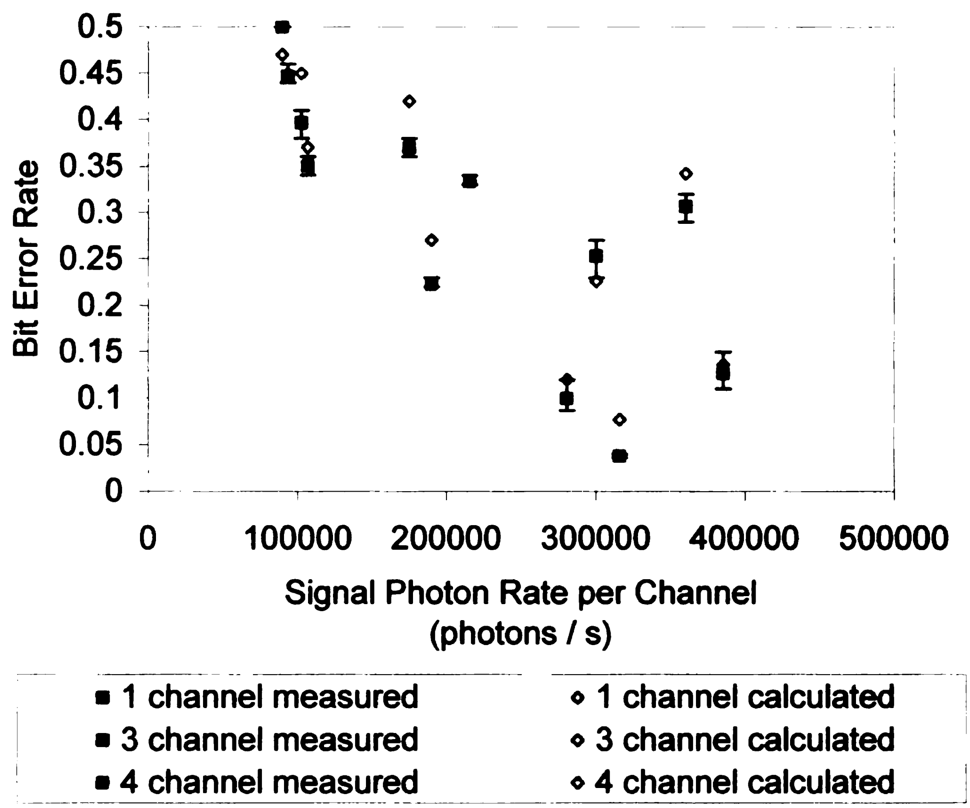

Figure 7.6: In this graph the variability of the Bit Error Rate as a function of Signal to Noise Ratio for the one, three and four channel configurations is shown. In this case only the signal level was changed and all other parameters were kept constant. The SNR in this case is the ratio of the signal to the average noise per channel as discussed in the previous experiment. The error bars for the measured data points are the maximum and minimum data values for that point.

There are two conclusions that can be taken from this data set. The first is that the equations developed in Chapter 3 to calculate the BER for given conditions fairly represent the measured data. Again the same sources of error, the independent measurement of background and signal counts and also beam wander, probably account for most of the discrepancy. The second conclusion is that the time coincident communication system is much more susceptible to performance degradation when the signal is reduced below a certain minimum level, which is around 10 coincidences per bit. In this experiment the photon coincidences were below this level for all of the data points. The average number of coincidences per bit was 5.5 at the maximum signal level and at an average of about 1 coincidence per bit at the lowest signal level. This conclusion regarding the performance degradation at low signal levels is also apparent from a general analysis of the coincident photon communication technique that is similar to the analysis for communication range in Chapter 3.

The coincident photon technique suppresses noise because for a narrow slice of time ambient photons have low probability of arrival and a pair of them occurring is even more improbable because, as they are independent probabilities, it is then equal to the product of two of these low probabilities. As signal strength falls below a minimum threshold, registering photon coincidences works against this technique because the probability of there being a signal coincidence is the product of two declining signal photon probabilities. This reduces the rate of signal coincidences more rapidly than the individual channels signal photon count rate declines. Note that in this case the photon probabilities are declining because of increased attenuation from neutral density filters, which is a good analog of lower power sources.

7.5 Experiment 3: Effect of varying coincidence time windows on system performance

In this experiment the effect that varying the coincidence time window has on the coincident photon communication system was examined. In this experiment the only parameter that was varied was the coincidence time setting for the receiver coincidence circuit. This setting affects both the number of signal and noise coincidences that are detected. The results of the experiment are shown in Figure 7.7.

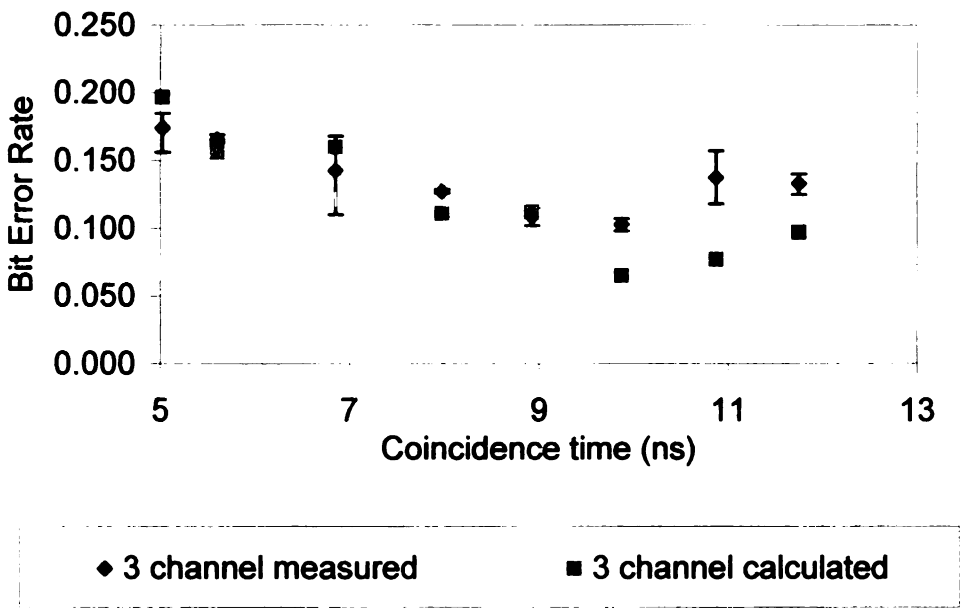

Figure 7.7: In this figure the performance of the 3 channel system is shown for various coincidence times. In this case only the coincidence time in the receiver coincidence circuit was changed and all other parameters were kept constant. The fixed parameters were: Aperture Diameter: 4.5 cm, Data Rate: 100 KBit/sec, Average Signal Counts per Channel: 500,000, Average Noise Counts per Channel:

985,000 and Average SNR: -2.88. The calculated data points in this case are made from signal and noise rates that have laser noise counted with the noise as discussed in the Experiment 1. The error bars for the measured data points are the maximum and minimum data values for that point.

This experiment was performed with a high noise level. The laser noise compensated signal to average channel noise level was measured for each data point and varied between -2.3 dB and -3.6 dB. The nominal coincidence time for all other experiments performed with this system was 11.75 ns, which was the maximum coincidence time of the circuit. In this experiment the coincidence time was varied from 11.75 ns down to 5 ns.

In Figure 7.7, it is best to examine the data from the nominal operating point, which is at the end of the graph, and go backwards from there. In going from 11.75 ns coincidence time down to 9.9 ns the BER is decreasing. This is because the dominate affect is that the noise level is being reduced by the shorter coincidence times. For progressively shorter coincidence times below this point the noise level continues to be reduced but the BER is increasing. This is because not only is the noise level being reduced but also the signal coincidences are being reduced. The reason the signal coincidences are being reduced is because the pulse widths of the particular lasers used in the experiment can only be made as small as about 14 ns. If one detector counts a photon at the beginning of the pulse and the other coincident detector does not detect a photon until the end of the pulse, a coincidence will not be registered if the coincidence time is less than time between photon events. So with laser pulses being as long as 14 ns it is apparent that the signal must be significantly degraded as the coincidence time gets significantly smaller than 14 ns. The drop in signal coincidences therefore dominates between 9.9 ns and 5 ns and the performance degrades even though the coincident noise level continues dropping.

7.6 Experiment 4: Data rate effect on system performance

In this experiment the affect that varying data rate has on system performance is examined. Only the three channel configuration was tested in this case. As in the previous experiments, all other parameters were held the same and only the data rate was varied. The lasers were still pulsed 10 times per bit in order to get a significant number of signal coincidences for each bit. Also the pulse durations were kept to 14 ns, but the time between pulses was increased to decrease the data rate.

The results from this experiment are shown in Figure 7.8. Some parameters that help to explain the operation of the system follow. Even though the signal level was not purposely adjusted, the number of measured signal coincidences did change a little throughout the experiment. They were an average 5.25 signal coincidences for the shortest bit period and these decreased to about 4.1 for the longer bit periods. This was probably caused by differences in the lasers pulse power with different time between pulses. This however was not the largest contributor to the increasing error rate. The increased error rate was due to the noise level increasing as the bit period increased. A longer bit period leads to proportionately greater accumulation of noise coincidences, as can be seen from Equation [3-30]. It was found the average noise coincidences per bit increased from 0.1 for the shortest bit period to 1 for the longest. This is an increase of 10 times the noise level for an increase of 16 times greater bit period. The increase in noise coincidences should have been the same as the increase in the bit period. The discrepancy in this case was caused by a 32% reduction in noise photons as the experiment progressed. This reduction of noise photons completely accounts for the discrepancy. The noise reduction was caused by a lower number of noise photons from the lasers due to changes in operating parameters required ti operate the lasers with more time between pulses. There was also a slight change in the noise photons from the noise lamps as the experiment progressed.

The threshold level was not changed in this experiment to consistently optimize the BER. It was instead held constant at a level of 1. It is readily apparent that at the longest bit period the probability of a '0' bit being incorrectly interpreted as a '1' bit is about 50 % when the average noise coincidences are approximately equal to the threshold value. The potential of the '1' bit value being incorrectly interpreted as a '0' is very small in this case so the average of the two error probabilities is about 25%. The error probability measured for the longest bit period was about 20%. The difference between what is expected and what was measured is because in this implementation when the number of coincidence measured was equal to the threshold the bit was arbitrarily assigned a '0' bit value.

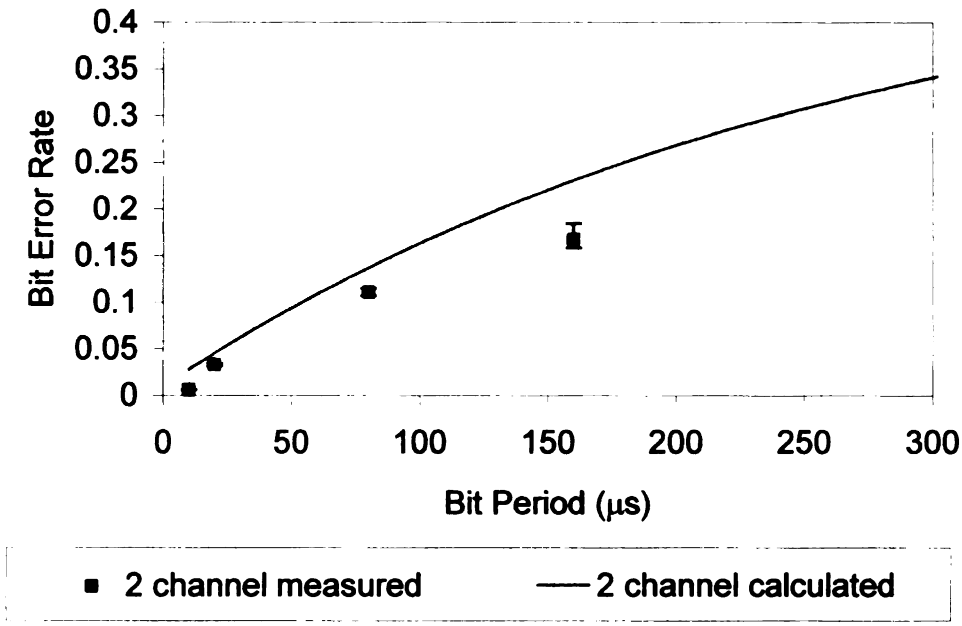

Figure 7.8: In this figure the performance of time coincident communication system at multiple bit periods is shown. In this case only the transmitter bit period was changed and all other parameters were kept constant. The calculated data points in this case are made from signal and noise rates that have laser noise counted with the noise as discussed in the Experiment 1. The error bars for the measured data points are the maximum and minimum data values for that point.

The calculated data in Figure 7.8 gives a fairly good approximation of the measured data. The discrepancy at the 160 microsecond bit period is also due to the operating parameters shifting as the experiment progressed. If each calculated data point was individually calculated there would have been better agreement, but the curve would not have been shown and it was decided that it was more valuable to show the general trend of the experiment.

7.7 Experiment 5: Effect of (Simulated) range on system performance

This experiment was performed to simulate how transmitting at further ranges will affect the performance of the coincident photon communication system. It was not feasible to transmit at longer ranges because of space limitations so instead the size of the receiver aperture was varied. By varying the receiver aperture the amount of the transmitted beam that is captured is reduced. This simulates how with increasing range less of the transmitted beam is captured by a fixed aperture because the transmitted beam spreads as it propagates. The size of the receiver aperture was varied by placing a variable aperture in front of the telescope and taking measurements as the aperture diameter is reduced. In this experiment three different configurations were tested. The single channel baseline and 2 channel coincident photon configurations were tested using OOK bit coding. Also the three channel configuration was tested using two state bit coding.

The laser beam diameter did not fill the entire receiver aperture and so reducing the aperture did not exactly simulate increased range until the aperture was closed to a diameter of 2 cm. To help illustrate this situation, the noise and laser (signal) photon detection counts for one representative detector (C) are graphed in Figure 7.9 for the different aperture settings. In this figure it can be seen that the photon counts from the laser remain constant until the aperture diameter is decreased to 2 cm while the noise photon counts steadily decrease as the aperture diameter is decreased. This is because the noise uniformly illuminates the receiver aperture while the laser beam has a diameter of only 2 cm. So the data points that correspond to the 2 cm or less aperture do simulate an increased range, or at least they simulate increased range with a spatially limited background noise source. Note that if the background noise source extended beyond the field of view the noise would remain constant for a fixed aperture receiver were moved to greater distances. While the other data points do not simulate increased range they are helpful in that this experiment provides another situation, like Experiment 3, where noise is initially decreased and then the noise and signal are decreased concurrently. So the results here will be a nice comparison to the results for Experiment 3.

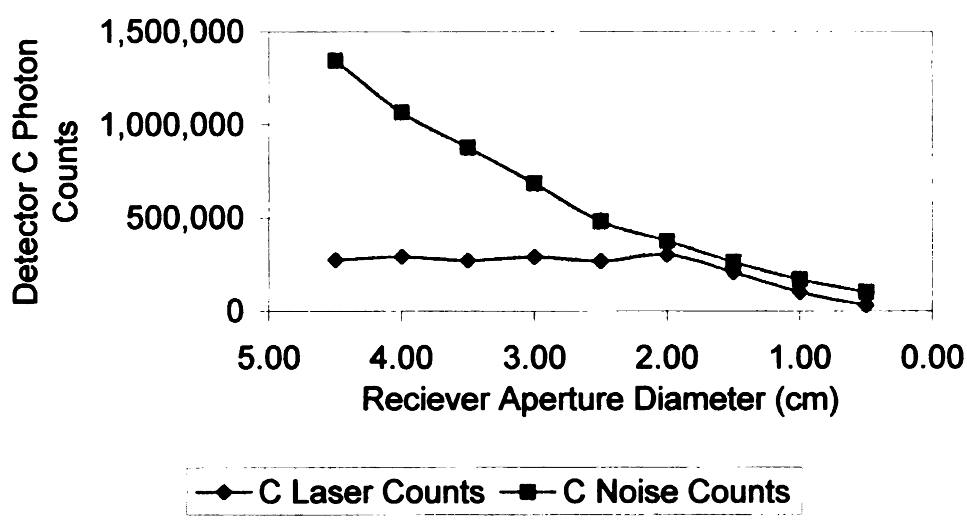

Figure 7.9: In this figure the noise and laser (signal) photon detection counts for one representative detector (C) are graphed for the different aperture settings. This figure shows that the laser beam had a beam diameter of about 2 cm and so all

aperture settings larger than 2 cm affected only noise while all aperture settings smaller than 2 cm affected noise and signal.

As the aperture is decreased from 4.5 cm to 2 cm the SNR for all three configurations improves as the noise is decreased. This is shown in Figure 7.10 where the SNR as a function of aperture diameter is graphed. After reducing the aperture below 2 cm the SNR begins to drop for all three configurations. These trends of SNR provide further insight into the relative affect that noise and signal changes have on system performance.

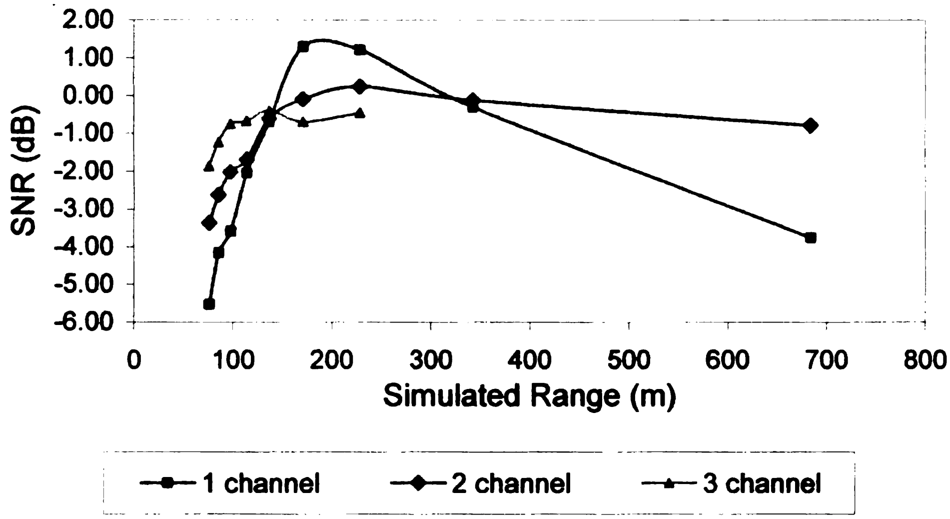

Figure 7.10: In this figure the laser noise compensated signal to noise ratio for each configuration is graphed according to the simulated range. The points greater than 200 m simulate the affect of greater range. Below 200 m it does not successfully simulate increased range because the SNR is increasing.

The system performance results of the simulated range experiment for all three configurations are shown in Figure 7.11. In interpreting this graph it is helpful to begin at the shortest range. Initially the two and three channel systems have a lower BER than the one channel system. As the noise level is decreased, for the first 4 data points, the one channel system performance improves but the two and three channel systems remain the same. The two and three channel systems are very insensitive to the change in noise level. This finding further supports the conclusions in experiment 1 that the coincident photon communication has significantly less sensitivity to noise than traditional photon counting communication.

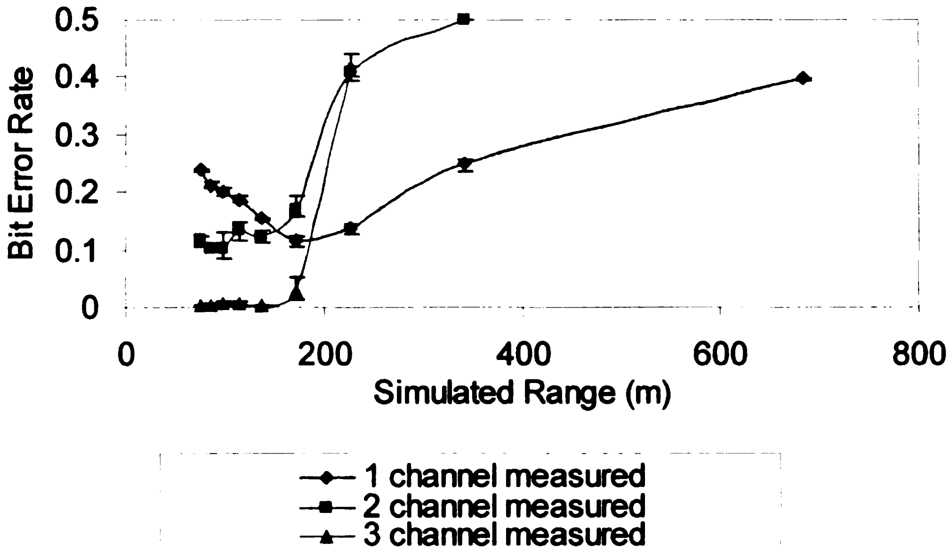

Figure 7.11: This figure shows the experimental results that different simulated ranges (inverse receiver aperture diameters) have on system performance. These results show that the coincident communication systems (2 and 3 channel) are more sensitive to changes in signal, but less sensitive to changes in noise, than the single channel traditional photon counting system. The error bars are the maximum and minimum data values for that point.

After the first five data points the closing of the aperture begins to roughly simulate greater range. For the next two data points, which are for simulated distances of 171 m and 228 m, the signal-to-noise ratios approximately level out for all three configurations. The BER for the single channel system increases only slightly. The BER for the 2 and 3 channel systems however increases substantially. This is because the signal was at a low level to begin with and the loss of signal affects the coincident photon communication system more than the single channel system. This supports the conclusions in Chapter 3 regarding the relative affect of range on the two different systems, which was that the coincident communication system dropped at $1/R^4$, where R is range, and the traditional system dropped off at $1/R^2$ when beyond the range at which the laser beam is entirely captured by the receiver collection optic. The conclusion of experiment 2 is also supported by this data. The single channel system BER nicely follows the trend in SNR for that system. However, the coincident communication system is more affected by signal strength and so this system more closely follows trends in signal strength.

7.8 Discussion

The general conclusion of all these experiments is that the coincident photon communication system is a photon counting communication technique that is effective even with significant ambient noise. The second conclusion is that the coincident photon counting technique is very sensitive to signal strength, in general more sensitive than traditional photon counting communication. This is to be expected and can be explained by comparing the equations for SNR for the 1 channel case to the 2 channel case. The SNR, in terms of photon counts registered by the receiver, for the one channel system, with an ideal detector that has $\alpha = 1$, is equal to

$$SNR_1 = \frac{R_1}{r_1} \qquad [7\text{-}1].$$

In this case changes in noise level affect the SNR in a way that is directly proportional to the noise level. The SNR for the two channel case is derived from the equations for average signal count per bit for a one bit [Equation 3-27] and average noise count per bit for a zero bit [Equation 3-30]. This SNR, again with ideal detectors, is represented by

$$SNR_2 = \frac{\frac{[R_1 R_2]}{R_p T_p}}{[r_1 r_2]} \qquad [7\text{-}2].$$

These equations are more readily comparable if we assume the signal rates and the pulse rate are all the same and also all of the noise rates are the same, and they simplify to

$$SNR_1 = \frac{R}{r} \qquad [7\text{-}3]$$

$$SNR_2 = \frac{\frac{R}{T_p}}{r^2} \qquad [7\text{-}4].$$

In the case where the signal photons are equal to the background photons the SNR for one channel is equal to 1 while the SNR for the 2 channel case is the ratio of 1 over the pulse time divided by the background noise count. If the background noise count is 1 million photons per second and the pulse time is 10 nano seconds then the SNR is 100 as shown here

$$SNR_2 = \frac{\frac{1}{10^{-8}}}{10^6} = 10^2 \qquad [7\text{-}5].$$

Since these rates and pulse widths are representative of the numbers found in the experiment we can see that error in the communications has more to do with the signal than it does from the noise. Keep in mind that a SNR of 100 can still produce a high BER if the signal is on the order of 5 coincidences per bit and the noise is .005 because a Poisson distribution with an average of 5 will have quite a few zeros, and so there will be quite a few bits with no signal. In the data taken for these experiments the numbers of coincidences for the 2, 3 and 4 channel cases were in general in the single digits per bit, so even without any noise there would have been a BER of at least 10^{-5} just because of a fraction of bits having no signal. Any reduction of signal, when the signal is already low, therefore significantly impacts system performance.

The experiments performed here demonstrate the potential for this technique for a very low power system. The bit error rates achieved are not those that would be required for a planetary mission. In that case the BER would have to be in the range of 10^{-7}. While that hasn't been demonstrated with this experimental system there is significant potential to reach this level. Improvements in the transmitter and receiver to reduce the pulse time to 1 ns and the coincidence time to 1ns would significantly improve the BER. Also increasing the number of pulses to 15 or 20 would significantly improve the BER. Also it is possible that Pulse Position Modulation could be used to further decrease the power per bit and Forward Error Correction coding could likewise improve the BER.

To illustrate how improvements in the system can affect overall performance Figure 7.12 was created. In this figure the performance of a two state 4 channel system is presented for three different situations. The data points were calculated using Equations [3-22, 23, 24, 27, 28, 29 and 30] and the Mathcad worksheet shown in Appendix D. The first data series is denoted as 'Experiment Configuration' and these data points represent the system performance of the experimental system with transmission loss neglected. The second curve is denoted as 'Coincidence / pulse time 1 ns' and this shows improvement in system performance by reducing the coincidence time and laser pulse width time to 1 ns. The third curve, denoted as 'Shorter coincidence time with 15 pulses per bit', shows how the overall system performance is improved by both reducing the pulse width / coincidence time and increasing the number of pulses to 15 per bit.

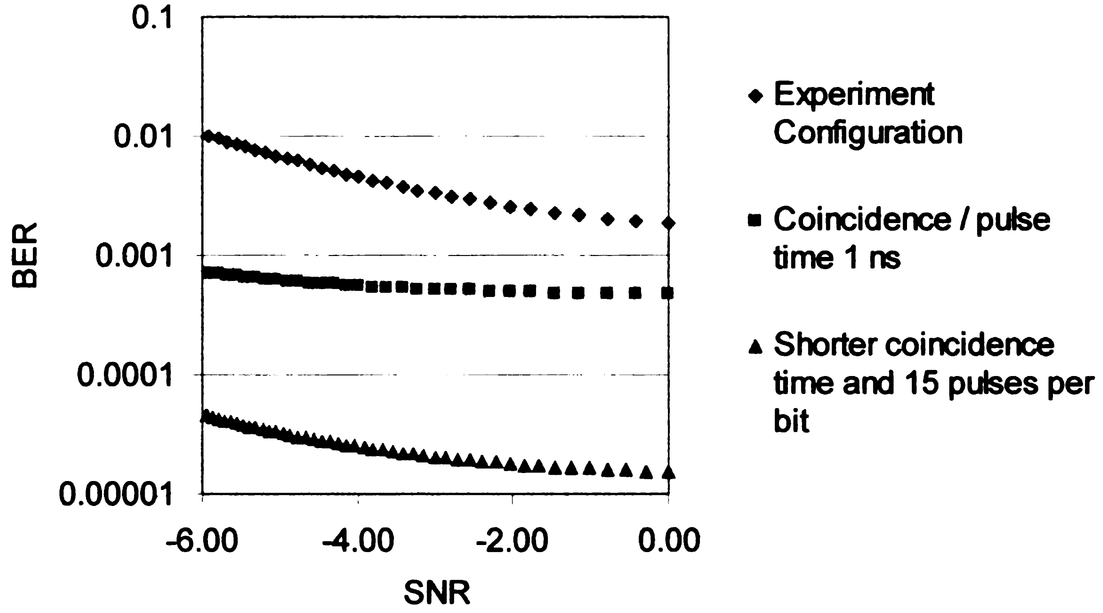

Figure 7.12: In this figure the system performance is graphed for the experimental configuration (diamonds), an improved system with a 1 ns pulse width and coincidence time (squares) and a further improved system that uses 15 pulses instead of 10 (triangles).

Figure 7.12 shows that reducing the pulse width of the lasers from 14 ns to 1ns and also reducing the coincidence time from 11.25 ns to 1 ns produces an order of magnitude reduction in BER. By further improving the system by increasing the number of pulses per bit from 10 to 15 the BER is reduced by another order of magnitude. With these two improvements the system has better than a 10^{-4} BER and the radiated power would still be less than 1 nW. The technique has demonstrated significant noise immunity in the presence of background noise and with further system refinement such as these and with the inclusion of standard coding and modulation techniques it has significant potential to enable free space communication for miniature sensor stations.

7.9 Summary

In this chapter experiments testing the low power optical communication system has been presented. In contrast to traditional photon counting the system is made significantly immune to background noise by only counting photon coincidences. Experiments conducted with this system have shown that a signal of just 360 pW can have an effective range of 70 meters even in the presence of ambient light levels similar to what can be expected outdoors. The experiment, while not optimized, has demonstrated low error communication at significantly lower signal to noise ratios than is possible with traditional photon counting. Previously this type of coincident photon communication method has been accomplished using non linear systems to generate quantum entangled photons. The system presented here has been developed because it can more readily utilize the smallest high efficiency sources that tend to have low total power levels. With sources such as these, the transmitter electrical energy can be as low as a billionth of a watt, which would overcome a significant hurdle for miniature planetary sensor platforms.

Chapter 8 Conclusion

This work has been focused on further developing low power optical communications based on the utilization of both Quantum Entangled (QE) photons and also pulsed pairs of photons. In this final chapter the new knowledge and accomplishments of this work are summarized. Also, a comparison of the results of this work with State-Of-the-Art (SOA) low power communication systems is made. The chapter, and this work, is completed with a discussion of the next steps that might be taken in developing miniature low power optical transmitters.

8.1 Dissertation accomplishments:

When this work began a list of planned accomplishments was created. These accomplishments were generated to further define the scope and significance of the work. The list is repeated here and how these accomplishments have been met is also included with each accomplishment.

1. <u>Develop two state error probabilities and build a 2 state transmitter utilizing quantum entangled photons.</u>

   The error probabilities for both the Quantum Entangled (QE) and the pulsed coincident photon communication systems for the two state bit coding were developed in Chapter 3. In Chapter 5 calculated BER values using the equations for the QE system were compared to experimental values and they had very good agreement. Likewise in Chapter 7 calculated values for the coincident photon system were compared to experimental results and had good agreement.

A transmitter based on quantum entangled photons was built that has two states, one for each bit value. One bit value was coded by sending photons of like polarization and the second bit value was coded by sending photons with orthogonal polarizations. The transmitter and receiver designs for this system were described in Chapter 4 and an experiment testing the system was described in Chapter 5. The findings from this accomplishment were: The system successfully transmitted data at a remarkably low power level, a received optical power of 1 Pico joule per bit, in the presence of significant background noise. As mentioned, this experiment had very good agreement to the theoretical prediction and so it confirmed the method for two state BER calculation developed in Chapter 3.

2. Contrast Ratio Calculation

The contrast ratio calculation, which is the ratio of the average of the '1' bit value to the '0' bit value - similar to SNR, was completed and described in Chapter 3. This calculation showed that the QE based communication system can produce much higher bit contrast ratios in very high noise environments, up to -20 dB SNR, than is possible with traditional photon counting systems.

3. <u>Modify Probabilistic Mathematical Model to account for solid state transmitter instead of existing QE based transmitter</u>

The method for calculating the average number of received photon pairs for the system based on coincidently pulsed source is described in Chapter 3. This method was adapted from the previously developed formulation for QE photon pairs [Man 1984, Hon 1985]. Once the average numbers of photon pairs can be determined, the BER can be calculated by analyzing the Poisson probability functions generated from these averages. The BER calculation for on / off keying was directly taken from the previous work for the QE system. The BER calculation for the two state keying was developed as part of this work and also appears in Chapter 3. This calculation is applicable to both the QE system and the coincidently pulsed sources system.

4. <u>Develop energy efficient transmitter concept and build an experimental transmitter and receiver and test the concept</u>

The transmitter concept was completed and described in detail in Chapter 6. This concept was considered to be very novel and so the National Aeronautics and Space Administration has filed for a patent on it in May 2006. Both the transmitter and receiver were built to test the pulsed photon pair concept and they were described in Chapter 6.

This concept was tested in several experiments and the results of these experiments were described in Chapter 7. The experimental results confirmed that the technique does indeed allow for photon counting communications in the presence of significant background noise. They also confirmed that the mathematical model developed in this dissertation does accurately predict BER. The final finding, and potentially most significant, from this accomplishment is that the system was able to achieve a BER of $2*10^{-3}$ while having a data rate of 100 Kbits/ sec, transmitting over a distance of 70 meters with a background level that was above the signal level (received SNR was -0.7) using only 760 pW of transmitted power. This translates to only 7.6 femto watts of transmitted power per bit. This confirms the low power optical communications concept that was the goal of this work.

One final accomplishment that deserves mention was unplanned. This accomplishment was the calculation in Chapter 3 regarding the differences in performance, as a function of range, between a QE based system and a system that is based on pulsed pairs of sources. It was assumed when this work began that the issue of range was solved, as it had been reported in the publication by Jackson et.al. [Jackson 2002]. The QE system however has been shown to have the potential for a significantly greater effective range than the system based on coincidently pulsed sources. These calculations have shown that the QE system can have an effective range hundreds of times greater than the pulsed pair system [Lekki 2008-1].

8.2 Comparison of general results from QE, coincident photons and SOA communication methods

The QE based system, coincidently pulsed sources system, the SOA optical and Radio Frequency systems all have some advantages and disadvantages for low power communication applications. The SOA has been covered in Chapter 2 so the advantages and disadvantages of the two techniques will only be discussed here.

The SOA miniature RF systems have several advantages. They have already been operated at 100 μw of electrical power and are Omni-directional, so pointing and tracking are not issues. The chief disadvantage of a miniature RF system is that it has a range of generally only 10 meters when operating at the 100 μw power level. For optical communication, the most promising systems for low power transmission are photon counting systems that use Geiger mode detectors. The advantages of these systems are that the receivers are extremely sensitive, as they can detect single photons, and they have very low noise, in the hundreds of counts per second. The optical sources can be made to be very small and also very energy efficient. Also, because small optical transmitters are more directional than RF transmitters of the same size, the photon counting system has greater range than the RF system. The directionality however does introduce issues with pointing and tracking problems for mobile stations. These SOA optical systems have been used to achieve nearly 1 photon per bit free space communication, but the chief disadvantage is that they have, until now, been limited to situations with "little or no background noise" [Maj 2008]. The advantages of photon counting communications and this specific disadvantage, is the essential motivator for developing the time coincident photon pair communication techniques.

The QE system has two chief advantages. The first is that a QE source intrinsically produces photons nearly simultaneously and so the receiver can have very short coincidence times. This would be very important in a situation with very high background light levels. The second advantage of a QE system is that because of the momentum entanglement it is possible to have hundreds of times further range than a pulsed pair system. The chief disadvantage of the QE system is that it is not energy efficient to produce QE photons. Without a more efficient method of producing QE photons this disadvantage may make it impossible for the QE system to be utilized in a miniature low power station. If the energy efficiency is increased then there are significant opportunities for this system to be implemented for long distance low power communication.

The system based on coincidentally pulsed sources has significant advantages. It has all of the advantages of a traditional photon counting communication system with the further advantage that it is a photon counting technique that can work in the presence of significant background noise. This system also has better range than the RF system as it has been demonstrated to 70 meters and a simulated range of about 175 meters. This was achieved with a signal power of 760 of picowatts. Even with very low electrical to optical energy efficiency ~1%, an optimized optical system utilizing this technique would still only use 76 nw of electrical power. This is a three orders of magnitude power improvement over the RF device while achieving greater range. The chief disadvantage to this system is that the signal falls off proportional to $1/R^4$ beyond the point where most of the beam is captured by the receiver.

Since the QE based system can have significantly greater effective range than the pulsed coincident source system and the QE system has lower energy efficiency it is not clear at this point which one will be more effective in the future. For shorter ranges the coincidently pulsed sources is clearly better. For ranges beyond that several questions, such as how much can the energy efficiency of QE sources be improved and also can the longer range transmissions by QE systems be realized, before a clearly preferred technique is determined.

8.3 Future Work

The accomplishments in this work can be expanded upon in numerous areas. Both the system based on Quantum Entanglement and the coincident photon communications systems have significant improvements that can be made. There are also areas in bit coding and error correction that can be applied to both these systems that can significantly enhance the system performance. Finally, pointing, tracking and synchronization techniques need to be implemented and tested for these systems.

For the QE based system further work towards improving the efficiency of spontaneous down conversion and work to confirm the increased range possible with QE photons are both reasonable next steps. The efficiency of spontaneous down conversion can be increased by placing the non linear crystal in an optical cavity. The cavity will increase the number of times that the pump photons passes through the crystal and will therefore increase the potential that a pump photon will down convert into two QE photons, thereby improving the energy efficiency of the system. Also, building and testing a QE transmitter that recombines the beams in a geometrically symmetric fashion would make it possible to test the conclusions in Chapter 3 regarding the improvement that can be realized at long ranges when utilizing the QE system rather than a pulsed pair system.

The next step for the pulsed pair system would be to improve the light sources so that a shorter pulse width can be achieved. The pulse width has lots of room for improvement as the sources used in this work could only generate pulse widths down to14 ns. A source with pulse widths of a fraction of a nano second would allow for the coincident time of the receiver to like wise be reduced to a fraction of a nano second. This will reduce the noise coincidences by at least a factor of ten and will significantly improve the BER of the system.

The BER for both these systems can be improved by utilizing error correction techniques. This will come at a loss of bandwidth and increase in the energy per bit, but the overhead is probably necessary to achieve BERs on the order of 10^{-7}, which is the general minimal requirement for planetary missions. Further work in bit coding can reduce the energy per bit. The 3 and 4 channel systems could be encoded so that they would have 3 and 4 bit states respectively. This would allow the 4 channel system to send twice the information of the two channel system. The number of channels and the number of states could like wise be increased beyond 4 by adding sources of different wavelengths. Even more out of the ordinary, Orbital Angular Momentum states could be used to add additional channels. The benefit of OAM states is that they are mutually orthogonal and so it is straight forward to add channels by simply increasing the OAM of the photons. This is highly speculative however because the OAM modes have there own range limitations based on the size of the aperture.

Finally, work in pointing, tracking and synchronization are other future steps that are necessary. Traditional tracking and synchronization techniques for optical communications would be applicable for systems such as these and so work in applying these techniques should be undertaken in the future. To initiate correct pointing, the low power transmitter can work in cooperation with larger higher power relay stations. These higher power stations can transmit higher power communication signals to the low power stations to give them a beacon to orient towards. The relay station will have to in turn listen for the low power transmissions as it scans an area with its receiver. This scanning may not be difficult as the small low power stations will probably have limited mobility and so the area that needs to be scanned may not be very large once the sensor has been initially localized.

8.4 Concluding Remarks

A concept for low power communication has been demonstrated to allow communication up to 70 meters utilizing Pico watts of radiated power. There is significant potential for improvement beyond this, as has been described in the previous section. This work has led to the potential of building future miniature planetary explorers that can communicate with nano watts of power. This is a power level that is readily 'scavenged' from the environment. It is therefore possible that robotic explorers, utilizing a communication technique such as this, might work as self sustaining swarms to study an area from many vantage points and collect a wealth of information in places we so very much want to explore.

APPENDIX A

MATHCAD WORKSHEET FOR CALCULATING BER FROM EXPERIMENT COINCIDENCE DATA

Mathcad 11 worksheet for calculating the Bit Error Rate of 2 state quantum entangled photon communication. Created: 11/9/2007 by John Lekki.

$N_1 := 55.66$	Number of 1 state coincindences measured when '1' bit transmitted
$N_{01} := 23.28$	Number of 0 state coincidences measured when '1' bit transmitted
$N_0 := 53.95$	Number of 0 state coincindences measured when '0' bit transmitted
$N_{10} := 23.67$	Number of 1 state coincidences measured when '0' bit transmitted

$$P_{10} := \sum_{z=1}^{20} e^{-(N_{10}+N_0)} \left(\frac{N_{10}}{N_0}\right)^{\frac{z}{2}} \cdot \mathrm{In}\left(z, 2\sqrt{N_{10} \cdot N_0}\right)$$

$$P_{10} = 1.813 \times 10^{-4}$$

$$P_{01} := \sum_{z=0}^{20} e^{-(N_{01}+N_1)} \left(\frac{N_{01}}{N_1}\right)^{\frac{z}{2}} \cdot \mathrm{In}\left(z, 2\sqrt{N_{01} \cdot N_1}\right)$$

$$P_{01} = 1.219 \times 10^{-4}$$

$$BER := \frac{P_{10} + P_{01}}{2}$$

$$BER = 1.516 \times 10^{-4}$$

APPENDIX B

COMMUNICATION DATA ANALYSIS FOR ON / OFF KEYED DATA

Mathcad 11 Worksheet
Latest Edit 2/1/2008

timebase := 1.000006

Time base multiplier to compensate for variability in clock pulse duration

CommunicationData :=

CommunicationData =

	0	1
0	0	"0 ps"
1	1	"210.000 ns"
2	1	"1.250,000 us"
3	1	"120.000 ns"
4	1	"160.000 ns"
5	1	"500.000 ns"
6	1	"200.000 ns"
7	1	"650.000 ns"
8	1	"390.000 ns"

Data File read into array

Column 1 is the amount of time from the last coincidence registered to present coincidence

x := 1 .. rows(CommunicationData) − 1

numrows := rows(CommunicationData)

numrows = 65536

$$\text{CommDataSifted}_{x,1} := \text{substr}\left(\text{CommunicationData}_{x,1}, \text{strlen}\left(\text{CommunicationData}_{x,1}\right) - 2, 2\right)$$

$$\text{CommDataSifted}_{x,0} := \text{str2num}\left(\text{substr}\left(\text{CommunicationData}_{x,1}, 0, 5\right)\right)$$

$$\text{CommData}_{x,0} := \text{CommDataSifted}_{x,0} \cdot \text{if}\left(\text{CommDataSifted}_{x,1} = \text{"us"}, 10^{-6}, 10^{-9}\right)$$

$$\text{CommData}_{x,1} := 0$$

$$\text{CommData}_{x,1} := \text{CommData}_{x-1,1} + \text{CommData}_{x,0}$$

$$\text{CommData}_{x,2} := 0$$

$$\text{CommData}_{x,2} := \text{CommunicationData}_{x,0}$$

CommDataSifted =

	0	1
0	0	0
1	210	"ns"
2	1.25	"us"
3	120	"ns"
4	160	"ns"
5	500	"ns"
6	200	"ns"
7	650	"ns"
8	390	"ns"
9	50	"ns"
10	560	"ns"
11	490	"ns"
12	830	"ns"
13	390	"ns"

The data has been seperated so that the time can be turned into a numerical value

CommData =

	0	1	2
0	0	0	0
1	$2.1\cdot10^{-7}$	$2.1\cdot10^{-7}$	1
2	$1.25\cdot10^{-6}$	$1.46\cdot10^{-6}$	1
3	$1.2\cdot10^{-7}$	$1.58\cdot10^{-6}$	1
4	$1.6\cdot10^{-7}$	$1.74\cdot10^{-6}$	1
5	$5\cdot10^{-7}$	$2.24\cdot10^{-6}$	1
6	$2\cdot10^{-7}$	$2.44\cdot10^{-6}$	1
7	$6.5\cdot10^{-7}$	$3.09\cdot10^{-6}$	1
8	$3.9\cdot10^{-7}$	$3.48\cdot10^{-6}$	1
9	$5\cdot10^{-8}$	$3.53\cdot10^{-6}$	1
10	$5.6\cdot10^{-7}$	$4.09\cdot10^{-6}$	1
11	$4.9\cdot10^{-7}$	$4.58\cdot10^{-6}$	1
12	$8.3\cdot10^{-7}$	$5.41\cdot10^{-6}$	1
13	$3.9\cdot10^{-7}$	$5.8\cdot10^{-6}$	1
14	$1.32\cdot10^{-6}$	$7.12\cdot10^{-6}$	1
15	$7.9\cdot10^{-7}$	$7.91\cdot10^{-6}$	1

The CommData array has the time between coincidence events in column 0 and the time of the even from the beginning of the data aquisition in column 1

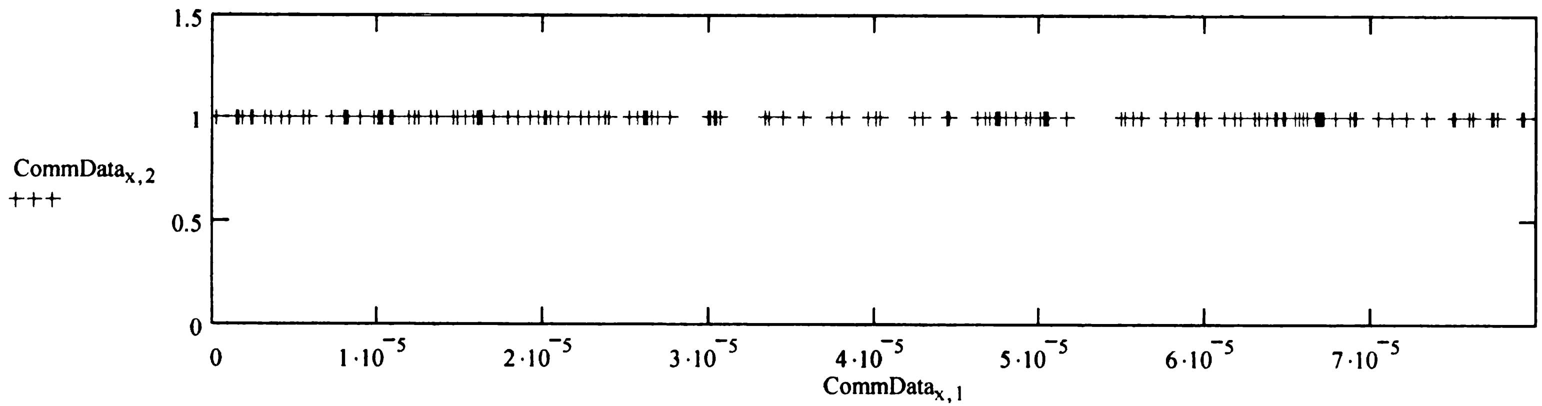

$\mathrm{Start} := 2\cdot10^{-6}$

$$\mathrm{bits} := \mathrm{floor}\left(\frac{\mathrm{CommData}_{\mathrm{numrows}-1,1}}{10\cdot10^{-6}}\right) - 5$$

$\mathrm{bits} = 3066$

The number of bits are determined and 5 are subtracted so partial bits are not used on either end of the data set

```
DataFit(data, numrows, timebase) :=
  bits ← floor( data_{numrows-1,1} / (10·10^-6) ) - 5
  MaxOnes ← 0
  Phase ← 0
  totalones ← 0
  for s ∈ 0..19
      Event ← 0
      DataFit ← 0
      for bit ∈ 0..bits - 1
          DataFit_{bit,2} ← 0  if mod(bit,2) = 0
          DataFit_{bit,2} ← 1  if mod(bit,2) = 1
          while [ data_{Event,1} < s·10^-6 + (bit + 1)(timebase)·10^-5 ]
              DataFit_{bit,1} ← DataFit_{bit,1} + 1  if data_{Event,1} > s·10^-6 + bit·10^-5
              Event ← Event + 1
          totalones ← totalones + DataFit_{bit,1}·DataFit_{bit,2}
      if (totalones > MaxOnes)
          Phase ← s
          MaxOnes ← 0
          MaxOnes ← totalones
      totalones ← 0
  Phase
```

This program determines when the first full bit starts in the data set

$\text{starttime} := \text{DataFit}(\text{CommData}, \text{numrows}, \text{timebase})$

$\text{starttime} = 14$

The DataSync function counts the number of coincedences in a bit period

$$
\text{DataSync}(\text{data}, \text{numrows}, \text{starttime}, \text{timebase}) := \left|
\begin{array}{l}
\text{bits} \leftarrow \text{floor}\left(\dfrac{\text{data}_{\text{numrows}-1,1}}{10 \cdot 10^{-6}}\right) - 6 \\
\text{MaxOnes} \leftarrow 0 \\
\text{Phase} \leftarrow 0 \\
\text{totalones} \leftarrow 0 \\
\text{Event} \leftarrow 0 \\
\text{DataFit} \leftarrow 0 \\
\text{for } \text{bit} \in 0..\text{bits} - 1 \\
\quad \left| \begin{array}{l}
\text{DataFit}_{\text{bit},2} \leftarrow 0 \text{ if } \text{mod}(\text{bit},2) = 0 \\
\text{DataFit}_{\text{bit},2} \leftarrow 1 \text{ if } \text{mod}(\text{bit},2) = 1 \\
\text{while } \left[\text{data}_{\text{Event},1} < \text{starttime} \cdot 10^{-6} + (\text{bit}+1)(\text{timebase}) \cdot 10^{-5}\right] \\
\quad \left| \begin{array}{l}
\text{DataFit}_{\text{bit},1} \leftarrow \text{DataFit}_{\text{bit},1} + 1 \text{ if } \text{data}_{\text{Event},1} > \text{starttime} \cdot 10^{-6} + \text{bit} \cdot 10^{-5} \\
\text{Event} \leftarrow \text{Event} + 1
\end{array} \right.
\end{array} \right. \\
\text{DataFit}
\end{array} \right.
$$

$\text{SyncedData} := \text{DataSync}(\text{CommData}, \text{numrows}, \text{starttime}, \text{timebase})$

SyncedData =

	0	1	2
0	0	24	0
1	0	15	1
2	0	9	0
3	0	17	1
4	0	17	0
5	0	22	1
6	0	21	0
7	0	22	1

The Synced data array has the syncronized data with numbers of coincidences stored in column 1 and the correct bit value in column 2

$$\mathrm{syncedrows} := \mathrm{rows}(\mathrm{SyncedData})$$

$$\mathrm{NumberOnes} := \sum_{n=0}^{\mathrm{syncedrows}-1} \mathrm{SyncedData}_{n,2}$$

$$\mathrm{NumberZeros} := \mathrm{syncedrows} - \mathrm{NumberOnes}$$

$$\mathrm{Threshold} := 25$$

$$\mathrm{NumberCorrectOnes} := \sum_{n=0}^{\mathrm{syncedrows}-1} \left(\mathrm{SyncedData}_{n,1} > \mathrm{Threshold} \wedge \mathrm{SyncedData}_{n,2} = 1\right)$$

$\text{IncorrectOnes} := \text{NumberOnes} - \text{NumberCorrectOnes}$

$$\text{CorrectZeros} := \sum_{n=0}^{\text{syncedrows}-1} \left(\text{SyncedData}_{n,1} \le \text{Threshold} \wedge \text{SyncedData}_{n,2} = 0\right)$$

$\text{IncorrectZeros} := \text{NumberZeros} - \text{CorrectZeros}$

$$\text{BER} := \frac{(\text{IncorrectOnes} + \text{IncorrectZeros})}{\text{syncedrows}}$$

NumberOnes = 1532

NumberZeros = 1533

NumberCorrectOnes = 307

IncorrectOnes = 1225

CorrectZeros = 1322

IncorrectZeros = 211

BER = 0.468515497553018

BER is determined by comparing the number of coincidences in the SyncedData array to the threshold value and comparing the measured value to the correct bit value

path := "C:\Archived Documents\Processed Data\"

FileName :=

OutFile:= concat(path, FileName)

OutDataFile:= concat(path, "ProcData", FileName)

$\text{Parameters}_0 := \text{syncedrows}$

$\mathrm{Parameters}_1 := \mathrm{NumberOnes}$

$\mathrm{Parameters}_2 := \mathrm{NumberCorrectOnes}$

$\mathrm{Parameters}_3 := \mathrm{IncorrectOnes}$

$\mathrm{Parameters}_4 := \mathrm{NumberZeros}$

$\mathrm{Parameters}_5 := \mathrm{CorrectZeros}$

$\mathrm{Parameters}_6 := \mathrm{IncorrectZeros}$

$\mathrm{Parameters}_7 := \mathrm{BER}$

$\mathrm{Parameters}_9 := \mathrm{Threshold}$

WRITEPRN(OutDataFile) := CommData

WRITEPRN(OutFile) := Parameters

APPENDIX C

COMMUNICATION DATA ANALYSIS FOR TWO-STATE DATA

timebase := 1.00000

FileName:= "Exp1-3-12.dat"

CommunicationData :=

CommunicationData =

	0	1
0	0	"0 ps"
1	1	"1.300,000 us"
2	1	"1.010,000 us"
3	1	"1.990,000 us"
4	10	"3.010,000 us"

$x := 1 .. \text{rows}(\text{CommunicationData}) - 1$

$\text{nrows} := \text{rows}(\text{CommunicationData})$

$\text{nrows} = 65536$

$\text{CommDataSifted}_{x,1} := \text{substr}\left(\text{CommunicationData}_{x,1}, \text{strlen}\left(\text{CommunicationData}_{x,1}\right) - 2, 2\right)$

$\text{CommDataSifted}_{x,0} := \text{str2num}\left(\text{substr}\left(\text{CommunicationData}_{x,1}, 0, 5\right)\right)$

$\text{CommData}_{x,0} := \text{CommDataSifted}_{x,0} \cdot \text{if}\left(\text{CommDataSifted}_{x,1} = \text{"us"}, 10^{-6}, 10^{-9}\right)$

$\text{CommData}_{x,1} := 0$

$\text{CommData}_{x,1} := \text{CommData}_{x-1,1} + \text{CommData}_{x,0}$

$\text{CommData}_{x,2} := 0$

$CommData_{x,2} := CommunicationData_{x,0}$

CommDataSifted =

	0	1
0	0	0
1	1.3	"us"
2	1.01	"us"
3	1.99	"us"
4	3.01	"us"
5	1.99	"us"
6	1.01	"us"

CommData =

	0	1	2
0	0	0	0
1	$1.3 \cdot 10^{-6}$	$1.3 \cdot 10^{-6}$	1
2	$1.01 \cdot 10^{-6}$	$2.31 \cdot 10^{-6}$	1
3	$1.99 \cdot 10^{-6}$	$4.3 \cdot 10^{-6}$	1
4	$3.01 \cdot 10^{-6}$	$7.31 \cdot 10^{-6}$	10
5	$1.99 \cdot 10^{-6}$	$9.3 \cdot 10^{-6}$	10
6	$1.01 \cdot 10^{-6}$	$1.031 \cdot 10^{-5}$	10
7	$9.9 \cdot 10^{-7}$	$1.13 \cdot 10^{-5}$	10

In CommData Array the zero column is the delta time between the previous event and the latest one. The one comumn is the absolute time of the events. Column two is the bit that transitioned to a one. A '1' indicates bit one went high and '10' indicates bit two went high.

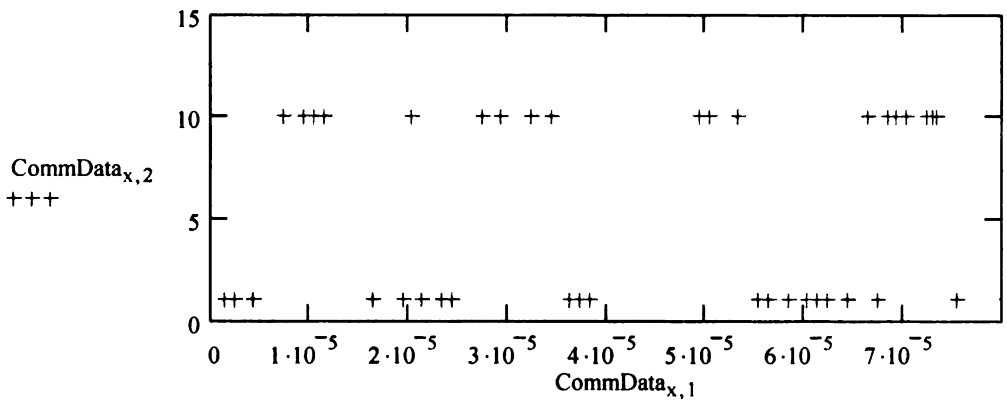

$$\text{bits} := \text{floor}\left(\frac{\text{CommData}_{\text{nrows}-1,1}}{10\cdot 10^{-6}}\right) - 3$$

$\text{bits} = 12653$

This is the total number of bits given a T = 10 microsecond bit time. Three bits have been trimmed to allow for bits lost during synchronization.

```
DatFit(data, nrows, timebase) :=
  bits ← floor( data[nrows−1, 1] / (10·10^−6) ) − 3        Determine the number of bits in the file
  MaxOnes ← 0
  Phase ← 0
  totalones ← 0
  for s ∈ 0..19
      Event ← 0                                           Loop through the start times
      DatFit ← 0
      for bit ∈ 0..bits − 1
          DatFit[bit,3] ← 0  if mod(bit,2) = 0             Loop through the bits
          DatFit[bit,3] ← 1  if mod(bit,2) = 1             Build the clock signal
          while [ data[Event,1] < s·10^−6 + (bit + 1)·(timebase)·10^−5 ]     Loop as long as the data times fall in the bit period
              DatFit[bit,1] ← DatFit[bit,1] + 1  if [ (data[Event,1] > s·10^−6 + bit·10^−5) ∧ (data[Event,2] = 1) ]
              Event ← Event + 1
          totalones ← totalones + DatFit[bit,1]·DatFit[bit,3]
      if (totalones > MaxOnes)
          Phase ← s
          MaxOnes ← 0
          MaxOnes ← totalones
      totalones ← 0
  Phase
```

$$starttime := DatFit(CommData, nrows, timebase)$$

$$starttime = 5$$

$$
DatSync(data, nrows, starttime, timebase) := \left|
\begin{array}{l}
bits \leftarrow floor\left(\dfrac{data_{nrows-1,1}}{10 \cdot 10^{-6}}\right) - 3 \\
MaxOnes \leftarrow 0 \\
Phase \leftarrow 0 \\
totalones \leftarrow 0 \\
Event \leftarrow 0 \\
DatFit \leftarrow 0 \\
\text{for } bit \in 0..bits-1 \\
\quad \left|
\begin{array}{l}
DatFit_{bit,3} \leftarrow 0 \text{ if } mod(bit,2) = 0 \\
DatFit_{bit,3} \leftarrow 1 \text{ if } mod(bit,2) = 1 \\
\text{while } \left[data_{Event,1} < starttime \cdot 10^{-6} + (bit+1) \cdot (timebase) \cdot 10^{-5}\right] \\
\quad \left|
\begin{array}{l}
DatFit_{bit,1} \leftarrow DatFit_{bit,1} + 1 \text{ if } \left[\left(data_{Event,1} > starttime \cdot 10^{-6} + bit \cdot 10^{-5}\right) \wedge \left(data_{Event,2} = 1\right)\right] \\
DatFit_{bit,2} \leftarrow DatFit_{bit,2} + 1 \text{ if } \left[\left(data_{Event,1} > starttime \cdot 10^{-6} + bit \cdot 10^{-5}\right) \wedge \left(data_{Event,2} = 10\right)\right] \\
Event \leftarrow Event + 1
\end{array}
\right.
\end{array}
\right. \\
DatFit
\end{array}
\right.
$$

$$SyncedData := DatSync(CommData, nrows, starttime, timebase)$$

SyncedData =

	0	1	2	3
0	0	0	4	0
1	0	5	1	1
2	0	0	4	0
3	0	3	0	1
4	0	0	3	0
5	0	7	0	1
6	0	1	7	0
7	0	4	0	1
8	0	0	5	0
9	0	5	1	1
10	0	0	3	0
11	0	7	1	1
12	0	1	5	0
13	0	6	0	1

$$\mathrm{syncedrows} := \mathrm{rows}(\mathrm{SyncedData})$$

$$\mathrm{NumberOnes} := \sum_{n=0}^{\mathrm{syncedrows}-1} \mathrm{SyncedData}_{n,3}$$

$$\mathrm{NumberZeros} := \mathrm{syncedrows} - \mathrm{NumberOnes}$$

$$\mathrm{NumberCorrectOnes} := \sum_{n=0}^{\mathrm{syncedrows}-1} \left(\mathrm{SyncedData}_{n,1} > \mathrm{SyncedData}_{n,2} \wedge \mathrm{SyncedData}_{n,3} = 1\right)$$

$$\mathrm{IncorrectOnes} := \mathrm{NumberOnes} - \mathrm{NumberCorrectOnes}$$

$$\mathrm{CorrectZeros} := \sum_{n=0}^{\mathrm{syncedrows}-1} \left(\mathrm{SyncedData}_{n,1} \le \mathrm{SyncedData}_{n,2} \wedge \mathrm{SyncedData}_{n,3} = 0\right)$$

$$\mathrm{IncorrectZeros} := \mathrm{NumberZeros} - \mathrm{CorrectZeros}$$

$$\mathrm{BER} := \frac{(\mathrm{IncorrectOnes} + \mathrm{IncorrectZeros})}{\mathrm{syncedrows}}$$

$\mathrm{NumberOnes} = 6326$

$\mathrm{NumberZeros} = 6327$

$\mathrm{NumberCorrectOnes} = 6309$

$\mathrm{IncorrectOnes} = 17$

$\mathrm{CorrectZeros} = 6319$

$\mathrm{IncorrectZeros} = 8$

path := "C:\Archived Documents\Processed Data\"

OutFile := concat (path , FileName)

OutDataFile := concat (path , "ProcData" , FileName)

$Parameters_{0}$:= syncedrows

$Parameters_{1}$:= NumberOnes

$Parameters_{2}$:= NumberCorrectOnes

$Parameters_{3}$:= IncorrectOnes

$Parameters_{4}$:= NumberZeros

$Parameters_{5}$:= CorrectZeros

$Parameters_{6}$:= IncorrectZeros

$Parameters_{7}$:= BER

WRITEPRN (OutDataFile) := CommData

WRITEPRN (OutFile) := Parameters

$$\mathrm{AverageOneHighValue} := \frac{\displaystyle\sum_{n=0}^{\mathrm{syncedrows}-1} \mathrm{SyncedData}_{n,1} \cdot \left(\mathrm{if}\left(\mathrm{SyncedData}_{n,3} = 1, 1, 0\right)\right)}{\mathrm{NumberOnes}}$$

$$\mathrm{AverageOneHighValue} = 5.43771735693961$$

$$\mathrm{AverageOneLowValue} := \frac{\displaystyle\sum_{n=0}^{\mathrm{syncedrows}-1} \mathrm{SyncedData}_{n,2} \cdot \left(\mathrm{if}\left(\mathrm{SyncedData}_{n,3} = 1, 1, 0\right)\right)}{\mathrm{NumberOnes}}$$

$$\mathrm{AverageOneLowValue} = 0.226683528295922$$

$$\mathrm{AverageZeroHighValue} := \frac{\displaystyle\sum_{n=0}^{\mathrm{syncedrows}-1} \left[\mathrm{SyncedData}_{n,2} \cdot \left(\mathrm{if}\left(\mathrm{SyncedData}_{n,3} = 0, 1, 0\right)\right)\right]}{\mathrm{NumberZeros}}$$

$$\mathrm{AverageZeroHighValue} = 4.38217164532954$$

$$\text{AverageZeroLowValue} := \frac{\sum_{n=0}^{\text{syncedrows}-1} \left[\text{SyncedData}_{n,1} \cdot \left(\text{if}\left(\text{SyncedData}_{n,3} = 0, 1, 0\right)\right)\right]}{\text{NumberZeros}}$$

$$\text{AverageZeroLowValue} = 0.219693377588114$$

$$\text{OneContrast} := \frac{\text{AverageOneHighValue}}{\text{AverageOneLowValue}}$$

$$\text{OneContrast} = 23.9881450488145$$

$$\text{ZeroContrast} := \frac{\text{AverageZeroHighValue}}{\text{AverageZeroLowValue}}$$

$$\text{ZeroContrast} = 19.9467625899281$$

$$\text{BER} = 0.001975816012013$$

APPENDIX D

BIT ERROR CALCULATION FOR TIME COINCIDENT PHOTON COMMUNICATION

Mathcad 11 worksheet for calculating the Bit Error Rate of 2 state time coincident photon communication. Created: 11/9/2007 by John Lekki.

$R_1 := 50000($

$R_2 := 500000$

$R_3 := 500000$

$R_4 := 500000$

$r_1 := 500000$

$r_2 := 500000$

$r_3 := 500000$

$r_4 := 500000$

$\alpha_1 := 0.7$

$\alpha_2 := \alpha_1$

$\alpha_3 := \alpha_1$

$\alpha_4 := \alpha_1$

$\delta t := 11.5 \cdot 10^{-9}$

$T_p := 15 \cdot 10^{-9}$

$T_s := 2 \times 10^{-5}$

$R_p := 10$

$$N_1 := R_1 \cdot \alpha_2 \cdot \frac{\delta t}{T_p} T_s + \left[\left[\left(1 - \alpha_2\right) R_1 r_2 + \left(1 - \alpha_1\right) R_2 r_1 + r_1 \cdot r_2\right] \cdot \delta t\right] \cdot T_s$$

Number of 1 state coincidences measured when '1' bit transmitted

$$N_{01} := r_3 \cdot r_4 \cdot \delta t \cdot T_s$$

Number of 0 state coincidences measured when '1' bit transmitted

$$N_0 := R_3 \cdot \alpha_4 \cdot \frac{\delta t}{T_p} T_s + \left[\left[\left(1 - \alpha_4\right) R_3 r_4 + \left(1 - \alpha_3\right) R_4 r_3 + r_3 \cdot r_4\right] \cdot \delta t\right] \cdot T_s$$

Number of 0 state coincidences measured when '0' bit transmitted

$$N_{10} := r_1 \cdot r_2 \cdot \delta t \cdot T_s$$

Number of 1 state coincidences measured when '0' bit transmitted

$N_1 = 5.459$

$N_{01} = 0.058$

$N_0 = 5.459$

$N_{10} = 0.058$

$$P_{10} := \sum_{z=1}^{20} e^{-(N_{10}+N_0)} \left(\frac{N_{10}}{N_0}\right)^{\frac{z}{2}} \cdot \mathrm{In}\left(z, 2\sqrt{N_{10} \cdot N_0}\right)$$

$$P_{10} = 2.77 \times 10^{-4}$$

$$P_{01} := \sum_{z=0}^{20} e^{-(N_{01}+N_1)} \left(\frac{N_{01}}{N_1}\right)^{\frac{z}{2}} \cdot \mathrm{In}\left(z, 2\sqrt{N_{01} \cdot N_1}\right)$$

$$P_{01} = 5.663 \times 10^{-3}$$

$$\mathrm{BER} := \frac{P_{10} + P_{01}}{2}$$

$$\mathrm{BER} = 2.97 \times 10^{-3}$$

REFERENCES

Abouraddy, A. F., Saleh, B. E. A., Sergienko, A. V. and Teich, M. C., "Role of Entanglement in Two-Photon Imaging", *Physical Review Letters* **87**(12), 123602 1-4 (2001).

Alde, D. M., Dyer, P., Luther, G. G., Morgan, G. L. and Schauer, M., "Quantum Cryptography", *Los Alamos National Laboratory Publication LA-UR-95-806.*

Andrews, L. C. and Phillips, R. L., *Laser Beam Propagation through Random Media*, SPIE Optical Engineering Press, Bellinham, Washington (1998).

Arakawa, Y., "Connecting the Dots", *OEMagazine*, January, 18-20 (2002).

Arnon, S., "Effects of atmospheric turbulence and building sway on optical wireless-communication systems", *Optics Letters* **28**(2), 129-131 (2003).

Atkin, G. E. and Fung, K. L., "Coded Multipulse Modulation in Optical Communication Systems", *IEEE Trans. on Comm.* **42**(2/3/4), 574-582 (1994).

Banaszek, K., Dragan, A., Wasilewski, W. and Radzewicz, C., "Experimental demonstration of entanglement-enhanced classical communication over a quantum channel with correlated noise", *Phys. Rev. Letters* **92**(25), 257901 1-4 (2004).

Barnett, S. M., Phoenix, S. J. D., "Information theory, squeezing and quantum correlations", Phys. Rev. A 44(1), 535-545 (1991).

Bouwmeester, D., Ekert, A. and Zeilinger, A., *The Physics of Quantum Information*, Springer, Berlin (2000).

Burnham, D. C. and Weinberg, D. L., "Observation of Simultaneity in Parametric Production of Optical Photon Pairs", *Phys. Rev. Letters* **25**(2), 84-87 (1970).

Dmitriev, V. G., Gurzadyan, G. G. and Nikogosyan, D. N., *Handbook of Nonlinear Optical Crystals 3rd. edition*, Springer, Berlin (1999).

Eckardt, R. C., Masuda, H., Fan, Y. X. and Byer, R. L., "Absolute and Relative Nonlinear Optical Coefficients of KDP, KD*P, BaB_2O_4, $LiIO_3$, MgO: $LiNbO_3$, and

KTP Measured by Phase-Matched Second-Harmonic Generation", *IEEE J. Of Quantum Electronics* **26**(5), 922-933 (1990).

Friberg, S., Hong, C. K., and Mandel, L., "Intensity Dependence of the Normalized Intensity Correlation Function in Parametric Down-Conversion", *Optics Communications* **54**(5), 311-316 (1985).

Gourley, P., "Nanolasers", *Scientific American* Magazine; March 1998, p. 56-61.

Grant, K. J., Corbett, K. A., Clare, B. A., Nener, B. D., Boettcher-Hunt, A., and Davies, J. E., "Dual Wavelength Free Space Optical Communications", *Proceedings of CLEO / QELS / Phast Conference*, Baltimore, Md. (2005).

Haight, F., *Handbook of the Poisson Distribution*, New York, New York (1967).

Hecht, E., *Optics (3rd Edition)*, Addison-Wesley, New York (1998).

Hong, C., Friberg, S. and Mandel, L., "Optical communication channel based on coincident photon pairs", *Applied Optics* **24**(22), 3877-3882 (1985).

Jackson, D., Hockney, G. and Dowling, J., "Quantum communication noise rejection using correlated photons", *Journal of Modern Optics* **49**, 2383-2388 (2002).

Joobeur, A. and Saleh, B. E. A., "Spatiotemporal coherence properties of entangled light beams generated by parametric down-conversion", *Phys. Rev. A* **50**(4), 3349-3361 (1994).

Karim, M. A., *Electro-Optical Devices and Systems*, PWS-Kent, Boston (1990).

Kim, I. I., Hakakha, H., Adhikari, P., Korevaar, E., and Majumdar, A. K., "Scintillation reduction using multiple transmitters," *Free-Space Laser Communication Technologies IX, Proc. SPIE* **2990**, 102-113 (1997).

Kim, I. I., Stieger, R., Koontz, J. A., Moursund, C., Barclay, M., Adhikari, P., Schuster, J., Korevaar, E., Ruigrok, R., and DeCusatis, C., "Wireless optical transmission of fast Ethernet FDDI, ATM and ESCON protocol data using the Terralink laser communication system", *Opt. Eng.* **37**(12), 3143-3155 (1998).

Kimble, M., Anderson, E., Jayne, K., and Woodman, A., "Micro-Tubular Fuel Cells", NASA Tech Briefs, April 2004.

Kurtsiefer, C., Oberparleiter, M. and Weinfurter, H., "High efficiency photon pair collection in type II parametric fluorescence", *Phys. Rev. A* **64**(2), 023802 1-4 (2001).

Kwiat, P. G., Mattle, K., Weinfurter, H., Zeilinger, A., Sergienko, A. V., and Shih, Y., "New High-Intensity Source of Polarization-Entangled Photon Pairs", *Phys. Rev. Letters* **75**(24), 4337-4341 (1995).

Lee, H. and Kim, J., "Quantum teleportation and Bell's inequality using single-particle entanglement", *Phys. Rev. A* **63**, 012305 1-5 (2000).

Lekki, J. D., Nguyen, Q., Nguyen, B. and Hizlan, M., "Quantum Optical Communication for Micro Robotic Explorers", *Proceedings of the AIAA Infotech@Aerospace Conference*, Arlington, Va., September (2005).

Lekki, J. D., Nguyen, Q., and Nguyen, B., "An Extremely Low Power Quantum Communication Link for Autonomous Robotic Explorers", *Proceedings of AIAA Infotech@Aerospace Conference*, Rohnert Park, Ca, May (2007).

Lekki, J., "Quantum entanglement enables low-power optical communication to orbital ranges", *Optical Engineering* **47**(1), (2008).

Lekki, J. D., Nguyen, Q., and Nguyen, B., "An extremely low power quantum optical communication link for miniature planetary sensor stations", *Journal of Aerospace Computing, Information and Communication*, (Submitted March 2008).

Majumdar, A. and Ricklin, J., *Free Space Laser Communications: Principles and Advances*, Springer, New York 2008, p 184.

Mandel, L. and Wolf, E., "Coherence Properties of Optical Fields," *Rev. Mod. Phys.* **37**, 231 (1965).

Mandel, L., "Proposal for almost noise-free optical communication under conditions of high background", *J. Opt. Soc. Am. B*, Vol 1, March (1984), p. 108-110.

Mao, S. S., "Nanolasers: Lasing from Nanoscale Quantum Wires", *Int. J. of Nanotechnology* **1**(1/2), 42-85 (2004).

McEliece, R. J., "Practical Codes for Photon Communication", *IEEE Trans. on Information Theory* **27**(4), 393-398 (1981).

Miyazawa, T., Tatebayashi, J., Nakaoka, T., Ishida, S., Iwamoto, S., Takatsu, M., Arakawa, Y., Hirose, S., Takemoto, K., Usuki, T. and Yokoyama, N., "Electroluminescence from a Single Quantum Dot at Telecommunication Wavelength", *Proceedings of CLEO / QELS conference*, Baltimore (2005).

National Science and Technology Council, Committee on Technology, Subcommittee on Nanoscale Science, Engineering and Technology, "National Nanotechnology Initiative: The Initiative and Its Implementation Plan", July 2000, Washington D.C., p. 61-62.

Nielsen, M. and Chuang, I., *Quantum Computation and Quantum Information*, Cambridge University Press, Cambridge (2000).

Nordholt et Al., "Present and Future Free-Space Quantum Key Distribution", SPIE Conference: Free-Space LASER Communications Technologies XIV, 20-25 JAN 2002, San Jose, CA

Nordholt, J. E., Hughes, R. J., Morgan, G. L., Peterson, C. G. and Wipf, C. C., "Present and future free-space quantum key distribution", *Los Alamos National Laboratory Publication LA-UR-01-6817* (2002).

Oberparleiter, M. and Weinfurter, H., "Cavity-enhanced generation of polarization-entangled photon pairs", *Optics Communications* **183**, 133-137 (2000).

Ortiz, G., Sandusky, J., and Biswas, A., "Design of an Opto-Electronic Receiver for Deep-Space Optical Communications", *TMO Progress Report* 42-142, August (2000).

Pierce, J. R., "Optical Channels: Practical Limits with Photon Counting", *IEEE Trans. On Communications* **26**(12), 1819-1821 (1978).

Pittman, T. B., Shih, Y. H., Strekalov, D. V. and Sergienko, A. V., "Optical imaging by means of two photon quantum entanglement", *Phys. Rev. A* **52**(5), 3429-3432 (1995).

Polishuk, A., "Communication performance analysis of microsatellites using and optical phased array antenna", *Opt. Eng.* **42**(7), 2015-2024 (2003).

Rabaey, J., Ammer, J., Karalar, T., Li, S., Otis, B., Sheets, M., Tuan, T., "PicoRadios for Wireless Sensor Networks: The Next Challenge in Ultra-Low-Power Design," Proc. of the Int'l Solid-State Circuits Conf., San Francisco, CA, February 3-7, (2002).

Rarity, J. G. and Tapster, P. "Experimental Violation of Bell's Inequality Based on Phase and Momentum", *Phys. Rev. A* **64**(21), 2495-2498 (1990).

Rarity, J. G. and Tapster, P. R., "Quantum Communications", *Appl. Phys. B* **55**, 298-303 (1992).

Rarity, J. G., "Getting Entangled in Free Space", *Science* **301**, 604-605 (2003).

Rarity, J. G., "Quantum communications and beyond", *Phil. Trans. R. Soc. Lond. A* **361**, 1507-1518, (2003).

Saleh, B. E. A. and Teich, M. C., *Fundamentals of Photonics*, Wiley-Interscience, New York (1991).

Shannon, C. E., "A Mathematical Theory of Communication", *The Bell System Technical Journal* **27**, 379-423 & 623-656 (1948).

Siegman, A. E., *Lasers*, University Science Books, Mill Valley, California (1986).

Sklar, B., *Digital Communications Fundamentals and Applications*, Prentice Hall, New Jersey (2000).

Stephens, D. R., *Phase-locked Loops for Wireless communications: Digital, Analog and Optical Implementations*, Kluwer Academic, New York (2002).

Strickland, B. R., Lavan, M. J., Woodbridge, E. and Chan, V., "Effects of fog on the bit-error rate of a free-space laser communication system", *Applied Optics* **38**(3), 424-431 (1999).

Takeuchi, S., "Beamlike twin-photon generation by use of type II parametric down conversion", *Optics Letters* **26**(11), 843-845 (2001).

Vilnrotter, V. and Lau, C. W., "Quantum Detection Theory for the Free-Space Channel", *IPN Progress Report 42-146*, (2001).